

# Functionality of recycled concrete fines

An experimental study on the mechanical performance of recycled concrete fines at mortar level

M. Farchich



# Functionality of recycled concrete fines

An experimental study on the mechanical performance of recycled concrete fines at mortar level

By

Mohammed Farchich

in partial fulfillment of the requirements for the degree of

**Master of Science**  
in Civil Engineering

at the Delft University of Technology,  
to be defended publicly on Wednesday December 11, 2024 at 11:00.

Supervisor:	Dr. ir. M. Ottelé	TU Delft
Thesis committee:	Prof. dr. H. M. Jonkers, Dr. S. C. Barbosa Nunes, Ir. A. T. M. Alberda van Ekenstein	TU Delft TU Delft TU Delft & Rutte Groep

An electronic version of this thesis is available at <http://repository.tudelft.nl/>.

Cover photo: Van der Wegen (2020)



# Preface

This thesis is written as partial fulfillment of the requirements for the degree of Master of Science in Civil Engineering at the Delft University of Technology. It is the culmination of my time as a student and also marks the end of a challenging academic journey.

This study focuses on the potential of recycled concrete fines as a sustainable alternative of ordinary cement. Concrete, with cement as its main component, is one of the most widely used materials in construction, forming the backbone of modern infrastructure. However, the production of cement is a great contributor to the global carbon dioxide emissions, accounting for nearly 8% of the total emissions. With the pressing challenges of climate change and resource depletion, the need for sustainable alternatives to conventional cement has never been more urgent.

In this research the performance of recycled concrete fines obtained from the novel Smart Liberator technique as replacement of ordinary Portland cement at mortar level is assessed. It is expected that these fine fractions consist mostly of whether or not hydrated cementitious materials. Several treatment methods, such as flash calcination and grinding, are used for enhancing the reactivity of the recycled concrete fines. Strength tests gave insight into the performance of the recycled concrete fines at mortar level.

The findings in this research aim to contribute to the ongoing efforts in mitigating climate change and promoting resource efficiency in the construction industry, paving the way for a more sustainable built environment.

I want to express my gratitude to everyone who helped, supported and encouraged me throughout this journey. I am grateful to Dr.ir. M. Ottelé, Prof.dr. H.M. Jonkers, Dr. S.C. Nunes and Ir. A.T.M. Alberda van Ekenstein for being part of my graduation committee. Thank you for your guidance through this process and your valuable insights, it helped me a lot in shaping this thesis and broadening my understandings. I also want to thank the team at Rutte Groep, particularly René, Silvio and Ousmane for their assistance and for granting me access to the necessary resources and equipment. Furthermore, I would like to thank the technical staff of TU Delft for their help and guidance during the experiments. Last but not least, a special thanks to my family, friends and fellow students for their support and encouragement throughout this journey.

As I present this thesis, I hope it serves as a small but meaningful contribution to the field and inspires further research on concrete recycling.

*M. Farchich  
Delft, December 2024*

# Abstract

The pressing challenges of climate change and the increasing surplus of concrete waste is making it increasingly important to fully recycle concrete in a sustainable way. Since cement is by far the component that contributes most to the environmental footprint of concrete, it is of great importance to investigate the potential of upcycling secondary cementitious materials. Modern recycling techniques such as the Smart Liberator make it possible to efficiently separate the coarse and fine fractions in concrete waste. It also makes it possible to produce a fine powder fraction that shows potential to replace primary cement, which helps to mitigate CO<sub>2</sub> emissions. This study explores to which extent recycled concrete fines (RCF), obtained from advanced recycling technologies such as the Smart Liberator, can replace ordinary Portland cement (OPC) in mortar mixtures. It is assumed that the RCF consist mostly of cementitious materials. The aim of this study is to assess the performance of RCF when replacing OPC in different mortar mixtures. Several treatment methods were applied to enhance the reactivity of the RCF.

To be able to assess the performance of the RCF as replacement of ordinary Portland cement at mortar level, three reference mortar mixtures, made from CEM I, CEM II/B-V and CEM III/B, were prepared for comparison. Portland cement with strength class 52.5 R was used in for preparation of the reference mixtures. The used RCF were the 0-63 µm fraction obtained from the Smart Liberator. It is expected that the RCF are from CEM III origin based on documentation from the company Rutte Groep. However, due to limited stock, some of the mortar mixtures had to be prepared with a different type of RCF, consisting of RCF with a CEM I and CEM III origin that were mixed in a 1:1 ratio. The OPC in the reference mixtures was replaced with RCF at 50%, 75% and 100% ratios.

Grinding, carbonation, conventional heating and flash calcination were applied as treatments to enhance the reactivity of the RCF. Thermogravimetric analyses were used to assess the effects of the treatments on the decomposition of the compounds of the RCF. Mortar prisms made with treated and untreated RCF were tested for flexural and compressive strength after 28 days of curing, and their performance was compared to the reference mortars.

The results showed that the untreated RCF performed best when used in combination with blast furnace slag. This combination was the only one in which a 100% replacement resulted in measurable strengths and the measured strengths at the other replacement ratios were the highest, reaching up to 70% of the compressive strength of the reference prisms at 50% replacement. This indicates that the RCF are a suitable activator for blast furnace slag.

The effects of the treatments differed in the different mixtures and also varied across the replacement ratios. Grinding of the RCF improved their performance at the 50% and 75% replacement ratios in the CEM I variant, while their performance in the CEM II and CEM III variants was similar to or lower than the untreated RCF. The same conclusions are drawn from the results after carbonation. Heating of the RCF up to 900 °C for 30 minutes in a regular chamber furnace resulted in better results for the CEM I variants at all replacement ratios, while no significant improvements were measured for the CEM II variants. For the CEM III variants, only the 75% replacement ratio had a significant improvement. Lastly, flash calcination resulted in the most significant improvements for the CEM I and CEM II variants at all replacement ratios. For the CEM III variants, flash calcination significantly improved the strengths at the 100% and 75% replacement ratio, but not at the 50% replacement ratio. Since this does not align with each other, it is necessary to reconfirm these results.

As a conclusion, this study demonstrated that untreated RCF shows potential to BFS, while flash calcination is the most promising treatment for boosting RCF reactivity across most mixtures. Conventional heating also showed potential, especially for CEM I. However, grinding and carbonation had mixed results, with limited benefits for BFS combinations due to carbonation effects. Future research should confirm these findings and explore ways to optimize the treatment methods.

# Table of contents

Preface .....	4
Abstract .....	6
List of figures .....	9
List of tables .....	11
1. Introduction.....	12
1.1. Problem description .....	12
1.2. Research gaps.....	13
1.3. Research goal and scope .....	14
1.4. Research questions .....	14
1.5. Research method.....	14
1.5.1. Literature study .....	14
1.5.2. Experimental research .....	14
1.5.3. Comparative LCA review .....	15
2. Literature review .....	16
2.1. Cement .....	16
2.1.1. Definition.....	16
2.1.2. Common cements.....	16
2.1.3. Basic cement chemistry .....	20
2.1.4. Cement hydration.....	23
2.2. Cement recycling .....	28
2.2.1. Cement recycling in the Netherlands .....	28
2.2.2. Recycling methods.....	28
2.2.3. Treatment methods.....	32
2.2.4. Implementation routes for recycled concrete fines .....	36
2.3. Life Cycle Assessment.....	39
2.3.1. Overview.....	39
2.3.2. Objectives of LCA .....	39
2.3.3. Methodology of LCA .....	39
3. Materials and methods .....	42
3.1. Materials .....	42
3.2. Treatment methods.....	43
3.2.1. Further grinding .....	43
3.2.2. Heating .....	44
3.2.3. Carbonation .....	45
3.2.4. Flash calcination .....	45
3.2.5. Thermogravimetric Analysis and Differential Scanning Calorimetry .....	45
3.3. Flexural and compressive strength tests .....	46
3.4. Hypotheses.....	48
3.4.1. Samples with untreated RCF .....	48
3.4.2. Samples with carbonated RCF.....	48
3.4.3. Samples with further ground RCF .....	48
3.4.4. Samples with thermally treated RCF at 900 °C .....	49
3.4.5. Samples with flash calcined RCF .....	49
4. Results .....	50
4.1. TGA and DSC.....	50
4.2. Flexural and compressive strength tests .....	56
4.2.1. Reference specimens .....	56
4.2.2. Comparison of 'CEM I' variants.....	57
4.2.3. Comparison of 'CEM II' variants.....	59
4.2.4. Comparison of 'CEM III' variants.....	61
4.3. LCA review .....	63
4.3.1. Goal definition.....	63
4.3.2. Scope definition .....	63

4.3.3. Life Cycle Impact analysis.....	64
5. Discussion .....	67
6. Conclusions and recommendations .....	70
6.1. Conclusions .....	70
6.2. Recommendations .....	73
Bibliography .....	74
Appendices.....	80
Appendix A: Cement standards.....	80
Appendix B: Mixing procedure according to NEN-EN 196-1.....	92
Appendix C: Strength results .....	94
Reference prisms.....	94
Prisms with untreated RCF .....	95
Prisms with carbonated RCF .....	97
Prisms with ground RCF .....	99
Prisms with heated RCF .....	101
Prisms with flash calcined RCF.....	103
Appendix D: TGA and DSC.....	105
Untreated RCF .....	105
Carbonated RCF .....	106
Further ground RCF.....	107
Flash calcined RCF .....	108
Heated RCF.....	109



# List of figures

Figure 1.1: How cement and concrete are made (Cement Association of Canada, sd).....	12
Figure 2.1: The 27 products in the family of common cements according to EN 197-1 .....	17
Figure 2.2: An outline on cement manufacturing (ConstructionHow, 2020).....	18
Figure 2.3: Processing of Blast furnace slag (Satyendra, 2013).....	19
Figure 2.4: Generation of fly ash in a power plant (Satyendra, 2013).....	19
Figure 2.5: Compounds of Portland cement and their abbreviations (Mehta & Monteiro, 2006) .....	20
Figure 2.6: Approximate composition limits of Portland cement in weight % (Neville & Brooks, 1987) .....	21
Figure 2.7: Slag reactivity relations (Escalante, et al., 2001).....	22
Figure 2.8: Range of element oxides present in Class C and Class F fly ash (Hemalatha & Ramaswamy, 2017) .....	22
Figure 2.9: Heat of hydration of pure compounds .....	24
Figure 2.10: Strength development of pure compounds (Neville & Brooks, 1987).....	24
Figure 2.11: Schematic representation of the heat flow rate during hydration of OPC (Marchon & Flatt, 2016) .....	25
Figure 2.12: Comparison of the heat flow rates (Gruskovnjak et al., 2006) .....	25
Figure 2.13: Coupled hydration reaction of slag-blended Portland cement (Chen & Brouwers, 2006).....	26
Figure 2.14: Factors that influence the reactivity of slag in cement (Chen & Brouwers, 2006) .....	26
Figure 2.15: Chemical composition in % of OPC and fly ash (Sakai et al., 2005) .....	27
Figure 2.16: Mineral composition of fly ashes in % (Sakai et al., 2005).....	27
Figure 2.17: Basicity of glass phase in fly ashes (Sakai et al., 2005) .....	27
Figure 2.18: Relationship between the amount of Ca(OH) <sub>2</sub> and the replacement ratio of fly ash in fly ash cement (Sakai et al., 2015) .....	27
Figure 2.19: Reaction ratio of fly ash over time (Sakai et al., 2015) .....	27
Figure 2.20: Applicable crushers based on particle size (Balasubramanian, 2017) .....	29
Figure 2.21: Typical three stage crushing with different equipment and their reduction ratios (Balasubramanian, 2017).....	29
Figure 2.22: Indication of the Smart Liberator (Florea et al., 2013) .....	29
Figure 2.23: Schematic representation ADR principle (Gebremariam et al., 2020).....	30
Figure 2.24: Sketch of HAS with measurement points Q (flow) and T (temperature) (Gebremariam et al., 2020) .....	31
Figure 2.25: Quality improvement techniques of RCA (Tam et al., 2021).....	32
Figure 2.26a: Dissolution of calcium from residual...2.26b: Dissolution of silicon from residual concrete....	38
Figure 2.27: Relationship between the phases of an LCA (NEN-EN-ISO 14040, 2006) .....	40
Figure 3.1: Retsch Planetary Ball Mill PM 100 .....	43
Figure 3.2: EyeTech Particle size and shape analyzer.....	43
Figure 3.3: Particle size distribution before and after grinding.....	44
Figure 4.1: Comparison of the TG graphs of all treatments.....	50
Figure 4.2: Comparison of the DTG graphs of all treatments .....	51
Figure 4.3: Comparison of the DSC graphs of all treatments .....	52
Figure 4.4: TG comparison between the different untreated RCF types.....	53
Figure 4.5: TG comparison between the different flash calcined RCF types .....	53
Figure 4.6: DTG comparison between the different untreated RCF types .....	54
Figure 4.7: DTG comparison between the different flash calcined RCF types.....	54
Figure 4.8: Flexural strengths of CEM I variants .....	57
Figure 4.9: Compressive strengths of CEM I variants .....	57
Figure 4.10: Flexural strengths of CEM II variants .....	59
Figure 4.11: Compressive strengths of CEM II variants .....	59
Figure 4.12: Flexural strengths of CEM III variants .....	61
Figure 4.13: Compressive strengths of CEM III variants .....	61
Figure A1: Mechanical and physical requirements of standard cement strength classes according to EN 197-1 .....	811
Figure A2: Chemical requirements for common cements according to EN 197-1 .....	822
Figure A3: Requirements for sulfate resisting cements according to EN 197-1 .....	833

Figure A4: Grading requirements for filler aggregate .....	844
Figure A5: Categories for maximum values of acid-soluble sulfate content.....	844
Figure A6: Categories for influence of water-soluble materials from recycled aggregates on the initial setting time of cement paste .....	855
Figure A7: Categories for maximum values of fines content .....	866
Figure A8: Categories for maximum values of freeze-thaw resistance .....	877
Figure A9: Categories for maximum magnesium sulfate soundness .....	877
Figure A10: General requirements for admixtures.....	91
Figure D1: TGA and DSC results of untreated RCF.....	1055
Figure D2: TGA and DSC results of carbonated RCF .....	1066
Figure D3: TGA and DSC results of further ground RCF.....	1077
Figure D4: TGA and DSC results of flash calcined RCF .....	1088

# List of tables

Table 2.1: Chemical composition of blast furnace slag (Snellings et al., 2012) .....	21
Table 2.2: Available concrete rubble in the Netherlands 2018-2030 (Betonakkoord, 2021).....	28
Table 2.3: Obtained material from Smart Liberator (Ottelé, 2022) .....	30
Table 2.4: List of 11 basic environmental impact categories according to Dutch 'Bouwbesluit-2012 bepalingsmethode' (Jonkers, 2021) .....	40
Table 3.1: Reference cements compositions .....	42
Table 3.2: Names and descriptions of the reference cements and untreated samples .....	42
Table 3.3: Names and descriptions of the limestone samples.....	43
Table 3.4: Particle size distribution characteristic $D_{10}$ , $D_{50}$ and $D_{90}$ values of the RCF.....	44
Table 3.5: Reactions at different temperature ranges (Verweij, 2020)    Table 3.6: Mass losses.....	45
Table 3.7: Characteristic temperature intervals with corresponding reactions (Alarcon-Ruiz et al., 2005) ...	46
Table 3.8: Mortar mix designs for reference cements and replacement ratio's 100%, 75% and 50% to prepare three test samples .....	46
Table 4.1: Flexural ( $R_f$ ) and compressive ( $R_c$ ) strengths of reference prisms [MPa] .....	56
Table 4.2: Flexural ( $R_f$ ) and compressive ( $R_c$ ) strengths of CEM I variants as ratio to reference values .....	58
Table 4.3: Flexural and compressive strengths of CEM II variants as ratio to reference values .....	60
Table 4.4: Flexural and compressive strengths of CEM III variants as ratio to reference values .....	62
Table 4.5: Environmental impacts per kg of OPC according to different studies .....	64
Table 4.6: Environmental impacts of the processing of 1 ton EoL concrete with the Smart Liberator method (Koullapis, 2022).....	65
Table 4.7: Environmental impacts per kg of RCF obtained with the Smart Liberator method .....	65
Table A1: Composition of CEM I, CEM II/B-V and CEM III/B cements according to EN 197-1 .....	80
Table A2: K-value of fly ash according to NEN-EN 206 and NEN 8005 .....	88
Table A3: k-value of silica fume according to NEN-EN 206.....	88
Table A4: k-value of silica fume according to NEN-EN 206 and NEN 8005.....	89
Table C1: Fracture loads of reference prisms [N].....	94
Table C2: Flexural strengths of reference prisms [MPa].....	94
Table C3: Maximum compressive load at fracture of reference prisms [N].....	94
Table C4: Compressive strengths of reference prisms [MPa].....	94
Table C5: Fracture loads of prisms containing untreated RCF [N] .....	95
Table C6: Flexural strength of prisms containing untreated RCF [MPa] .....	95
Table C7: Maximum compressive loads of the prisms containing untreated RCF [N].....	95
Table C8: Compressive strengths of prisms containing untreated RCF [MPa] .....	96
Table C9: Fracture loads of prisms containing carbonated RCF [N].....	97
Table C10: Flexural strength of prisms containing carbonated RCF [MPa] .....	97
Table C11: Maximum compressive loads of the prisms containing carbonated RCF [N] .....	97
Table C12: Compressive strength of prisms containing carbonated RCF [MPa] .....	98
Table C13: Fracture loads of prisms containing further ground RCF [N] .....	99
Table C14: Flexural strength of prisms containing further ground RCF [MPa].....	99
Table C15: Maximum compressive loads of the prisms containing further ground RCF [N] .....	99
Table C16: Compressive strength of prisms containing further ground RCF [MPa].....	100
Table C17: Fracture loads of prisms containing heated RCF [N].....	101
Table C18: Flexural strength of prisms containing heated RCF [MPa].....	101
Table C19: Maximum compressive loads of the prisms containing heated RCF [N].....	101
Table C20: Compressive strength of prisms containing heated RCF [MPa].....	102
Table C21: Fracture loads of prisms containing flash calcined RCF [N].....	103
Table C22: Flexural strength of prisms containing flash calcined RCF [MPa].....	103
Table C23: Maximum compressive loads of the prisms containing flash calcined RCF [N].....	103
Table C24: Compressive strength of prisms containing flash calcined RCF [MPa].....	104

# 1. Introduction

## 1.1. Problem description

Since the beginning of the Industrial Revolution in the 18<sup>th</sup> century, the world has experienced major technological and political transformations. Industrial automation has led to immense economic and population growth. These changes have also had big social impacts, leading to widespread urbanization and the development of large cities (Miller et al., 2016).

As cities grew, so did the demand for concrete, a fundamental material in the construction industry. Concrete is essential for building infrastructure that supports key functions such as housing, healthcare and education. It is also vital for constructing roads and bridges, which facilitate the transport of goods and people. Furthermore, concrete is used in protective structures like storm surge barriers and dams to provide protection against natural disasters. With all the developments in the past centuries, concrete has become the world's second-most consumed material, after water (The Guardian, 2019).

While concrete has been essential to global progress, its production significantly harms the environment. The primary issue lies in cement, a key component of concrete, which is a major contributor to climate change due to the high amount of CO<sub>2</sub> that is released during its production. Each year, over 4 billion tons of cement are produced, contributing about 8% of global CO<sub>2</sub> emissions (Lehne & Preston, 2018). With ongoing economic growth, particularly in Asia, demand for concrete (and therefore cement) is expected to increase by 12-23% by 2050 compared to 2014 levels (International Energy Agency & World Business Council for Sustainable Development, 2018).

The problem of high CO<sub>2</sub> emissions from cement production is expected to grow even bigger, with potentially serious consequences for the planet if left unaddressed. But CO<sub>2</sub> emissions aren't the only concern. Producing more cement also means using more raw materials and fossil fuels, which are needed in the manufacturing process. This leads to the depletion of these important resources. Figure 1.1 shows how cement and concrete are made.

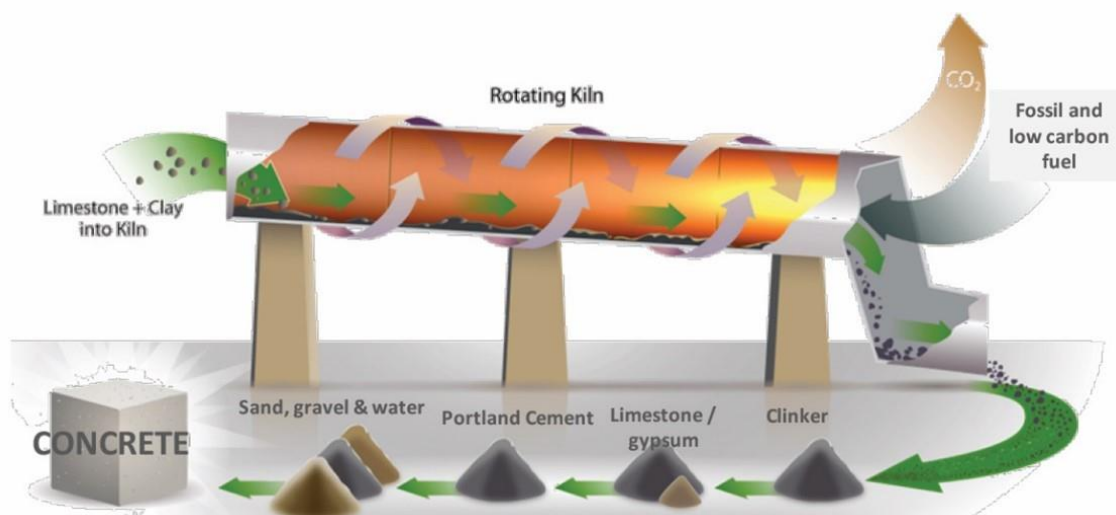


Figure 1.1: How cement and concrete are made (Cement Association of Canada, sd)

A solution is urgently needed. In recent decades, much research has focused on addressing these problems. One of the most promising ways to reduce CO<sub>2</sub> emissions from cement production is recycling old concrete. Currently, end-of-life (EoL) concrete is mostly either landfilled or used in road foundations. However, neither option is a sustainable way to handle concrete waste.

Adding to the challenge, demand for road materials is decreasing, while volumes of EoL concrete keep rising as many buildings and structures from the 1950s reach the end of their life. This creates a growing surplus of concrete waste. By recycling EoL concrete so it can be reused in new concrete, it becomes possible to make productive use of this surplus (Lotfi et al., 2013).

## 1.2. Research gaps

Most of the research on the recycling of EoL concrete focuses on the suitability of coarse aggregates in new concrete mixtures, often overlooking the bigger picture in the development of recycling technologies. Nowadays, many new recycling methods are under development. The four main techniques are the Smart Liberator, C2CA (Concrete to Cement and Aggregate), Circulair Mineraal and Mangeler (Ottel , 2022).

Gebremariam et al. (2020) describes the development of two large-scale recycling technologies named Advanced Dry Recovery (ADR) and Heating Air classification System (HAS). These technologies make it possible to separate EoL concrete into coarse (4-12 mm), fine (0.25-4 mm) and ultrafine (0-0.25 mm) particles. ADR and HAS are part of the C2CA recycling method. It was concluded that full incorporation of the coarse and fine aggregates resulted in a compressive strength comparable to that of the reference concrete. Additionally, ADR and HAS are designed to be mobile, so that the concrete can be recycled on site or close to the concrete plants. This reduces heavy construction related traffic and thus traffic-related CO<sub>2</sub>-emissions. Therefore, these technologies have a great potential in reducing the environmental burden of concrete.

In the Netherlands, the most advanced recycling technology is the Smart Liberator (Van der Wegen, 2020). Due to the fact that the Smart Liberator only crushes the cement stone and does not break straight through the sand and gravel, the amount of produced concrete fines and the cleanness of the aggregates is much higher compared to a conventional crusher (Florea, Ning, & Brouwers, 2014). This development created a new starting point for further investigation into how the ultrafine retrieved fraction from old concrete could be reused as secondary binder for new concrete.

One method for upcycling recycled concrete fines is thermal treatment. In a study by Wang et al. (2018), secondary cement paste was produced at four different temperatures: 120 °C, 450 °C, 750 °C, and 1150 °C. They found that 450 °C was the optimal temperature, producing cement paste with the highest compressive strength, comparable to the strength of Ordinary Portland Cement. However, the cement paste's workability was poor and needed improvement by adding ground-granulated blast-furnace slag. For practical use, it's also important to assess the long-term performance and durability of recycled cement.

Another promising study was conducted by Alberda van Ekenstein (2020), focusing on secondary cementitious binder obtained through the Smart Liberator technique. CEM I and CEM III/B cements were used as references. Thermal treatments at 500 °C, 800 °C and 1400 °C were applied for upcycling of the secondary materials. The treated materials were analyzed and compared to each other and it was concluded that the thermal treatment at 800 °C was the best approach due to the presence of alite and belite after the treatment. This suggested possible reactivity in the treated material. However, the material's strength could not be measured accurately due to poor compaction, which was affected by high water demand. Further research is needed to fully understand the reactivity of secondary cementitious binders.

In another study, Zhutovsky et al. (2021) examined phase changes in hydrated cement pastes with and without carbonation when subjected to thermal treatment between 600 °C and 1450 °C. For the experiments, cement paste made with CEM I 52.5 N was used. The results were encouraging, showing that it is possible to produce new secondary Portland cement clinker from hydrated cement paste through thermal treatment.

### 1.3. Research goal and scope

Although there are many studies which focus on the recycling of concrete, there is still no practical application found for the fine fraction retrieved from old concrete. This research will focus on determining how recycled concrete fines can be used to make it applicable as partial or full replacement of cement. Recycled concrete fines can, in theory, help to drastically decrease the environmental footprint of concrete since there would be no need for producing new cement. This means that the demand for raw materials and the CO<sub>2</sub>-emissions due to the production of cement will decrease significantly. Also, it could make concrete a fully circular building material, which brings the goal of a fully circular economy a step closer.

The main goal of this research is to evaluate the potential of recycled concrete fines as a sustainable material for replacement, whether partial or not, of ordinary Portland cement in mortar. More specifically, this research aims to determine the 28-day compressive and flexural strength of mortar when recycled concrete fines are used in the mix design. The outcomes are used to assess the functionality and viability of recycled concrete fines in reducing the environmental impact of concrete production.

The secondary goal of this research is to assess the potential improvement in terms of environmental impact of recycled concrete fines compared to traditional Portland cement. This is done by means of a comparative Life Cycle Assessment (LCA) review in which the recycling process including extra material treatments are taken into account. With the outcomes of the LCA review, the question whether the replacement of cement by recycled concrete fines leads to a significant reduction of the environmental impacts can be answered.

### 1.4. Research questions

The main research question of this study is as follows:

*'To what extent can recycled concrete fines replace traditional cement?'*

To help to answer this question the following sub-questions are formulated:

1. *What is the impact of different replacement percentages of recycled concrete fines on the compressive and flexural strength of the mortar prisms?*
2. *What is the effect of the treatment methods on the strength of the recycled concrete fines?*
3. *How do the strength characteristics of mortar prisms with varying recycled concrete fines percentages relate to those of standard mortar mixtures with traditional cement?*
4. *How does the environmental impact of the recycled concrete fines relate to that of ordinary Portland cement?*

### 1.5. Research method

This research is divided into three main parts, followed by a concluding part based on the findings. The first part is a literature review, the second involves experimental research and the third is a comparative Life Cycle Assessment (LCA) review. Each part is explained in more detail in the following sections.

#### 1.5.1. Literature study

In this part of the research, key topics relevant to the study are reviewed through literature. It starts with an overview of the chemistry of traditional cement. Then, the essential requirements that binders must meet, according to cement standards, are outlined along with a summary of these key standards. This provides a basis for evaluating recycled concrete fines (RCF) for potential practical applications. Additionally, the four main separation techniques, which are Smart Liberator, C2CA, Circulair Mineraal, and Mangeler, are discussed. Finally, the literature review focuses on treatment methods that can enhance the reactivity of recycled concrete fines.

#### 1.5.2. Experimental research

In this stage of the research, experiments will assess the functionality and potential of recycled concrete fines (RCF) obtained through the Smart Liberator technique by Rutte Groep. These fines, called "Freement fine", have particle sizes ranging from 0 to 63 µm. Since the focus is on testing the RCF's functionality, mortar

prisms will be prepared using RCF and tested for flexural and compressive strength following the European cement standard EN 196 series.

Because untreated RCF may lack reactivity, various treatments will be applied to enhance their performance. These treatments include carbonation, further grinding, and two types of thermal treatments: one in a high-temperature chamber furnace and another in a Flash Calciner. The main difference between a regular furnace and a Flash Calciner is that the latter rapidly heats up and cools down the material. Slow cooling can lead to undesirable reactions which is prevented by rapid cooling. Also, the regular furnace is more static, whereas in the flash calciner the material moves within an airflow.

Finally, the strength results from the RCF mortar prisms will be compared to reference mortar samples made with CEM I, CEM II/B-V, and CEM III/B, all using ordinary Portland cement as the binder.

### 1.5.3. Comparative LCA review

In addition to the experimental research, a comparative Life Cycle Assessment review based on existing literature will be conducted to compare the environmental impact of RCF and ordinary Portland cement based on existing LCA studies. This will help to determine to what extent the upcycling of RCF leads to a lower environmental burden compared to producing ordinary Portland cement.

## 2. Literature review

### 2.1. Cement

To assess the functionality of secondary cementitious materials, it is important to understand the basics of cement. These basics will be discussed in this chapter consisting of the definition of cement, its chemistry and its hydration. Also the applicable requirements to the three most common cements in the Netherlands CEM I, CEM II/B-V and CEM III (Betonhuis, 2020) according to the European norm EN 197-1 will be discussed.

#### 2.1.1. Definition

According to EN 197-1 cement is a hydraulic binder, which means that it is a ground inorganic material which forms a paste when mixed with water and sets and hardens by means of hydration reactions. Also, the strength and stability of the cement will be retained after hardening, even under water (The Netherlands Standardization Institute, 2011).

CEM cement is cement which conforms to the EN 197-1 standard. This type of cement shall be capable of producing concrete or mortar, when it is appropriately batched and mixed with water and aggregates. The workability of this concrete or mortar should retain its workability long enough and shall attain specified strength levels after defined periods. Another important property is its long-term volume stability.

#### 2.1.2. Common cements

The European standard EN 197-1 distinguishes the following five types of common cements:

- CEM I            Portland cement
- CEM II          Portland-composite cement
- CEM III        Blast furnace cement
- CEM IV        Pozzolanic cement
- CEM V        Composite cement

The two most common types of cement in Dutch construction industry are Portland cement or CEM I and Blast furnace cement or CEM III. Their share in the total cement usage in the Netherlands has reached about 90% to 95%. The other 5% to 10% consists of among others fly ash cement, which is also noted as CEM II/B-V (Betonhuis, 2020). This research will consider these three main types of cement, while the other types of cement are left out of the scope of this thesis. Figure 2.1 shows the 27 products in the family of common cements according to EN 197-1.



Main types	Notation of the 27 products (types of common cement)		Composition (percentage by mass <sup>a</sup> )										Minor additional constituents	
			Main constituents											
			Clinker	Blast-furnace slag	Silica fume	Pozzolana		Fly ash		Burnt shale	Limestone			
						natural	natural calcined	siliceous	calcareous		L	LL		
K	S	D <sup>b</sup>	P	Q	V	W	T	L	LL					
CEM I	Portland cement	CEM I	95-100	–	–	–	–	–	–	–	–	–	–	0-5
CEM II	Portland-slag cement	CEM II/A-S	80-94	6-20	–	–	–	–	–	–	–	–	–	0-5
		CEM II/B-S	65-79	21-35	–	–	–	–	–	–	–	–	–	0-5
	Portland-silica fume cement	CEM II/A-D	90-94	–	6-10	–	–	–	–	–	–	–	–	0-5
	Portland-pozzolana cement	CEM II/A-P	80-94	–	–	6-20	–	–	–	–	–	–	–	0-5
		CEM II/B-P	65-79	–	–	21-35	–	–	–	–	–	–	–	0-5
		CEM II/A-Q	80-94	–	–	–	6-20	–	–	–	–	–	–	0-5
		CEM II/B-Q	65-79	–	–	–	21-35	–	–	–	–	–	–	0-5
	Portland-fly ash cement	CEM II/A-V	80-94	–	–	–	–	6-20	–	–	–	–	–	0-5
		CEM II/B-V	65-79	–	–	–	–	21-35	–	–	–	–	–	0-5
		CEM II/A-W	80-94	–	–	–	–	–	6-20	–	–	–	–	0-5
		CEM II/B-W	65-79	–	–	–	–	–	21-35	–	–	–	–	0-5
	Portland-burnt shale cement	CEM II/A-T	80-94	–	–	–	–	–	–	6-20	–	–	–	0-5
		CEM II/B-T	65-79	–	–	–	–	–	–	21-35	–	–	–	0-5
	Portland-limestone cement	CEM II/A-L	80-94	–	–	–	–	–	–	–	6-20	–	–	0-5
		CEM II/B-L	65-79	–	–	–	–	–	–	–	21-35	–	–	0-5
		CEM II/A-LL	80-94	–	–	–	–	–	–	–	–	6-20	–	0-5
CEM II/B-LL		65-79	–	–	–	–	–	–	–	–	–	21-35	0-5	
Portland-composite cement <sup>c</sup>	CEM II/A-M	80-88	←----- 12-20 ----->										0-5	
	CEM II/B-M	65-79	←----- 21-35 ----->											
CEM III	Blast furnace cement	CEM III/A	35-64	36-65	–	–	–	–	–	–	–	–	–	0-5
		CEM III/B	20-34	66-80	–	–	–	–	–	–	–	–	–	0-5
		CEM III/C	5-19	81-95	–	–	–	–	–	–	–	–	–	0-5
CEM IV	Pozzolanic cement <sup>c</sup>	CEM IV/A	65-89	–	←----- 11-35 ----->						–	–	–	0-5
		CEM IV/B	45-64	–	←----- 36-55 ----->						–	–	–	0-5
CEM V	Composite cement <sup>c</sup>	CEM V/A	40-64	18-30	–	←----- 18-30 ----->			–	–	–	–	0-5	
		CEM V/B	20-38	31-49	–	←----- 31-49 ----->			–	–	–	–	0-5	

<sup>a</sup> The values in the table refer to the sum of the main and minor additional constituents.

<sup>b</sup> The proportion of silica fume is limited to 10 %.

<sup>c</sup> In Portland-composite cements CEM II/A-M and CEM II/B-M, in pozzolanic cements CEM IV/A and CEM IV/B and in composite cements CEM V/A and CEM V/B the main constituents other than clinker shall be declared by designation of the cement (for examples, see Clause 8).

Figure 2.1: The 27 products in the family of common cements according to EN 197-1

### 2.1.2.1. Portland cement

Portland cement is defined as a cement that is obtained by burning and grinding a mixture of calcareous and argillaceous, or other silica-, alumina-, and iron oxide-bearing materials. Examples of calcareous materials are limestone and chalk. Clay and shale are typical examples of silica and alumina. Materials other than gypsum, water or grinding aids may not be added to the clinker after burning. Gypsum is commonly added for controlling the setting of the cement. It was a Leeds builder named Joseph Aspdin who patented the Portland cement back in 1824 (Neville & Brooks, 1987).

According to NEN-EN 197 Portland cement clinker is a hydraulic material which mass consists of at least two-third of calcium silicates with molecular formulas  $3\text{CaO}\cdot\text{SiO}_2$  and  $2\text{CaO}\cdot\text{SiO}_2$ . The remaining one-third of the mass consists, among others, of aluminum and iron containing clinker phases. The ratio of  $\text{CaO}/\text{SiO}_2$  by mass should be at least 2.0 and the magnesium oxide (MgO) content by mass may not be higher than 5.0%.

There are several types of Portland cement, of which Ordinary Portland cement (OPC) is the most common, which is obtained by mixing Portland cement clinker with 6-15% of blended materials and gypsum (Zhang, 2011). Figure 2.2 shows an outline of the manufacturing process of cement.

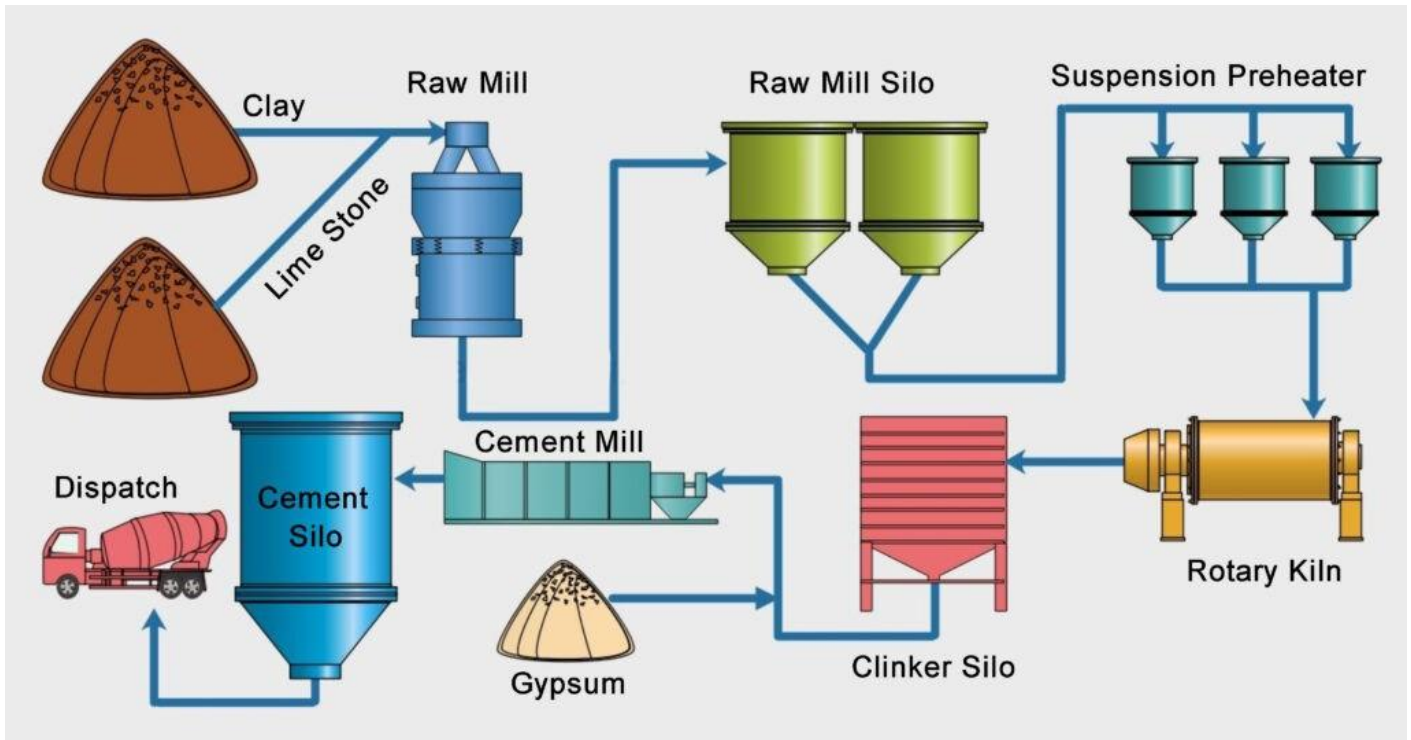


Figure 2.2: An outline on cement manufacturing (ConstructionHow, 2020)

#### 2.1.2.2. Blast furnace cement

Portland blast furnace cement, also known as Blast furnace cement, is a cement type which is produced by blending Portland cement clinker with granulated blast furnace slag and gypsum. The amount of granulated blast furnace slag that is mixed in cement is 20-70% by weight (Zhang, 2011). According to NEN-EN 197 granulated blast furnace slag consists of at least two-thirds by mass of glassy slag and possesses hydraulic properties when activated suitably. The sum of the mass of calcium oxide (CaO), magnesium oxide (MgO) and silicon dioxide (SiO<sub>2</sub>) should be at least two-thirds of the total mass. The remainder consists of aluminum oxide (Al<sub>2</sub>O<sub>3</sub>) and small amounts of other compounds. Also, the ratio by mass (CaO + MgO)/SiO<sub>2</sub> should be higher than 1.0.

Granulated blast furnace slag is a waste product in the manufacture of pig iron. Therefore, the usage of blast furnace slag leads to a lower energy consumption during the cement production process (Neville & Brooks, 1987).

After the blast furnace slag has left the blast furnace in the manufacture of pig iron, it is molten and it has a temperature of around 1450 °C. The blast furnace slag will have to be cooled rapidly through pelletization or granulation to obtain a reactive product. Slowly air cooled slag is hardly reactive and mainly used as a back-fill material in road construction or as aggregate in the production of concrete (Matthes et al., 2017). Figure 2.3 gives an overview of the processing of blast furnace slag.

## Blast furnace slag and its processing

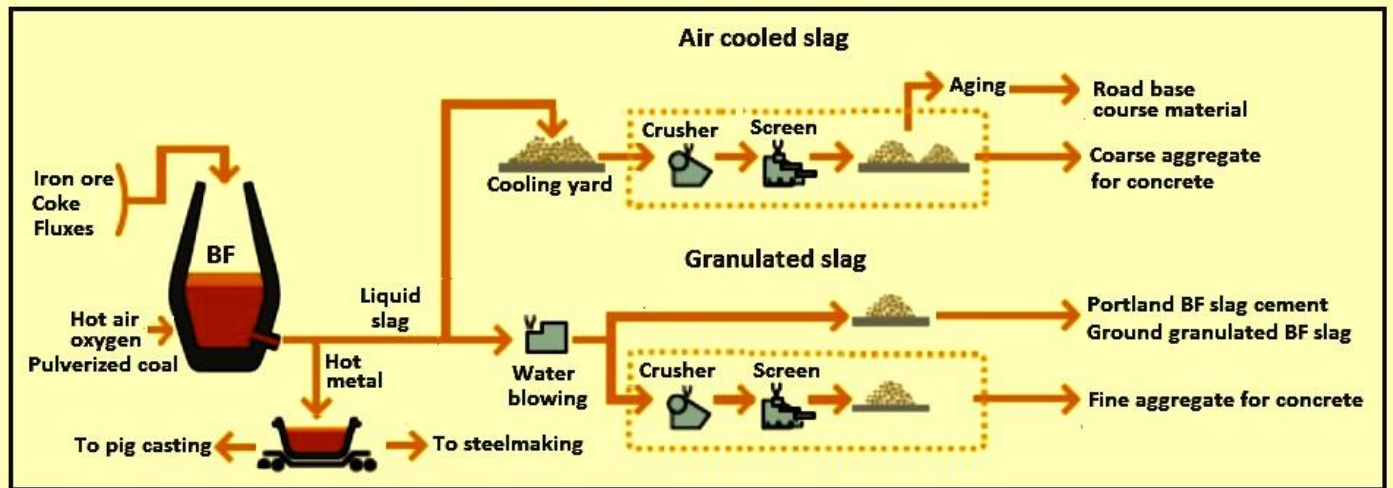


Figure 2.3: Processing of Blast furnace slag (Satyendra, 2013)

### 2.1.2.3. Fly ash cement

The European standard EN 450-1 defines fly ash as a fine powder with pozzolanic properties which consists of mainly spherical, glassy particles, derived from burning pulverized coal, with or without combustion materials and its essential chemical constituents are  $\text{SiO}_2$  and  $\text{Al}_2\text{O}_3$ . Fly ash is obtained by electrostatic or mechanical precipitation of dust-like particles from the flue gases of the power stations and it may be processed. The processing can be done by, for example, classification, sieving, blending, selection, drying, grinding or carbon reduction, or by combining these processes in adequate production plants. According to EN 197-1, CEM II/B-V consists of 65-79% clinker and 21-35% siliceous fly ash. Figure 2.4 shows the production process of fly ash in a power plant.

## Generation of fly ash in a power plant

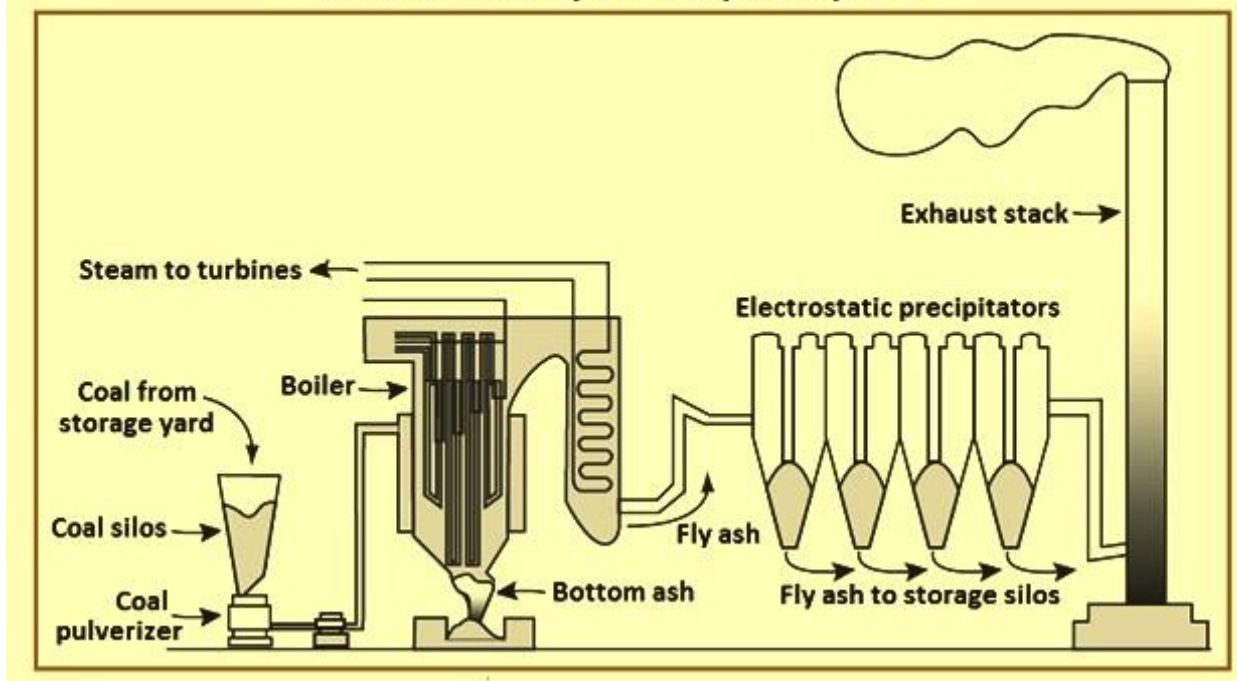


Figure 2.4: Generation of fly ash in a power plant (Satyendra, 2013)

Fly ashes are generally sub-divided into two categories: Class F and Class C fly ashes. Class F fly ash is produced by burning bituminous or anthracite coal which meets the requirements applicable to this class and it has pozzolanic properties. Class C fly ash is produced by burning bituminous or lignite coal which meets the requirements applicable to this class. Class C fly ash possesses both pozzolanic and cementitious properties. Some Class C fly ashes may have a lime content of more than 10% (Wesche, 1991).

### 2.1.3. Basic cement chemistry

In this section the basic chemistry of Portland cement blast furnace cement and fly ash cement will be discussed.

#### 2.1.3.1. Portland cement

Lime, silica, alumina and iron oxide are the main compounds that are used for the production of Portland cement. The interaction of these compounds with each other in the kiln, under high temperatures of up to 1500 °C, leads to the formation of a series of products with higher complexity and the reaching of a state of chemical equilibrium, apart from a small residue of uncombined lime which did not have sufficient time to react. After leaving the kiln, the obtained clinker is cooled down, but the chemical equilibrium is not maintained during the cooling process. The cooling rate also had an effect on the crystallization and the amount of amorphous material, known as glass, that is present in the cooled clinker. The properties of this glass are considerably different from those of crystalline compounds of similar chemical composition. The interaction of the liquid part of the clinker with the already present crystalline compounds gives another complication (Neville & Brooks, 1987).

However, the equilibrium existing at the clinkering temperature is assumed to be reproduced by the cooled products. This assumption is made in the calculation of the composition of commercial cements in which the measured quantities of oxides in the clinker as if full crystallization of equilibrium products had taken place are used to calculate the 'potential' composition.

There are four compounds that are regarded as the most important constituents of Portland cement, namely tricalcium silicate, dicalcium silicate, tricalcium aluminate and tetracalcium aluminoferrite. Although the calcium compounds are the essential compounds, the oxides of the elements are used to report the results of chemical analyses (Mehta & Monteiro, 2006). Also, it is usual to express the compounds by using abbreviations. Figure 2.5 gives an overview of these abbreviations.

Oxide	Abbreviation	Compound	Abbreviation
CaO	C	3CaO·SiO <sub>2</sub>	C <sub>3</sub> S
SiO <sub>2</sub>	S	2CaO·SiO <sub>2</sub>	C <sub>2</sub> S
Al <sub>2</sub> O <sub>3</sub>	A	3CaO·Al <sub>2</sub> O <sub>3</sub>	C <sub>3</sub> A
Fe <sub>2</sub> O <sub>3</sub>	F	4CaO·Al <sub>2</sub> O <sub>3</sub> ·Fe <sub>2</sub> O <sub>3</sub>	C <sub>4</sub> AF
MgO	M	4CaO·3Al <sub>2</sub> O <sub>3</sub> ·SO <sub>3</sub>	C <sub>4</sub> A <sub>3</sub> S̄
SO <sub>3</sub>	S̄	3CaO·2SiO <sub>2</sub> ·3H <sub>2</sub> O	C <sub>3</sub> S <sub>2</sub> H <sub>3</sub>
H <sub>2</sub> O	H	CaSO <sub>4</sub> ·2H <sub>2</sub> O	CŠH <sub>2</sub>

Figure 2.5: Compounds of Portland cement and their abbreviations (Mehta & Monteiro, 2006)

The potential composition of Portland cement is often referred to as the 'Bogue composition' and can be calculated with the Bogue equations listed below (Neville & Brooks, 1987). The oxides represent the weight percentages of the given oxides in the clinker.

- $C_3S = 4.07CaO - 7.60SiO_2 - 6.72Al_2O_3 - 1.43Fe_2O_3 - 2.85SO_3$
- $C_2S = 2.87SiO_2 - 0.754(3CaO \cdot SiO_2)$
- $C_3A = 2.65Al_2O_3 - 1.69Fe_2O_3$
- $C_4AF = 3.04Fe_2O_3$

The most important compounds of Portland cement are the two silicates Alite and Belite. They are responsible for the strength of the hydrated cement paste.

Celite is less desirable, because it has almost no contribution to the strength of the cement, except on the early strength. Another complication is the formation of calcium sulfoaluminate (ettringite), which may cause disruption when the hardened cement paste is attacked by sulfates. Nevertheless, the presence of Celite benefits the manufacture of cement, because it makes the combination of lime and silica possible.

Compared to the other compounds, Felite has no significant effect on the behavior of cement. However, its reaction with gypsum causes the formation of calcium sulfoferrite and its presence causes acceleration of the hydration of the silicates (Neville & Brooks, 1987).

What is crucial is the added amount of gypsum to the clinker, which also depends on the Celite and alkali content of the cement. The gypsum requirement is also dependent on the fineness of the cement. Increasing

the fineness of the cement has the effect of increasing the amount of Celite available at early stage, which leads to a higher gypsum requirement. However, the amount of gypsum has to be limited, because a surplus of gypsum causes expansion and consequent disruption of the set cement paste. The optimum amount of gypsum is determined based on the heat of hydration generation so that an eligible rate of early reaction occurs, ensuring that the availability of Celite for reaction is little after combination of all gypsum (Neville & Brooks, 1987).

In addition to the four main compounds of Portland cement, minor compounds also exist, such as MgO, TiO<sub>2</sub>, Mn<sub>2</sub>O<sub>3</sub>, K<sub>2</sub>O and Na<sub>2</sub>O. Usually no more than a few percent of the mass of cement consists of these compounds. However, their presence is still important, especially the two alkalis Na<sub>2</sub>O and K<sub>2</sub>O. The products of the reaction of these two compounds with some aggregates cause disintegration of the concrete and affect the strength gaining rate of cement (Neville & Brooks, 1987). Figure 2.6 shows the general composition limits in wt.% for the oxides in Portland cement.

Oxide	Content, per cent
CaO	60–67
SiO <sub>2</sub>	17–25
Al <sub>2</sub> O <sub>3</sub>	3–8
Fe <sub>2</sub> O <sub>3</sub>	0.5–6.0
MgO	0.1–4.0
Alkalis	0.2–1.3
SO <sub>3</sub>	1–3

**Figure 2.6: Approximate composition limits of Portland cement in weight % (Neville & Brooks, 1987)**

### 2.1.3.2. Blast furnace cement

Blast furnace slag is used in blast furnace cement. The slag behaves hydraulic when the melt is rapidly cooled or quenched below 800 °C in order to prevent the crystallization of merwinite and melilite, but activation of the slag is necessary. This type of blast furnace slag is called ground granulated blast furnace slag (GGBS). The chemical composition of slags vary widely. It depends on the composition of the raw materials that are used in the production process of the iron. However, the main components of blast furnace slag are CaO, SiO<sub>2</sub>, Al<sub>2</sub>O<sub>3</sub> and MgO (Snellings et al., 2012). Table 2.1 shows the approximate chemical composition of blast furnace slag.

**Table 2.1: Chemical composition of blast furnace slag (Snellings et al., 2012)**

Constituent	Content (weight %)
CaO	30 – 50
SiO <sub>2</sub>	28 – 38
Al <sub>2</sub> O <sub>3</sub>	8 – 24
MgO	1 – 18
S	1 – 2.5
Fe <sub>2</sub> O <sub>3</sub>	1 – 3
MnO	1 – 3
TiO <sub>2</sub>	< 4
Na <sub>2</sub> O + K <sub>2</sub> O	< 2

Typically the glass content of slags that are suitable for blending with Portland cement varies between 90% and 100% (Snellings et al., 2012). It is dependent on the cooling method and the temperature at which the cooling starts. The glass structure of the slag is largely dependent on the proportion of network forming elements and network-modifiers. Typical network forming elements are Si and Al, while network modifiers are elements such as Ca, Mg and to a lesser extent Al. Depending on the ratio of network-forming to network-modifying elements, the network-forming atoms exhibit variable degrees of polymerization or connectedness. They are coordinated tetrahedrally by oxygen atoms. The network depolymerization and reactivity are influenced by the amount of network modifiers, a larger amount of network modifiers leads to higher degrees of network depolymerization and higher reactivity (Goto, et al., 2007). The rate of cooling also influences the

reactivity. A higher cooling rate causes more structural defects in the glass phase, which leads to higher reactivity of the slag.

Next to the glass content, also the hydration temperature and the water-to-cement ratio influence the reactivity. The observations of Escalante et al. (2001) on the slag reactivity are summarized in Figure 2.7.

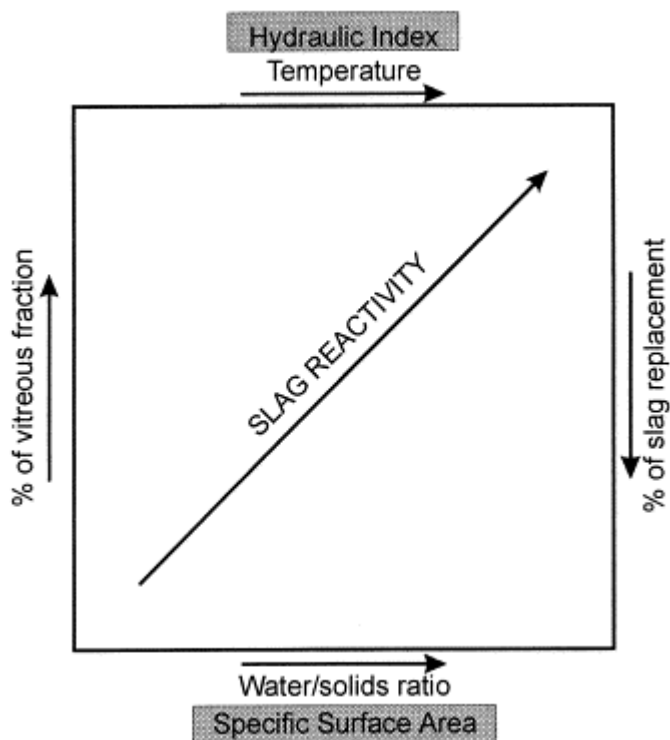


Figure 2.7: Slag reactivity relations (Escalante, et al., 2001)

### 2.1.3.3. Fly ash cement

Like ground granulated blast furnace slag, fly ash is also a supplementary cementitious material (SCM) which is used to lower the amount of Portland cement to be used. The usage of fly ash has many benefits for fresh and hardened concrete. It leads to lower mixing water requirement, higher workability and strength, higher durability, reduced heat of hydration and reduced permeability (American Coal Ash Association, 2003). Fly ash typically contains significant amounts of silicon dioxide ( $\text{SiO}_2$ ), calcium oxide ( $\text{CaO}$ ), aluminum oxide ( $\text{Al}_2\text{O}_3$ ) and iron oxide ( $\text{Fe}_2\text{O}_3$ ). Existing literature report different present element oxides percentages in Class C and Class F fly ash. Figure 2.8 gives an overview of the ranges of element oxides present in fly ash according to existing literature. The wide variations within the categories may be attributed to the variations in processing conditions, sources et cetera.

Element oxides	Class C	Class F
	Percentage	
CaO	15.1–54.8	0.50–14.0
SiO <sub>2</sub>	11.8–46.4	37.0–62.1
Al <sub>2</sub> O <sub>3</sub>	2.6–20.5	16.6–35.6
Fe <sub>2</sub> O <sub>3</sub>	1.4–15.6	2.6–21.2
MgO	0.1–6.7	0.3–5.2
K <sub>2</sub> O	0.3–9.3	0.1–4.1
Na <sub>2</sub> O	0.2–2.8	0.1–3.6
SO <sub>3</sub>	1.4–12.9	0.02–4.7
P <sub>2</sub> O <sub>5</sub>	0.2–0.4	0.1–1.7
TiO <sub>2</sub>	0.6–1.0	0.5–2.6
MnO	0.03–0.2	0.03–0.1
Loss on Ignition (LOI) (%)	0.3–11.7	0.3–32.8

Figure 2.8: Range of element oxides present in Class C and Class F fly ash (Hemalatha & Ramaswamy, 2017)

The chemical composition of fly ash mainly determines its performance when used in concrete (Shehata & Thomas, 2000). Apart from the chemical composition of fly ash, its physical properties are also important for the properties of fly ash cement and concrete. Especially the shape and size of the fly ash particles play an important role (Hemalatha & Ramaswamy, 2017). Chindaprasirt et al. (2004, 2007a, 2007b) conducted several studies to investigate the influence of the fineness of fly ash on different properties of cement and concrete, such as strength, chloride penetration, sulphate resistance, drying shrinkage et cetera. They concluded that the incorporation of finer fly ash in cement led to enhancement of the hydration and pozzolanic reaction, packing effect and nucleation effect. This resulted in a more homogeneous cement paste with a denser structure and lower  $\text{Ca}(\text{OH})_2$  compared to the paste with coarser fly ash (Chindaprasirt et al., 2007). Also, the water demand was reduced by incorporating fine fly ash, while coarse fly ash increased the water requirement due to the rougher surface of the particles. Considering the strength properties, fine fly ash leads to higher strength, caused by higher reactivity due to a high surface area. Furthermore, the packing effect led to higher compressive strength of the mortar. Although the drying shrinkage was reduced by all fly ashes, a difference was observed between the fine and coarse fly ash due to their difference in water content. Fine fly ash mortar required less water and had a relatively low drying shrinkage compared to coarse fly ash with a high water content. However, coarse fly ash performed better in the case of resistance to sulfuric acid attack (Chindaprasirt et al., 2004). Considering the resistance to chloride penetration of concrete, fine fly ash had the best performance which resulted from the reduced average pore size, reduced water/binder ratio and improvement of the interfacial zone. The spherical and smooth surface of the fine fly ash particles attribute most to its benefits (Chindaprasirt et al., 2007).

#### 2.1.4. Cement hydration

In this section the hydration of CEM I, CEM II/B-V and CEM III will be discussed. Hydration is the reaction of cement with water, producing hardened cement paste (Neville & Brooks, 1987).

##### 2.1.4.1. Hydration of Portland cement

When water is present, the silicates and aluminates of Portland cement listed in Figure 2.9 form hydration products or hydrates, which produce the hardened cement paste (Neville & Brooks, 1987).

In commercial cements, the calcium silicates  $\text{C}_3\text{S}$  and  $\text{C}_2\text{S}$  contain small impurities from some of the present oxides. The hydrated silicates are strongly affected by these impurities. The impure forms of  $\text{C}_3\text{S}$  and  $\text{C}_2\text{S}$  are known as respectively alite and belite.

When alite hydrates, some lime separates out as crystalline  $\text{Ca}(\text{OH})_2$  in the production of the microcrystalline hydrate  $\text{C}_3\text{S}_2\text{H}_3$ . The same happens when belite hydrates, however less lime is produced during this process. The calcium silicate hydrates are nowadays referred to as C-S-H. The approximate hydration reactions are written as follows (Neville & Brooks, 1987).

- Hydration of alite: 
$$2\text{C}_3\text{S} + 6\text{H} \rightarrow \text{C}_3\text{S}_2\text{H}_3 + 3\text{Ca}(\text{OH})_2$$
  

$$[100] \quad [24] \quad [75] \quad [49]$$
- Hydration of belite: 
$$2\text{C}_2\text{S} + 6\text{H} \rightarrow \text{C}_3\text{S}_2\text{H}_3 + 3\text{Ca}(\text{OH})_2$$
  

$$[100] \quad [21] \quad [99] \quad [22]$$

The most reactive phase in cement is  $\text{C}_3\text{A}$ . The reaction of pure  $\text{C}_3\text{A}$  with water is very fast and leads to a so called 'flash set'. Flash set is a rapid and unintended setting of the cement. To prevent this and make sure that the workability will be kept for a certain period before setting, gypsum is added to the clinker (Marchon & Flatt, 2016). The approximate hydration reaction of  $\text{C}_3\text{A}$  is written as follows (Neville & Brooks, 1987).

- Hydration of  $\text{C}_3\text{A}$ : 
$$\text{C}_3\text{A} + 6\text{H} \rightarrow \text{C}_3\text{AH}_6$$
  

$$[100] \quad [40] \quad [140]$$

Although  $\text{C}_3\text{A}$  is the most reactive phase in cement, the hydration of OPC is dominated by the hydration of alite, which is the main component of cement. Portland cement clinker consists for 50-70% of alite (Marchon & Flatt, 2016).

The hydration of cement is an exothermic reaction, which means that heat is released during the process. This released heat is defined as the heat of hydration and depends on the chemical composition of the cement. The total heat of hydration approximately equals to the sum of the heats of hydration of the separate

hydration of the individual compounds. Figure 2.9 shows a list of the typical heats of hydration of the pure main compounds of Portland cement (Neville & Brooks, 1987).

Compound	Heat of hydration	
	J/g	Cal/g
C <sub>3</sub> S	502	120
C <sub>2</sub> S	260	62
C <sub>3</sub> A	867	207
C <sub>4</sub> AF	419	100

**Figure 2.9: Heat of hydration of pure compounds**

As can be seen, the heat of hydration of C<sub>3</sub>A and C<sub>3</sub>S are the highest. From this follows that it is possible to control the heat and the rate of hydration of cement by controlling the amount of C<sub>3</sub>A and C<sub>3</sub>S. The total amount of heat liberation can only be controlled by the quantity of cement in the concrete mixture, while the development of the rate of hydration heat is affected by the fineness of the cement. The cementing properties of the compounds are not affected by heat of hydration (Neville & Brooks, 1987). Figure 2.10 shows the strength development of the main compounds over time in the first year.

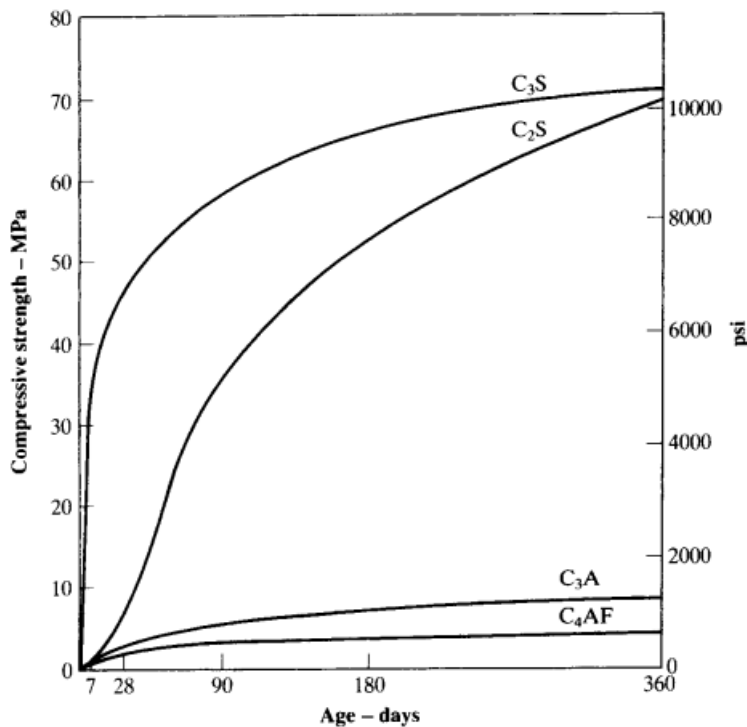


**Figure 2.10: Strength development of pure compounds (Neville & Brooks, 1987)**

It can be noticed from this graph that C<sub>3</sub>S and C<sub>2</sub>S are the main contributors to the strength of hydrated cement paste. C<sub>3</sub>S is primarily responsible for the early strength development in the first 28 days, while C<sub>2</sub>S influences the later strength development. However, after about 1 year, both silicates contribute almost equally to the strength. Compared to C<sub>3</sub>S and C<sub>2</sub>S, C<sub>3</sub>A and C<sub>3</sub>AF contribute significantly less to the final strength of the cement. However, C<sub>3</sub>A is the first compound to hydrate and it therefore contributes to the strength development in the first few days. And, as stated before, the hydration of C<sub>3</sub>A has to be slowed down by addition of a retarder, which is usually gypsum.

The overall hydration process of ordinary Portland cement can be divided into five stages, which mainly correspond to the hydration of alite (Marchon & Flatt, 2016). These stages are as follows:

- I. Initial dissolution
- II. Induction period
- III. Acceleration stage



- IV. Deceleration stage
- V. Diffusion stage

Figure 2.11 gives a schematic representation of the heat flow rates during these stages. As can be observed, a high exothermic peak occurs in the first stage. This peak is caused by the wetting of the cement surface and the quick dissolution of the anhydrous phases. Also, ettringite initially precipitates as a result of the highly reactive aluminates and the available calcium sulfate. After this, a tremendous slowdown of the reaction can be observed, which initiates the start of the induction period. The acceleration stage is characterized by the increment of the reaction speed up to the second peak. During this stage a large amount of hydration products CSH and CH is formed. The main cause of the increase in heat release is the dissolution of  $C_3S$ . The second peak is again followed by a deceleration of the reaction. During this second deceleration another peak can be observed from the graph. This peak represents the sulfate depletion point and corresponds to a higher dissolution of  $C_3A$  and a faster precipitation of ettringite. The last stage is the diffusion stage, during which the activity is low. A peak can be observed, which corresponds to the formation of AFm. The low activity is due to the slow diffusion of the species in the hardened cement (Marchon & Flatt, 2016).

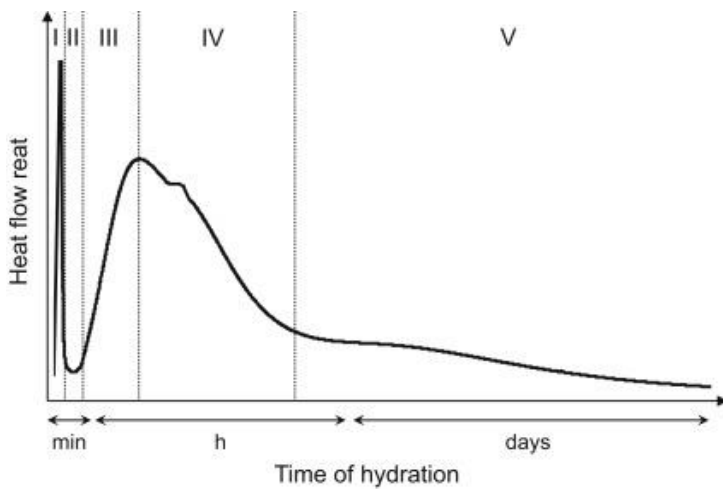


**Figure 2.11: Schematic representation of the heat flow rate during hydration of OPC (Marchon & Flatt, 2016)**

#### 2.1.4.2. Hydration of blast furnace cement

Ground granulated blast furnace slag can react with water on its own. However, the rate of hydration is very low and therefore an activator is needed to obtain a sufficient hydration rate. The hydraulic reactivity of GGBS is dependent on the surface morphology, glass phase content, chemical composition and particle size distribution. Portland cement, gypsum and alkalis are possible activators for GGBS (Song et al., 2000). Gruskovnjak et al. (2006) compared the hydration of an alkali-activated slag (AAS) with OPC. Figure 2.12 shows the heat flow rates of AAS, OPC and slag without activator.

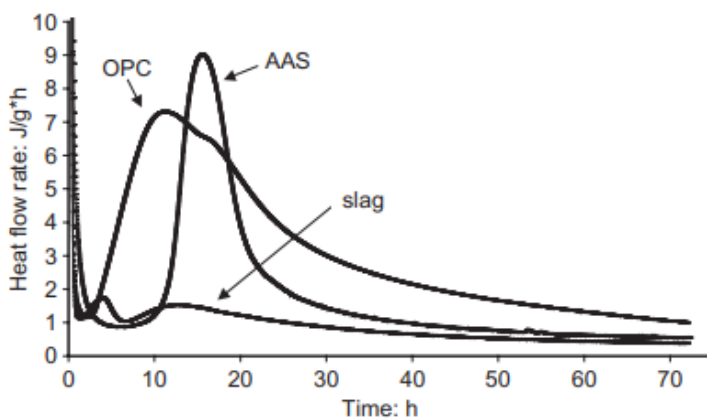


**Figure 2.12: Comparison of the heat flow rates (Gruskovnjak et al., 2006)**

Independent of the type of activator used, the main hydration product is CSH with a low Ca/Si ratio. When GGBS is activated by using Portland cement, which is the most popular activator, the hydration accelerates

due to the presence of calcium hydroxide and gypsum (Mehta & Monteiro, 2006). During the hydration of blast furnace cement, the slag component consumes some of the calcium hydroxide that is produced by the Portland cement component. Therefore it of interest to consider the blast furnace slag hydration influenced by the consumption of the calcium hydroxide. The glassy slag is activated due to the attack by hydroxyl ions provided by the calcium hydroxide (Richardson et al., 1989). The coupled reactions of the hydration of Portland cement activated slag are given in Figure 2.13.

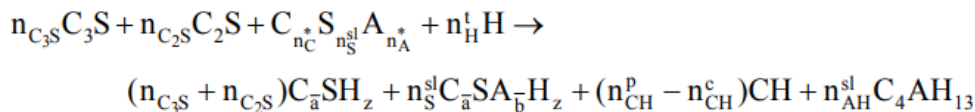


Figure 2.13: Coupled hydration reaction of slag-blended Portland cement (Chen & Brouwers, 2006)

In this reaction  $n_{C_3S}$  and  $n_{C_2S}$  are the moles of alite and belite in the Portland cement clinker,  $n_H^t$  is the total amount of water in the reaction products C-S-H and CH, the C/S-ratio in C-S-H is given by  $\bar{a}$  and the A/S-ratio in C-S-H is given by  $\bar{b}$ .  $n_S^{sl}$  is the moles of S from the slag,  $n_C^*$  and  $n_A^*$  are the moles of respectively C and A,  $z$  is the water content in C-S-H,  $n_{AH}^{sl}$  is the moles of tetracalcium aluminate hydrate,  $n_{CH}^p$  is the mole of CH produced by clinker hydration and  $n_{CH}^c$  is the mole of CH consumed by the slag reaction (Chen & Brouwers, 2006). Figure 2.14 gives an overview of the factors that affect the reactivity of the slag in cement.

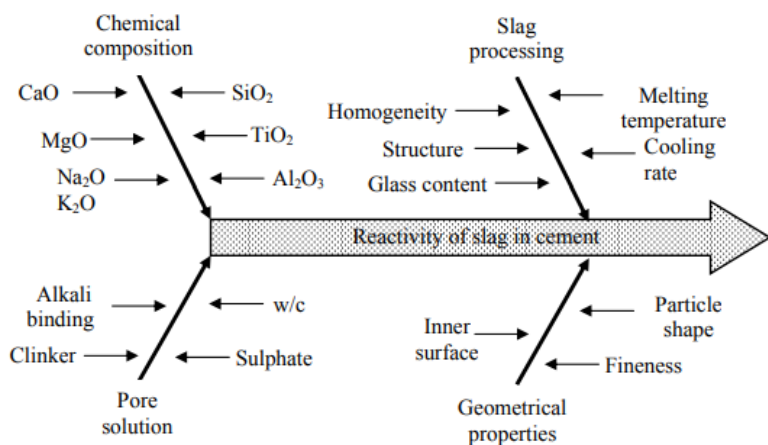


Figure 2.14: Factors that influence the reactivity of slag in cement (Chen & Brouwers, 2006)

### 2.1.4.3. Hydration of fly ash cement

In the hydration of fly ash cements, two phenomena can be distinguished: the hydration of the Portland cement clinker and the pozzolanic reaction of fly ash with the free lime (Baert et al., 2007).

Under normal curing conditions, the main reaction product of fly ash cement hydration and ordinary Portland cement are the same, namely calcium silicate hydrate (C-S-H). However, the hydration mechanisms are not the same. The effect of fly ash on the hydration of cement is complex and depends on different aspects, such as the chemical and physical nature of the fly ash, but also on the water to cement ratio of the mixture. Fly ash appears to cause retardation of the early hydration of  $C_3A$  and  $C_3S$  (Jawed, et al., 1991). Wang et al. (2004) concluded that fly ash content has a promoting role to the hydration of cement. But, when the fly ash content increases, the pozzolanic reaction degree of the fly ash reduces. Also, the total hydration degree of the system reduces with increasing fly ash content, due to the fact that cement has a higher reactivity than fly ash.

Sakai et al. (2005) also studied the hydration of fly ash cement. During their research they investigated the influence of the glass content and the basicity of glass phase on the hydration of fly ash cement. The hydration over a long curing time was characterized. Two types of fly ash were used: one with 38.2% glass content (F) and the other with 76.6% glass content (F'). Ordinary Portland cement (OPC) was used as reference material and compared to fly ash cements with replacement ratios 20%, 40% and 60% by mass. The chemical and mineral compositions and the basicities of the used samples can be found in Figures Figure 2.15, Figure 2.16, and Figure 2.17.

Samples	Ignition loss	SiO <sub>2</sub>	Al <sub>2</sub> O <sub>3</sub>	Fe <sub>2</sub> O <sub>3</sub>	CaO	MgO	TiO <sub>2</sub>	SO <sub>3</sub>	Na <sub>2</sub> O	K <sub>2</sub> O	Relative density
OPC	1.6	21.2	4.9	2.8	65.0	1.5	0.25	2.05	0.29	0.41	3.16
Fly ash F	1.1	56.3	34.2	3.2	1.2	1.3	1.87	0.26	0.27	0.50	2.24
Fly ash F'	1.2	62.0	25.5	4.3	2.2	1.2	1.10	0.40	1.30	0.80	2.22

Figure 2.15: Chemical composition in % of OPC and fly ash (Sakai et al., 2005)

FA	Glass content	Mullite	α-SiO <sub>2</sub>	Hematite	Magnetite	CaSO <sub>4</sub>	Ignition loss	Blaine (m <sup>2</sup> /kg)
F	38.2	41.9	17.1	0	0	1.7	1.1	406
F'	76.6	12.4	8.7	0	0.4	0.7	1.2	418

Figure 2.16: Mineral composition of fly ashes in % (Sakai et al., 2005)

FA	Basicity of glass phase (CaO+MgO+Al <sub>2</sub> O <sub>3</sub> )/SiO <sub>2</sub>
F	0.24
F'	0.40

Figure 2.17: Basicity of glass phase in fly ashes (Sakai et al., 2005)

The amount of formed Ca(OH)<sub>2</sub> was measured for all specimen at 28, 91 and 360 days. The measured data are shown in Figure 2.18. The straight line indicates the amount of Ca(OH)<sub>2</sub> formed in OPC and the difference between the straight line and the measured data gives the amount of Ca(OH)<sub>2</sub> that is consumed by pozzolanic reactions.

It was found that in all specimen, the fly ash in cement cured at 20 °C did not react until 7 days, regardless of the glass content and composition (Sakai et al., 2015). This is in line with the findings of Jawed et al. (2015), who found that fly ash causes retardation of early hydration. Therefore, it can be concluded that the glass content and composition do not need to be taken into consideration for the heat liberation of initial hydration. Also, over long curing periods with a duration of about one year, the glass content has little influence on the reactions and therefore the glass content may not be neglected. Figure 2.19 shows the reaction ratios of the different specimen over time.

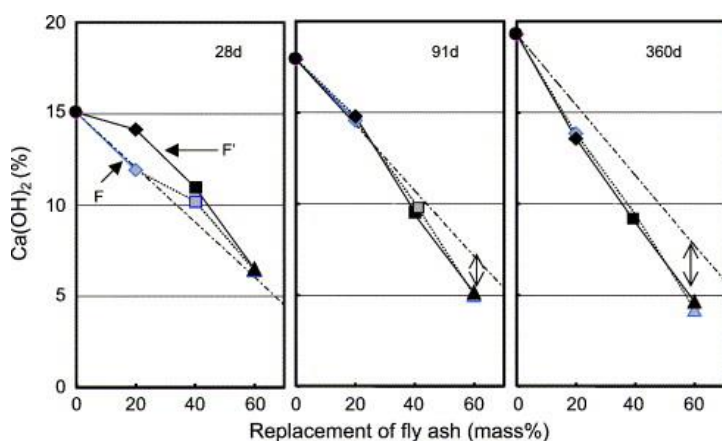


Figure 2.18: Relationship between the amount of Ca(OH)<sub>2</sub> and the replacement ratio of fly ash in fly ash cement (Sakai et al., 2015)

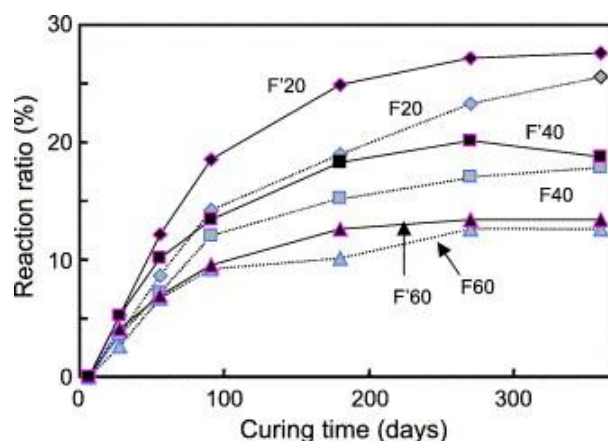


Figure 2.19: Reaction ratio of fly ash over time (Sakai et al., 2015)

## 2.2. Cement recycling

### 2.2.1. Cement recycling in the Netherlands

In the Netherlands a so called 'Betonakkoord' ('Concrete agreement') has been drawn up with the goal of the achievement of a 100% recycling of the concrete rubble by 2030 to reduce the CO<sub>2</sub> footprint (Betonakkoord, 2021). This is part of the ambition of the Dutch government to have a fully circular economy by 2050 (Rijksoverheid, n.d.). Multiple parties, such as the Dutch government, several municipalities and companies and clients from the concrete industry, participate in the Betonakkoord.

To be able to assess the potential of fully recycling the concrete rubble and specifically the cementitious binder within the concrete, it is of importance to get insight into the available amounts of waste material and the demand for concrete. Of interest for this research are the values of the Dutch construction and demolition waste. Table 2.2: gives an overview of the expected values in million tonnes of the Dutch construction and demolition waste (CDW) from 2018-2030. It is assumed that 60% of the CDW consists of concrete rubble.

**Table 2.2: Available concrete rubble in the Netherlands 2018-2030 (Betonakkoord, 2021)**

Material	2018	2020	2025	2030
<b>Total Dutch CDW (million tonnes)</b>	19.0	20.0	22.0	25.0
<b>Concrete rubble (million tonnes)</b>	11.4	12.0	13.2	15.0

In general, to produce 1 m<sup>3</sup> of concrete 325 kg of cement is used (Bouwbestel, n.d.). Under the assumption of a unit weight of concrete of 2400 kg/m<sup>3</sup>, it means that by 2030 in potential 2 million tonnes of cement can be recycled. In Europe, for each kg of produced cement, 0.7 kg of CO<sub>2</sub> is emitted (Hendriks et al., 1999). This means that, in the Netherlands, a total yearly reduction of CO<sub>2</sub>-emissions of 1.4 million tonnes can be achieved in 2030. Compared to the total amount of CO<sub>2</sub>-emissions in the Netherlands in 2021, this is approximately 1% (CBS, sd). However, this percentage is expected to be higher in 2030, since a lot of effort is put in to lower the CO<sub>2</sub> emissions.

### 2.2.2. Recycling methods

Before concrete can be recycled, it has to be processed in order to reduce the size of the debris and separate the different compounds based on particle size. For this, there exist multiple crushing and separation techniques, which can generally be divided into two groups: the conventional crushing methods and the more advanced separation techniques. The latter is of main interest for this research. However, both groups will be addressed in this section.

#### 2.2.2.1. Conventional crushing methods

Traditionally, crushing is used to produce rock or mineral fractions to be used as raw material in industrial production processes. It is the largest process operation in minerals processing and the quality parameters are normally size, shape and strength. There are two different types of machinery utilized in crushing operations. One involves employing crushers, and the other involves impactors.

The function of a crusher or crushing machine is to brake large rocks down into smaller rocks, gravel or rock dust by means of pressure crushing. Crushers can be used to for size reduction or form alternation of waste materials to make disposing, recycling or differentiating the material more easy. Impactors or impact crushers make use of impact rather than pressure to crush the material (Balasubramanian, 2017).

Crushing can be defined as the transfer of a force through a material made of molecules that have a stronger bond and are more resistant to deformation than those in the material being crushed. This force is magnified by mechanical advantage. The material keeps being crushed until the desired particle size is reached, after which the material can leave the crusher.

During impact crushing the crushed material is captured by a fast rotating rotor and smashed against an impact plate. This process repeats until the particles are small enough to pass through the gap between the rotor and impact plate. Impact crushers are mainly used as secondary crushers (Balasubramanian, 2017). There are multiple types of commonly used crushers and impactors, which are listed below.

- Jaw crushers
- Gyratory crushers
- Cone crushers

- Compound crushers
- Horizontal shaft impactors
- Vertical shaft impactors
- Mineral sizers

During the crushing process, the material can be crushed in different stages using different crushers for different particle sizes. The two types of crushers which are suitable for primary crushing of large debris are the jaw crusher and gyratory crusher, whereas the other types of crushers are used in later stages. Figures Figure 2.20 and Figure 2.21 show which types of crushers are suitable to use in different stages based on the particle sizes (Balasubramanian, 2017).

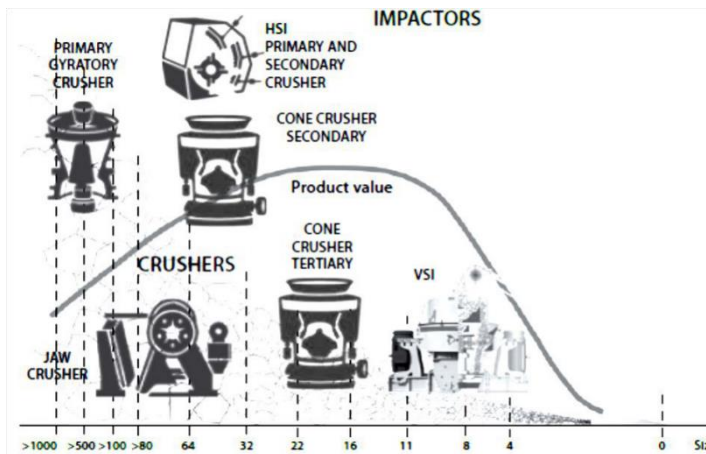


Figure 2.20: Applicable crushers based on particle size (Balasubramanian, 2017)

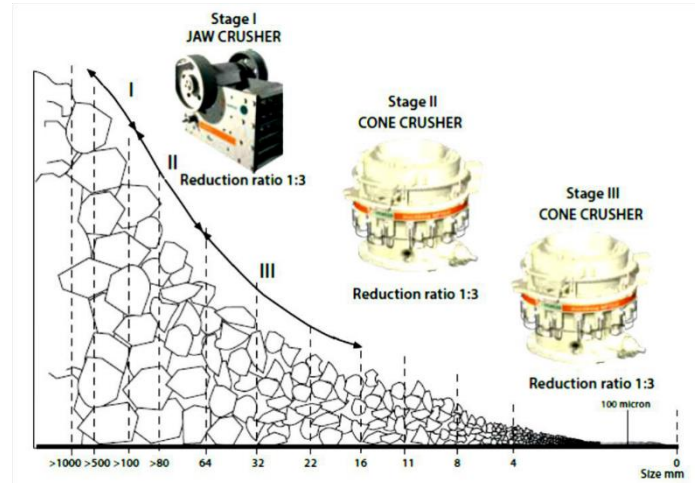


Figure 2.21: Typical three stage crushing with different equipment and their reduction ratios (Balasubramanian, 2017)

### 2.2.2.2. Innovative separation techniques

Besides the conventional crushing methods, there are the modern, more advanced separation techniques. These techniques focus on improving the quality of the recycled concrete granulate by removing the attached hardened cement. The four main separation techniques for concrete recycling in the Netherlands are Smart Liberator, C2CA, Circulair Mineraal and Mangeler (Ottel , 2022). Of main interest for this research is the Smart Liberator technique, which is the most advanced technique and it is used by the company Rutte Groep. The Smart Liberator and C2CA method will be discussed in this section.

#### Smart Liberator

Compared to the conventional crushing methods, the Smart Liberator crushes the pre-broken concrete rubble in such way that there is much less breakage. Whereas in the conventional crushing methods the debris is crushed by means of pressure crushing under high pressure forces, in the Smart Liberator the jaws move both vertically and horizontally such that the particle sized are reduced under shear forces. Due to the fact that the shear strength of concrete is much lower than the compressive strength, there is much less breakage and the process is less energy consuming compared to conventional crushing methods (Van der Wegen, 2020). Also, the Smart Liberator produces more fines than the conventional crusher and the particle size distribution of the obtained material, especially the aggregates, resembles the one of the initial concrete production materials. This indicates the separation of clean aggregates from the hardened cement paste (Florea et al., 2014). Figure 2.22 shows an indication of the Smart Liberator.

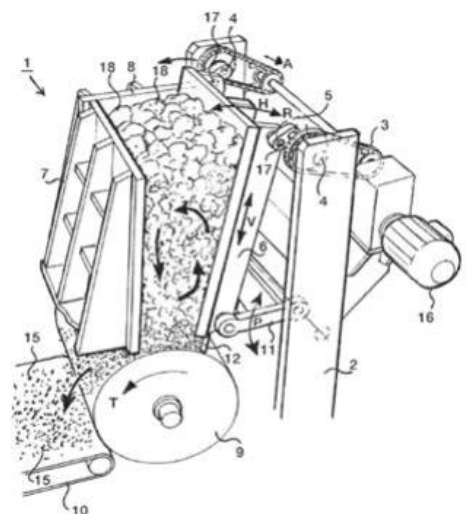







Figure 2.22: Indication of the Smart Liberator (Florea et al., 2013)

The material obtained from the Smart Liberator is separated afterwards based on particle sizes. Table 2.3 gives an overview of the obtained material from crushing concrete with the Smart Liberator of Rutte Groep together with the corresponding particle sizes, possible applications in new concrete and their product names and impressions.

**Table 2.3: Obtained material from Smart Liberator (Ottel , 2022)**

Material	Product name	Particle size [mm]	Application in new concrete	Impression
Gravel	Freegravel	> 4	Gravel	
Sand	Freesand	0.25 – 4	Sand	
Fine fraction	Freefiller C	0.08 – 0.25	Filler	
Superfine fraction	Freement	0.04 – 0.08	Cement/binder	
Ultrafine fraction	Freefiller F	0 – 0.04	Binder/activator	

**C2CA-method**

C2CA stands for ‘Concrete to Cement & Aggregate’ and originates from a spin-off from a joint venture between GBN Groep (part of Strukton) and TU Delft (Van der Wegen, 2020). In this method, the Advanced Dry Recovery (ADR) technology is used, often in combination with the Heating air and classification system (HAS). The ADR technology is a mechanical system which is used to for extraction of fines from moist crushed concrete aggregates. The system uses kinetic energy for the breakage of the water bond formed by moisture with the fine particles (Gebremariam et al., 2020). Figure 2.23 shows a schematic representation of the ADR principle.

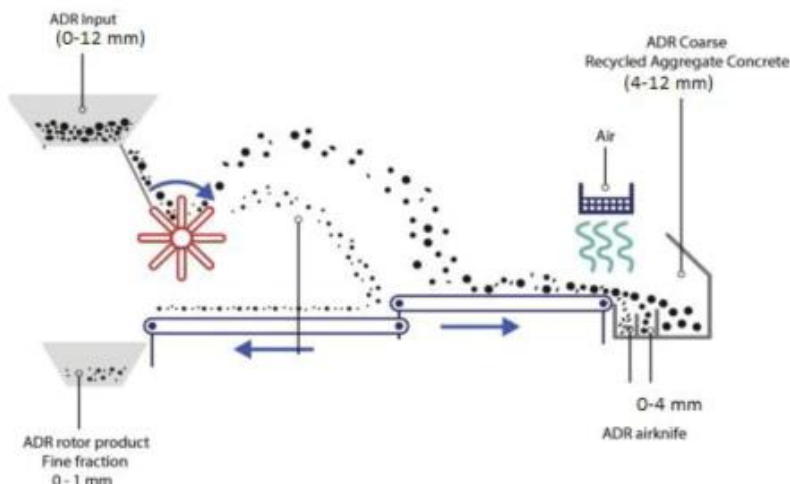


**Figure 2.23: Schematic representation ADR principle (Gebremariam et al., 2020)**

As can be seen in the figure, the input is concrete debris with a maximum particle size of 12 mm, which is separated into three fractions: 0-1 mm (rotor product), 1-4 mm (airknife product) and 4-12 mm. The fast-rotating rotor throws the particles away, which leads to the separation of the particles from each other. The small and lighter particles reach less far than the big heavier particles, which makes it possible, with help of the air sifter, to capture the different fractions separately. From these fractions, the coarse fraction (4-12 mm) is directly usable in new concrete. The fine fraction, however, must be further processed to extract the hardened cement paste from the sand before it can be used in new concrete. The ADR technology has three essential features: mobility, flexibility and affordability. The flexibility is thanks to the possibility to change certain variables, such as belt speed and air velocity, which makes the technology adaptable to different input materials. The affordability is in term of technology and refers to the energy efficiency and simplicity compared to conventional methods (Gebremariam et al., 2020).

Further processing of the fine fractions obtained with the ADR technology is usually done with the HAS. In the HAS the fine particles are exposed to a hot gas to dry the particles and get rid of possibly present undesired waste materials, such as wood and plastic. During the process, in a fluidized-type reactor, air is used to carry the heat and categorize the fine particles according to their particle size. The heat is used to dry the material and activate the ultrafine particles, which are primarily made up of hydrated cement. The main components of the HAS are the vibrator motors, burner, compressor, rotary sluice and cyclone. The burner generates hot gas up to 700 °C to dry the material. With the help of the compressor, air is drawn in, heated air from the cyclone is circulated and some air that has been saturated with vapor is blown into the atmosphere. Fine aggregates are ensured to flow downward through the staggered arrangement of tubes inside the HAS chamber using vibrators. Ultrafine particles (extracted from the feed) are separated from the air stream using a vortex separation mechanism called a cyclone. The separation zone is where the particles are classified in interaction with the air flow (Gebremariam et al., 2020). Figure 2.24 shows a sketch of the HAS.

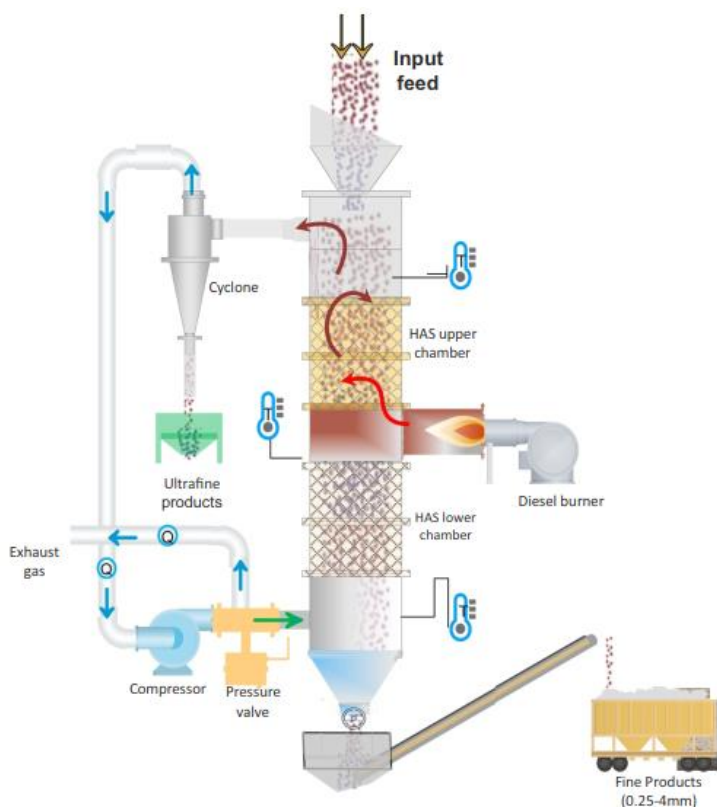


Figure 2.24: Sketch of HAS with measurement points Q (flow) and T (temperature) (Gebremariam et al., 2020)

### 2.2.3. Treatment methods

Tam et al. (2021) comprehensively reviewed almost all treatment methods for improving the quality of recycled concrete aggregate that are available in literature. Their study focused on the removal of adhered mortar from aggregate grains and its reuse. Similarly, Braymand et al. (2016) tested several treatment methods that allow complete separation and quantification of adhered mortar to determine their efficiency.

The treatment methods that are mentioned in literature can be separated into two categories: physical treatments and chemical treatments. Each of these categories consist of multiple different treatment methods. Tam et al. (2021) made a schematic diagram showing the treatment methods and reuse applications for the removed mortar from the concrete aggregates, which is shown in Figure 2.25. The treatment methods are discussed in the following sections.

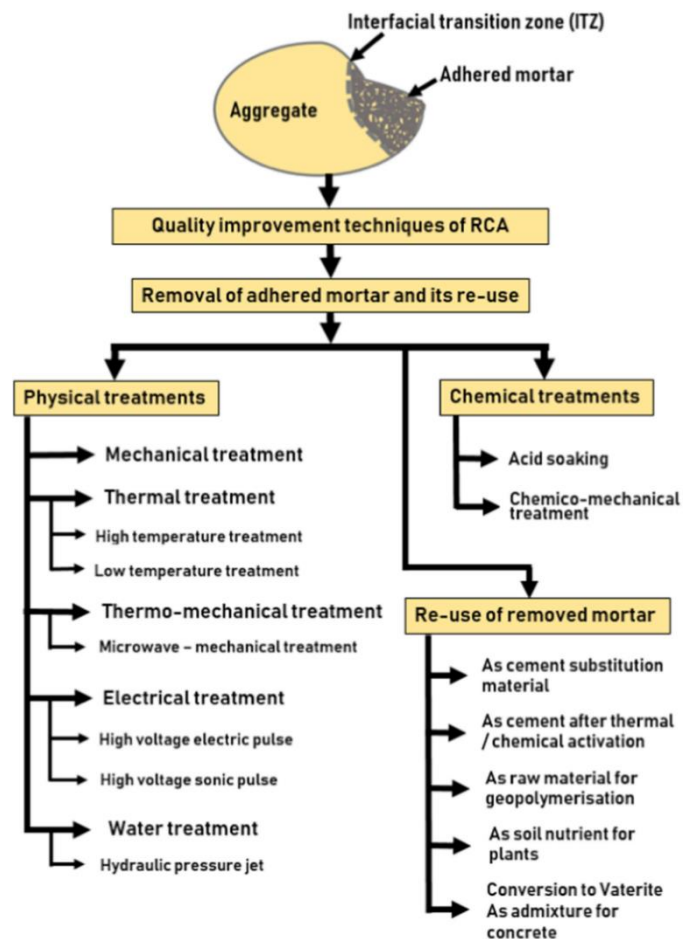


Figure 2.25: Quality improvement techniques of RCA (Tam et al., 2021)

#### 2.2.3.1. Physical treatments

Common examples of physical treatments in existing literature are mechanical treatments, thermal treatments, thermo-mechanical treatments, electrical treatments and water treatments (Tam et al., 2021). This section elaborates further on these treatment methods.

##### *Mechanical treatments*

Mechanical treatments are simple to apply and therefore they are commonly used for the improving the quality of recycled concrete aggregate (RCA). Various studies show that, with mechanical treatment, the produced secondary concrete has 25% lower strength compared to reference concrete. However, there are other studies which show that, by using high quality RCA, similar strength can be achieved (Tam et al., 2021). A drawback of applying mechanical treatments is that, during grinding, the breakage of RCA is high and micro cracks are induced, which negatively affects the strength properties. Tam et al. (2021) discuss the performance of 5 types of mechanical treatments, which are:

1. Autogenous cleaning
2. Ball/tube milling
3. Impact crushing
4. Eccentric shaft rotor
5. Screw abrading mill

During autogenous cleaning, RCA are added to a revolving mill drum with a diameter of 30 cm and a depth of 50 cm. The mill is up to 33% full of raw RCAs and rotated at 60 rotations per minute for varying time periods. After 10 or 15 minutes of rotating, the attached dust and impurities are removed with water. It was found that the water absorption capacity of the RCA progressively decreased with increasing duration of cleaning. After



28 days, an increase in compressive strength of 8% compared to uncleaned RCA was observed, while after 60 days an improvement of about 17% was observed. Compared to reference concrete, the compressive strength of the cleaned recycled aggregate concrete after 60 days was 8.9% lower (Pepe et al., 2014).

Ball/tube milling involves the usage of a ball or tube mill to effectively remove adhered mortar from RCA grains in a size range of 5-40 mm. This method is relatively cheap compared to other treatment methods. In a ball mill, steel balls are present against which the RCA grains are scrubbed to improve their quality and shape. Afterwards, high quality RCA is obtained which usually meets required specifications. However, ball milling can easily cause damage to the aggregate grains due to collision and attrition actions, which may induce micro cracks. Therefore, care should be taken when using this method (Tam et al., 2021).

During impact crushing, the attached mortar to RCAs is stripped by an impact roller in combination with wind pressure in a closed metallic structure. The adjustable wind pressure is generated by a fan, which is installed in a knife type supply device with variable directions. An air suction devices is used to capture the fine particles and dust that are released during the process (Tam et al., 2021).

In an eccentric shaft rotor, high quality RCA is obtained by removing the attached mortar by friction, compression, attrition, grinding and attrition. During this process the concrete rubble is inserted from the top and passes through between an inner and outer cylinder. The inner cylinder has an adjustable rotation speed. The grinding by compression and tumbled action from interaction of the cylinders with the aggregates and the aggregates with each other, cause removal of the adhered mortar from the aggregates. A second pass through the equipment may further improve the quality of the RCAs (Tam et al. 2021).

In a screw abrading mill, two cones in a cylindrical housing abrade and scrub the RCAs to improve their quality. The fine particles that are produced are collected in a discharge chute. This process may be repeated multiple times to obtain higher quality aggregates (Tam et al., 2021).

#### *Thermal treatments*

During thermal treatments the recycled concrete aggregates are exposed to high or low temperatures. Thermal treatments under high temperatures are based on heating the RCAs at temperatures of 300 °C and above. These high temperatures cause thermal stresses which lead to expansion of the RCAs and the attached mortar. Furthermore, at high temperatures, the attached mortar dehydrates. As a result, the mortar can detach easily. The efficiency of this type of thermal treatment can be improved by soaking the RCAs in water before heating them, due to higher vapor pressure. However, when the aggregates are exposed to temperatures higher than 500 °C, their properties may degrade due to micro cracks caused by the internal thermal stresses and phase transformation of minerals within the aggregates. Another way of improving the removal rates of the attached mortar is to immediately dip the treated aggregates in cold water, due to expansion and induced tension in the mortar (Tam et al., 2021).

Thermal treatments under low temperatures are based on the effect of freeze-thaw cycles on chemical or water soaked RCAs. Abbas et al. (2007) applied this treatment to remove residual mortar from RCAs. Their approach was based on inducing thermal and chemical stresses by using freeze thaw cycles and exposing the RCAs to a sodium sulphate solution. During the process, the attached residual mortar disintegrates due to the induced stresses. It was concluded that this method efficiently removes the attached residual mortar from the RCAs. However, with a duration of seven days, the overall procedure is time consuming.

#### *Thermal-mechanical treatments*

Tam et al. (2021) and Braymand et al. (2016) discuss the 'hybrid' thermal-mechanical treatments, which are based on a combination of thermal treatments, hot or cold, and mechanical post-treatments. Due to the primary thermal treatment of the RCAs, thermal stresses are generated which weaken the bonds between the attached mortar and aggregates. This makes it easy to remove the attached mortar in a mechanical post-treatment. Braymand et al. (2016) concluded that thermal-mechanical treatments are the most efficient, provided that the process is sequenced step by step.

### *Electrical treatments*

Electrical treatments are based on crushing concrete rubble with high electric pulse discharge (HVPD). Tam et al. (2021) distinguishes two types of electrical treatments: high voltage electric pulse and high voltage sonic pulse. In the high voltage electric pulse treatment shockwaves are induced by controllable high voltage electrical energy to concrete under water. These shockwaves create tensile stresses which result in removal of the attached mortar and breakage of concrete pieces into smaller pieces. Better results can be obtained by discharging more pulses. About 50 pulses are needed for effectively removing the attached mortar. This treatment is considered as a highly energy efficient and green technology. This is due to the fact that it does not create any noise and it is free of dust and/or harmful gases, which are common in other mechanical treatments.

In high voltage sonic pulse treatments, high frequency sonic waves generate stresses to the concrete rubble which result in separation of the attached mortar from the RCAs. During this process the aggregates are not damaged. Furthermore, the removal efficiency is much higher than with conventional mechanical treatments and depends on the aggregate sizes. For coarse aggregates (<24 mm) the removal efficiency is higher (70%) than for fine aggregates (<4 mm, 40%).

### *Water treatment*

The water treatment is based on high hydraulic pressure which erodes and damages the concrete by removing adhered mortar from aggregates (Tam et al., 2015). There are four main mechanisms that lead to erosion of the concrete: air bubble formation in high pressure liquids, shock waves generation due to symmetric bubbles implosion, micro-jets formation due to non-symmetric bubble implosion and micro-jets formation due to shock induced bubble collapse. During the implosion and collapse of cavitation bubbles, typically pressures of multiple hundred MPa are generated and stresses reach values in the order of multiple GPa. These pressure pulses lead to fracture of the concrete and removal of adhered mortar from aggregates. Usually, the erosion starts from the interfacial transition zone (ITZ). The ITZ is the weakest zone in concrete and has a low density and a low surface energy, which is at least one order of magnitude lower than that of the attached mortar and aggregates. Therefore, water treatment can be used for neat separation of mortar and aggregates.

### 2.2.3.2. **Chemical treatments**

The two types of chemical treatments that are discussed by Tam et al. (2015) are acid soaking and chemico-mechanical (hybrid) treatment. Another promising treatment is carbonation of the retrieved fines. Šavija and Luković (2016) reviewed the state of the art of the carbonation of cement paste.

#### *Acid soaking*

This treatment is based on dissolving the reaction products of cement mortar in an acid solution. Its efficiency to remove adhered mortar from RCA is dependent on several factors, such as the nature of the aggregates, the mortar porosity, the type and molar concentration of the acid solution and the treatment conditions. Tam et al. (2015) mention the three most effective acid solutions for this type of treatment, which are hydrochloric acid (HCl), acetic acid (C<sub>2</sub>H<sub>4</sub>O<sub>2</sub>) and sulfuric acid (H<sub>2</sub>SO<sub>4</sub>). From these treatments, the acetic acid treatment is considered as the cleanest, cheapest and safest. Moreover, the waste slurry produced by acetic acid treatment can be transformed into Vaterite, which is a polymorph of CaCO<sub>3</sub>, by using CO<sub>2</sub> sequestration. Vaterite can be added to concrete mixtures to increase the durability and strength. The other acids HCl and H<sub>2</sub>SO<sub>4</sub> may affect the durability of the produced recycled concrete due to possible increase of sulfate and chloride content of the recycled aggregates.

#### *Chemico-mechanical treatment*

In this treatment, the RCAs are subjected to mechanical treatment after being soaked in acid. It has similar advantages and disadvantages as 'ordinary' acid treatment. However, it has an extra advantage that the after grinding leads to higher removal ratios. An additional drawback is that it is a time consuming process.

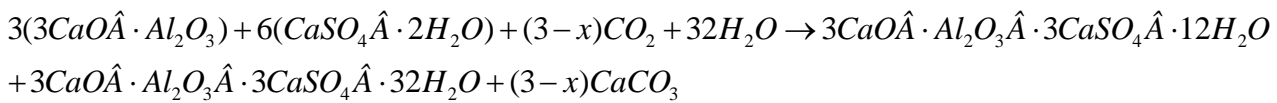
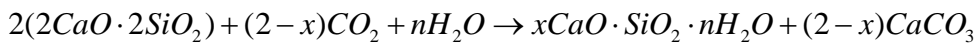
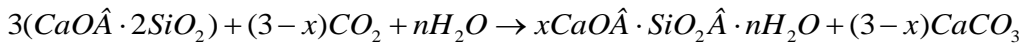
#### *Carbonation*

This treatment is based on the reaction of carbon dioxide from the atmosphere with hydrated cement in the presence of moisture, which affects both the cement microstructure and durability of (reinforced) concrete (Šavija & Luković, 2016). During their literature study, Šavija and Luković (2016) found that carbonation can be used as an active technology for the improvement of cementitious materials. It can for example be used to achieve high strength and improve the durability of cementitious materials. Furthermore, it shows promising

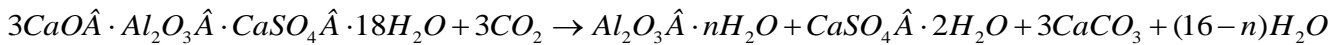
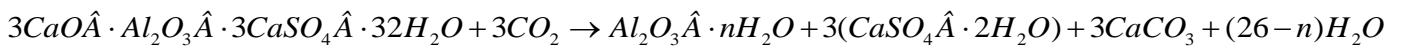
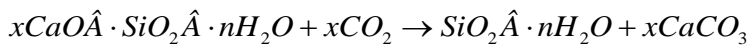
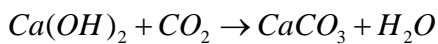
results in concrete recycling: it can be used to improve the adhered mortar on recycled aggregates and it makes reuse of waste hydrated cement paste possible. Carbonation can be achieved through dry or aqueous carbonation and its efficiency depends on the several conditions such as relative humidity, temperature, CO<sub>2</sub> concentration and carbonation duration ((Li & Wu, 2022), (Teune et al., 2023), (Xu, et al., 2022)).

Li et al. (2022) outlined the chemical reactions that take place during the carbonation of recycled concrete fines. During carbonation the CO<sub>2</sub> reacts with Portland clinker and its hydration products, forming a dense microstructure of C-S-H with CaCO<sub>3</sub> and Si-gel (Li et al., 2022). The carbonation equations are presented below:

- **Carbonation of Portland clinker:**



- **Carbonation of C<sub>3</sub>S, β-C<sub>2</sub>S, C<sub>3</sub>A and C<sub>4</sub>AF hydration compounds:**



It is expected that the recycled concrete fines contain hydrated cement paste, which is why the outlined reactions are also assumed as applicable for the carbonation of RCF.

Lu et al. (2018) investigated the effects of carbonation of hardened cement paste on the hydration and microstructure of Portland cement. In their research Portland cement pastes with a w/c ratio of 0.4 were prepared and compared to cement pastes in which the Portland cement was replaced by 10% to 30% with uncarbonated and carbonated cement paste powder. They found that replacement of cement by uncarbonated cement paste powder from 10% to 30% led to a decrement of the compressive strength at all ages, while the replacement of cement by carbonated cement paste powder from 10% to 20% increased the early compressive strength (after 1 and 7 days) and maintained the later compressive strength (after 28 and 90 days). Replacing 30% of the cement by carbonated cement paste powder decreased the compressive strength at all ages. Furthermore, the replacement of cement by 20% with carbonated cement paste powder decreased the porosity, while the cement paste with 20% uncarbonated cement paste powder had a higher porosity compared to Portland cement. Similar findings are done in the studies of Qin et al. (2019), Mehdizadeh et al. (2020) and Mehdizadeh et al. (2021). Another study of Mehdizadeh et al. (2022) showed that it is even possible to replace cement up to 30% with waste hydrated cement paste without losing strength. In their study they used two types of waste cement paste, one consisting of 50% fly ash and the other consisting of 50% blast furnace slag.

The reactivity of recycled hydrated cement paste is stimulated by the carbonation treatment, which results in the improvement of the mechanical strength of cement paste that contains recycled hardened cement paste. This improvement is due to the presence of CaCO<sub>3</sub> and Si-gel, which provide multiple additional sites for the nucleation and growth of calcium-silicate-hydrate. This process significantly speeds up the primary Portland cement hydration, thereby improving the mechanical strength (Li et al., 2018). Si-gel is highly reactive in the

presence of Portlandite. During the reaction of Si-gel with Portlandite, C-S-H gel is formed. Other recent studies that confirmed the pozzolanic reactivity of the formed Si-gel are the studies of Mao et al. (2024) and Zajac et al. (2024).

Moreover, the high  $\text{CaCO}_3$  content, which was about 55% in the carbonated recycled hardened cement paste, promotes the formation of dense calcium aluminate monocarbonate. This compound effectively inhibits the transformation of ettringite (Aft) to monosulfate (Afm) and increases the solid volume of Aft, which is beneficial for the early development of compressive strength in concrete. Finally, the filler effect of calcium carbonate and Si-gel in carbonated recycled hardened cement paste reduces the porosity of the concrete, contributing to an overall increase in mechanical strength (Li et al., 2022). These properties make that carbonated RCF show great potential to be used as a supplementary cementitious material.

#### 2.2.4. Implementation routes for recycled concrete fines

There are several implementation routes possible for the reuse of the retrieved fine fractions to lower the  $\text{CO}_2$ -emissions, as can be seen in Figure 2.25. Tam et al. (2021) performed a literature review on the applications of residual mortar powder. In the investigated studies, the presence of un-hydrated cement, calcium hydroxide  $\text{Ca}(\text{OH})_2$ , di-calcium silicates ( $\text{C}_2\text{S}$ ) and calcium carbonate  $\text{CaCO}_3$  have been validated in the powder fractions. These components have the ability, after activation, to hydrate and produce cement hydration products. The following five possible applications are discussed by Tam et al. (2021):

- As partial cement substitution/inert filler (type I addition)
- As cementitious material (type II addition)
- As a raw material for geopolymerization
- As soil nutrient fertilizer
- As admixture for improving concrete durability

Other possible applications are:

- As a raw material for clinker production
- As a raw material for blended cements
- As an activator for blast furnace slag or fly ash
- As a new binder

##### *As partial cement substitution (type I addition)*

It was concluded that thermally activated (at 800 °C) residual mortar powder is able to partially replace cement in concrete within the range 10%-20%, without significant loss of compressive strength ((Uygunoğlu, 2011), (Florea et al., 2014)). Also, mortar that was ground and passed through a 80  $\mu\text{m}$  sieve, was found to be a practical substitute for limestone filler in cement. With this solution the quarrying of limestone and the carbon footprint of cement can be reduced (Oksri-Nelfia et al., 2016).

In another study a similar grinding and sieving approach was used, which resulted in decreased calcium hydroxide content and an increased porosity of the mortars (Bordy et al., 2017). After comparison of different substitution percentages of residual mortar in cement paste, Topič et al. (2017) found that below 33% substitution the strength properties barely changed and were comparable to the reference samples. However, another study showed decreasing strength properties at all substitution ratios, but 20% substitution seemed the best option at which the flexural strength increased with 21% and the compressive strength decreased by 25.7% (Topič et al., 2017). Kalinowska-Wichrowska et al. (2020) found that the optimum temperature for maximum thermal activation of the mortar powder was 650 °C. The mortars made with 25% substitution ratio showed higher compressive strength compared to the reference sample after 28 days of curing.

Ruminy (2022) performed an experimental research in which the performance of primary materials and recycled concrete fines as fillers in mortar were compared to each other. Two types of RCF were distinguished: RCF obtained with traditional recycling methods and RCF obtained with the Smart Liberator technology. The particle size range of the used fillers was 0-250  $\mu\text{m}$  and the cement replacement percentage was 25% for all samples. Mass replacement and volume replacement were both considered, resulting in two outcomes. It was found that the samples with the Smart Liberator RCF generally performed better than the specimens with traditional RCF. Also, the samples in which the cement was replaced by volume performed

better than the samples in which the cement was replaced by mass. This can be explained by the greater amount of Portland Cement due to the higher density compared to RCF. The results show that the Smart Liberator samples with volume replacement meet the requirements set by both EN 197-1 and BRL 1804, while the samples with mass replacement and the samples with traditional RCF did not meet any of the mentioned standards.

#### *As cementitious material (type II addition)*

Shui et al. (2009) studied the cementitious characteristics and rehydration capability of dehydrated cement paste with thermal treatment under temperatures varying from 300 °C to 900 °C. It was concluded that the reactivity depends on the activation temperature and that the water demand for consistency has a linear relationship with the activation temperature, while maximum compressive strength was reached at an activation temperature of 800 °C. Ma et al. (2009) found that after thermal treatment at 750 °C, the mortar which consisted of only dehydrated cement paste, had a compressive strength and flexural strength of respectively 12.3 MPa and 3.5 MPa and a water requirement of 60%. These values implied that the dehydrated cement was reactive. Their study also showed that the substitution of Portland cement by 60% with dehydrated cement paste led to flexural and compressive strengths of 65% and 60% compared to the reference value.

#### *As raw material for geopolymerization*

Payá et al. (2012) concluded that it is possible to activate hydrated-carbonated cement by alkali-solutions to cause geopolymerization of alumina and silica gels in the carbonated material. The carbonation of the material took place for seven days in an atmosphere containing 95% CO<sub>2</sub>. A 3-day curing time at 20 °C and 65 °C resulted in compressive strengths of respectively 6.31 MPa and 14.11 MPa and the flexural strengths were respectively 1.34 MPa and 0.78 MPa. The results have shown that alkali-activation is a promising method for reusing the cementitious fractions from construction and demolition waste.

Ahmari et al. (2012) investigated the effects of different compositions and concentrations of alkaline solutions and ground waste concrete fines on the compressive strength of the produced geopolymer material by substitution of the fines with class F fly ash. They found that 50% was the optimum ground waste concrete content at 5 and 10 M NaOH and sodium silicate to sodium hydroxide (NaOH) ratios of 1 and 2. The measured compressive strengths were 26 MPa and 34.5 MPa.

Using similar mixing ratios of ground waste concrete to fly ash as Ahmari et al. (2021) with 10 M, 14 M and 18 M NaOH and a sodium silicate to NaOH ratio of 1.5, Chen et al. (2018) found that with 75% substitution, the compressive strength was 37.5 MPa after initial curing at 50 °C for 24 hours and further curing in open atmosphere.

An alternative study was carried out by Gong et al. (2014). The production of geopolymer using a 70/30 mixing ratio of residual mortar powder and slag powder while keeping a sodium silicate/NaOH ratio of 1.4. For 3- and 28-day curing, the specimens treated at 20 °C had compressive strengths of respectively 18.4 MPa and 45.4 MPa and flexural strengths of 4.4 MPa and 7.5 MPa.

#### *As soil nutrient fertilizer*

Mejía et al. (2016) dissolved the Ca<sup>+</sup> and Si that were present in the residual mortar powder by using citric acid of 0.04 M, 0.05 M and 0.055 M concentrations. For efficient dissolution of the mortar powder, the pH value of the acid was maintained at 2.2. Figure 2.26 shows the relationship between the dissolved percentages of Ca and Si and the dissolution time. The mixture was stirred at 110 rpm for 48 hours at a temperature of 28 °C. The retrieved leachate with a higher concentration of dissolved Ca and Si could functionate as fertilizer to provide nutrients for plants.

#### *As admixture for improving concrete durability*

Chen et al. (2017) removed residual cement mortar from recycled concrete aggregates (RCAs) with an acetic acid treatment. Their study did not only demonstrate that the acetic acid treatment leads to improvement of the properties of the RCAs, but also vaterite can be produced from the waste solution of the treatment and simultaneously CO<sub>2</sub> can be permanently stored in the vaterite. Vaterite is a useful, value-adding product that can be used in concrete mixtures to mitigate autogenous shrinkage. The produced vaterite had a higher water absorption (80% of the oven-dry weight) than traditional lightweight aggregates (5%-40%), which suggests that the vaterite can function as a water reservoir in internal curing and less vaterite is needed to have the effect as traditional curing agents. Therefore, by using vaterite as a curing agent, the potential harm caused by internal curing agents on the mechanical properties and durability of the concrete can be reduced. An

unique advantage of using vaterite as an internal curing agent is that it can also function as a binder in the concrete, due to its transformation into calcite after releasing water through the dissolving-recrystallization process. In this way the vaterite may contribute to improving the mechanical strength of the concrete and possibly other superior properties which are not yet explored (Chen, et al., 2017).

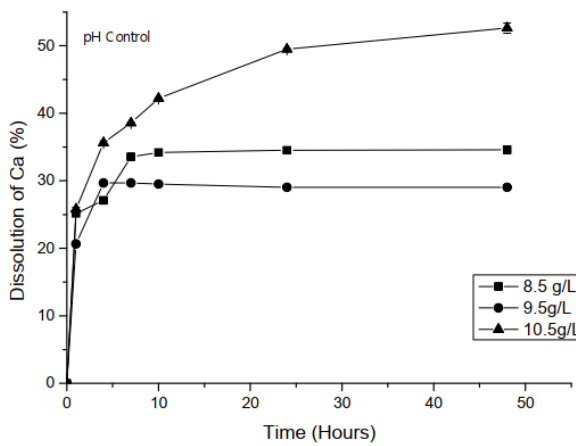


**Figure 2.26a: Dissolution of calcium from residual concrete with controlled pH (Mejía et al., 2016)**

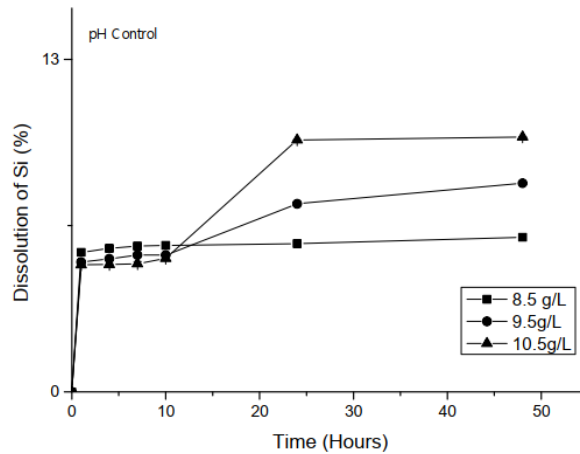


**Figure 2.26b: Dissolution of silicon from residual concrete with controlled pH (Mejía et al., 2016)**

#### *As a raw material for clinker production*

Schoon et al. (2015) studied the potential of using recycled concrete fines as an alternative raw material in Portland cement clinker production. They found that recycled fines can successfully replace traditional materials without significantly affecting the final mineral composition of the clinker. The study showed that these recycled fines could substitute regular raw materials, especially silica sources (SiO<sub>2</sub>), and even limestone, by increasing their calcium oxide (CaO) content. This substitution would reduce the need for burned limestone, helping to lower CO<sub>2</sub> emissions (Van der Wegen, 2020).

#### *As a raw material for blended cements*

Van der Wegen (2020) mentions the possible implementation of the retrieved fines as a raw material for blended cements, whether or not after full carbonation. The retrieved fines could replace the components in cements that are becoming more and more scarce, such as pulverized coal fly ash.

#### *As an activator for blast furnace slag or fly ash*

Blast furnace slag and fly ash are typically activated by Portland cement. However, also other materials can be used as an activator, such as gypsum and alkalis (Song et al., 2000). Since the recycled concrete fines may contain any of these materials, it can possibly be used as an activator. This has the great advantage that no primary materials are used and concrete waste can be effectively reused.

#### *As a new binder*

Theoretically, hydrated cement can be dehydrated and then rehydrated, allowing recycled concrete fines to act as a new binder. Many studies have explored the potential to create secondary cementitious binders from recycled materials. Wang et al. (2018), Alberda van Ekenstein (2020), and Zhutovsky et al. (2021) all used thermal treatments to investigate the dehydration and rehydration of cement. While these studies have not yet led to practical applications, their results remain promising.

## 2.3. Life Cycle Assessment

### 2.3.1. Overview

Life Cycle Assessment (LCA) is a systematic method that is used to evaluate the environmental impacts of a product during all stages of its life. From raw material extraction through production, use stage, and disposal. By examining the entire lifecycle, LCA provides a comprehensive view of the environmental aspects and potential impacts, offering valuable insights for improving sustainability and reducing negative environmental effects. LCA can be used to calculate the environmental costs or shadow costs of a product. However, this calculation is considered by the ISO 14040 standard as an optional element (Jonkers, 2021).

In an era where sustainability is getting more and more important, LCA plays a crucial role in guiding decisions across various sectors, including manufacturing, construction, and energy. It helps companies, policymakers, and researchers to identify areas where environmental impacts can be minimized, supports the development of more sustainable products, and provides a basis for environmental labeling and certification (Jonkers, 2021).

### 2.3.2. Objectives of LCA

LCA can be used for several objectives. Some of the primary objectives of LCA are quantification of environmental impacts, identification of highest impact spots, comparative analysis and support of sustainable development (Jonkers, 2021).

Quantification of environmental impacts includes the measurements of environmental burdens of products and/or processes. This includes energy consumption, resource depletion and emissions. Quantification of the environmental impacts of products and/or processes is essential for the assessment of their sustainability (Jonkers, 2021).

Identification of the stages and/or components that are causing the highest environmental burden enables targeted improvement. It also shows which stages and/or components need to be prioritized for improvements. Comparative analysis includes the comparison of the environmental impact of different products, processes, or scenarios in order to identify the most sustainable option. The outcomes can be used for decision-making. Support of sustainable development includes research and designing of products and/or processes with minimum environmental impact in order to support sustainable development (Jonkers, 2021).

### 2.3.3. Methodology of LCA

Conducting an LCA involves four main phases, as outlined by ISO 14040 and ISO 14044 standards.

The first phase of an LCA is the goal and scope definition, which establishes the context and boundaries of the study. Key elements of this phase include an objective to define the purpose of the LCA, a functional unit that serves as a reference to which inputs and outputs are normalized, system boundaries to determine which life cycle stages and processes are included in the LCA, and stating the assumptions and limitations of the study to provide context for the interpretation of the results. Definition of the cut-off criteria is also part of the definition of the system boundaries, since not all involved processes and materials are contributing significantly to the final product. Usually, materials which contribute less than 2-5% in weight to the final product are left out of the LCA (Jonkers, 2021).

The second phase is the Life Cycle Inventory (LCI). During this phase, any relevant data on inputs and outputs for each process within the system boundaries is collected and reported. Data collection is necessary for quantification of the environmental impact of each product or process, which is also part of the LCI phase. It is important to ensure the quality and representativeness of the data (Jonkers, 2021).

The third phase is the Life Cycle Impact Assessment (LCIA). In this phase, the potential environmental impacts are evaluated using various impact categories. The two main steps of this phase are the selection of relevant environmental impact categories and classification and characterization of inventory data. Life cycle inventory data that is collected in the second phase must be assigned to the chosen impact categories and converted to environmental impacts. In the Netherlands, the Dutch building regulations lists 11 basic impact categories that must be included in the LCA List of 11 basic environmental impact categories according to Dutch 'Bouwbesluit-2012 bepalingsmethode' (Jonkers, 2021). Table 2.4 gives an overview of these impact categories together with their abbreviations, specific unit equivalent, and shadow costs per unit equivalent.

**Table 2.4: List of 11 basic environmental impact categories according to Dutch ‘Bouwbesluit-2012 bepalingsmethode’ (Jonkers, 2021)**

Impact category	Abbreviation	Unit equivalent (UE)	Shadow costs per UE in Euros
Abiotic depletion non-fuel	ADP-non fuel	kg Antimone	0,16
Abiotic depletion fuel	ADP-fuel	kg Antimone (4,18E-4 kg Antimone/MJ)	0,16
Global warming	GWP100	kg CO <sub>2</sub>	0,05
Ozone layer depletion	ODP	kg CFC-11	30
Photochemical oxidation	POCP	kg Ethene	2
Acidification	AP	kg SO <sub>2</sub>	4
Eutrophication	EP	kg PO <sub>4</sub> <sup>3-</sup>	9
Human toxicity	HTP	kg 1,4-dichloro benzene	0,09
Fresh water aquatic ecotoxicity	FAETP	kg 1,4-dichloro benzene	0,03
Marine aquatic ecotoxicity	MAETP	kg 1,4-dichloro benzene	0,0001
Terrestrial ecotoxicity	TETP	kg 1,4-dichloro benzene	0,06

The fourth phase is the interpretation phase. This final phase involves analyzing the results to draw conclusions and provide recommendations. Although it is mentioned as the final phase, interpretation is done during all phases. Each phase requires interpretation of the data and all inputs and outputs, which is also why ISO 14040 connects interpretation to each phase. Interpretation includes identification of significant issues, hotspots and trends. Interpretation is also needed to assess the robustness of the results, which is an important part of drawing conclusions and providing recommendations (Jonkers, 2021).

Figure 2.27 illustrates the relationship between the four main phases of an LCA as outlined by ISO 14040.

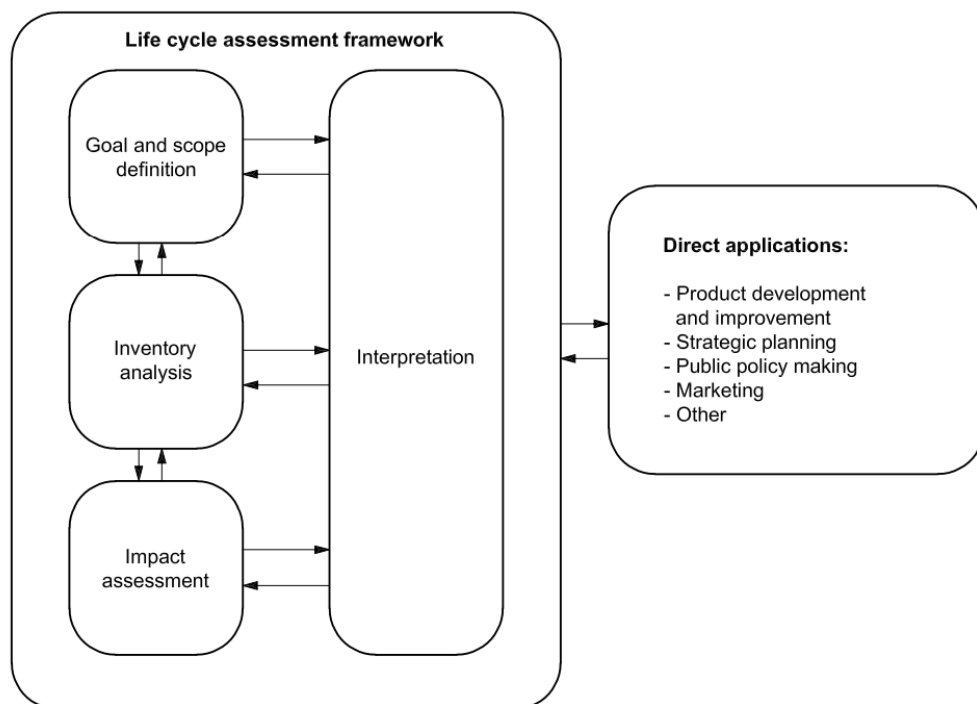


**Figure 2.27: Relationship between the phases of an LCA (NEN-EN-ISO 14040, 2006)**



## **Tools and resources**

The Life Cycle Inventory (LCI) table, which lists all required materials and processes in the second step of the LCA procedure, can contain up to thousands of data depending on the product that is being studied. This makes that manual processing of all these data is time consuming. That is why specialized programs have been developed to support LCA practitioners. Those programs target specific products for different applications. Examples of such programs that are being used in the construction sector in the Netherlands are (Jonkers, 2021):

- MRPI Free Tool
- GPR Buildings
- DGBC-Breeam Materials tool
- DuboCalc

The mentioned programs make use of environmental databases containing LCI data for many raw materials, (half)products, (prefab) elements and (transport) processes which are typically used in the construction sector. The LCI information for items found in environmental databases comes from the products' independently examined LCA-based Environmental Product Declarations (EPDs).

## **Applications of LCA**

LCA can be applied in various fields to achieve different goals, such as product and design development to inform eco-design and sustainable product development. LCA can also be applied in policy making to support regulations and standards aimed at reducing environmental impacts, corporate sustainability to guide corporate strategies for sustainability and reporting and to create public awareness about the environmental impacts of products and services (Jonkers, 2021).

## **Conclusion**

LCA is an important tool for understanding and improving the environmental performance of products, processes, and services. By providing a detailed and holistic view of environmental impacts, LCA helps to drive sustainability across industries and supports the transition to more sustainable practices and products. As global environmental challenges intensify, the importance of LCA in fostering sustainable development and reducing ecological footprints cannot be overstated (Jonkers, 2021).

# 3. Materials and methods

The focus of this research lies in assessing the performance of recycled concrete fines when used to make new cement mortar. This chapter outlines all the materials that are used during the research as well as procedures that have been followed for upcycling the recycled concrete fines and testing the specimens.

## 3.1. Materials

For this research different types of primary cement were used as reference material to evaluate the performance of the RCF. Mortar prisms made with CEM I, CEM II/B-V, and CEM III/B are used as reference samples. All cements are prepared with Portland cement with strength class 52.5 R. Table 3.1 gives an overview of the compositions of the used reference cements during this research. All reference materials are provided by the Stevin Lab of the TU Delft.

**Table 3.1: Reference cements compositions**

Cement type	Main constituents [%]		
	Clinker	Blast furnace slag	Fly ash
CEM I	100	-	-
CEM II/B-V	70	-	30
CEM III/B	30	70	-

Next to the reference cements, RCF provided by the company Rutte Groep are used to prepare mortar prisms in which the Portland cement is partially to fully replaced by the RCF starting from 50% in steps of 25%. The used RCF go by the product name 'Freement fine' and are obtained by means of the Smart Liberator method. According to the product specifications the fines have a particle size range of 0-63 µm and are therefore expected to contain most of the cement. The used RCF, which originate from buildings on the Haarlemmerweg, are expected to be a BFS containing cement based on documentation from Rutte Groep. Since it is most likely that most of the RCF consist of hydrated cement particles, different upcycling methods are applied to it in order to enhance the performance of the material. However, the untreated material is also tested to be able to assess the effects of the treatments. The applied treatments are further grinding, heating, flash calcination and carbonation. In the sample names, the treatments are abbreviated as respectively GR, HE, FC, and CAR.

For most of the flash calcination tests, a second type of RCF was used because the original RCF from Haarlemmerweg had run out. The new RCF was a mixture of CEM I and CEM III origin, mixed by hand in a 1:1 ratio. The downside of using different types of RCF is that their material characteristics vary, which could affect the strength development of the samples. This makes it harder to make reliable comparisons between the results.

The mortar prisms are prepared following the procedure outlined in NEN-EN 196-1. Table 3.2 shows the sample compositions along with their names. Note that the table only lists the names of the untreated samples. For the treated samples, the corresponding abbreviations are added to the sample names. The numbers 1, 2, and 3 in the sample names represent the cement type being compared, while the numbers 50, 75, and 100 indicate the percentage of Portland cement that is replaced compared to the reference samples.

**Table 3.2: Names and descriptions of the reference cements and untreated samples**

Sample	Description
REF1	Mortar made from 100% CEM I (100% Portland cement 52.5 R)
REF2	Mortar made from 100% CEM II/B-V (30% fly ash, 70% Portland cement 52.5 R)
REF3	Mortar made from 100% CEM III/B (70% BFS, 30% Portland cement 52.5 R)
SC1-100	Mortar made from 100% Smart Liberator fines
SC2-100	Mortar made from 30% fly ash and 70% Smart Liberator fines by mass
SC3-100	Mortar made from 70% BFS and 30% Smart Liberator fines by mass
SC1-75	Mortar made from 25% Portland cement 52.5 R and 75% Smart Liberator fines by mass
SC2-75	Mortar made from 30% fly ash, 17.5% Portland cement 52.5 R and 52.5% Smart Liberator fines by mass

SC3-75	Mortar made from 70% BFS, 7.5% Portland cement 52.5 R and 22.5% Smart Liberator fines by mass
SC1-50	Mortar made from 50% Portland cement 52.5 R and 50% Smart Liberator fines by mass
SC2-50	Mortar made from 30% fly ash, 35% Portland cement 52.5 R and 35% Smart Liberator fines by mass
SC3-50	Mortar made from 70% BFS, 15% Portland cement 52.5 R and 15% Smart Liberator fines by mass

To evaluate the effect of the RCF on the strength of the samples, three additional samples are tested, where the RCF is replaced by limestone (abbreviated as LS). Limestone is considered an inert filler and should not have a significant impact on the mortar's strength. Table 3.3 shows the names and compositions of these samples.

**Table 3.3: Names and descriptions of the limestone samples**

Sample	Description
CEM1-LS-50	Mortar made from 50% Portland cement 52.5 R and 50% limestone by mass
CEM2-LS-50	Mortar made from 30% fly ash, 35% Portland cement 52.5 R and 35% limestone by mass
CEM3-LS-50	Mortar made from 70% BFS, 15% Portland cement 52.5 R and 15% limestone by mass

### 3.2. Treatment methods

The following four treatments are applied to try to enhance the performance of the RCF:

1. Further grinding below 32  $\mu\text{m}$
2. Heating up to 900  $^{\circ}\text{C}$
3. Carbonation
4. Flash calcination up to 700-800  $^{\circ}\text{C}$

The next sections will further elaborate on the followed procedures for the treatments and testing and the equipment used throughout the process.

#### 3.2.1. Further grinding

The RCF that are used for this research are assumed to contain hydrated cement particles. However, the particles might still have unhydrated cores. In order to expose the unhydrated cores of the cement particles, the RCF are further ground by means of a ball mill. The aim was to grind the RCF until the particle size range reduced from 0-63  $\mu\text{m}$  to 0-32  $\mu\text{m}$ . For this treatment the Retsch Planetary Ball Mill PM 100 shown in Figure 3.1: Retsch Planetary Ball Mill PM 100 is used.



**Figure 3.1: Retsch Planetary Ball Mill PM 100**



**Figure 3.2: EyeTech Particle size and shape analyzer**

The RCF were ground by means of dry grinding with zirconium oxide balls with a diameter of 10 mm. The total grinding time that was needed to achieve the desired particle size range of 0-32  $\mu\text{m}$  was 40 minutes, which was determined by trial and error. Assessment of the grinding effectiveness was done with the EyeTech

particle size and shape analyzer from the Microlab at the TU Delft, which is shown in Figure 3.2: EyeTech Particle size and shape analyzer. Figure 3.3 show the particle size distributions of the RCF before and after grinding. Table 3.4 shows the characteristic particle sizes at the cumulative percentage values 10%, 50% and 90%. The corresponding values are called  $D_{10}$ ,  $D_{50}$  and  $D_{90}$ , respectively. They mean that 10%, 50% and 90% of the fractions consists of particles that have a lower size than the corresponding diameters. The measurements show that the  $D_{90}$  of the RCF reduced from 86.40  $\mu\text{m}$  to 30.45  $\mu\text{m}$  after 40 minutes of dry grinding.

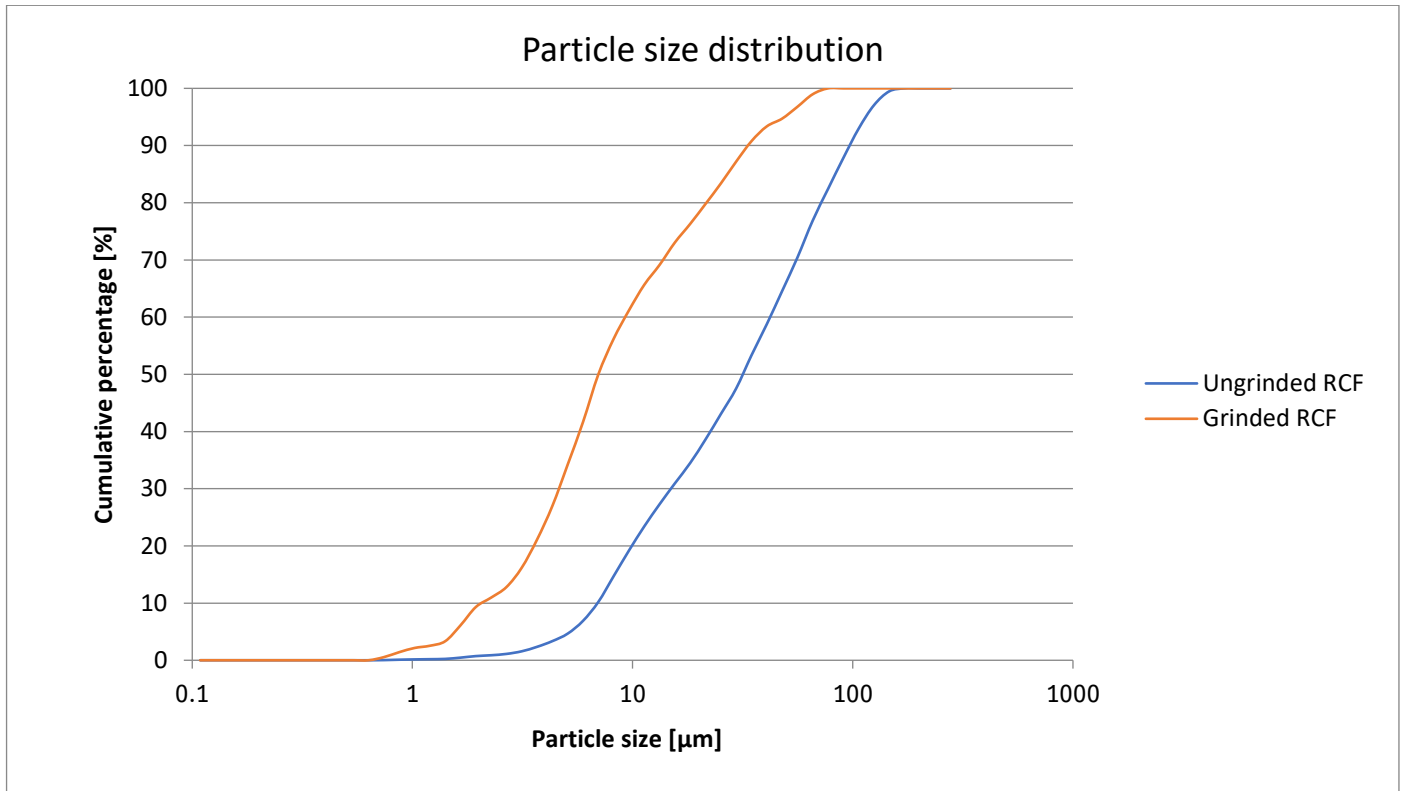


Figure 3.3: Particle size distribution before and after grinding

Table 3.4: Particle size distribution characteristic  $D_{10}$ ,  $D_{50}$  and  $D_{90}$  values of the RCF

Fraction	$D_{10}$ [ $\mu\text{m}$ ]	$D_{50}$ [ $\mu\text{m}$ ]	$D_{90}$ [ $\mu\text{m}$ ]
Unground RCF	6.30	29.14	86.40
Ground RCF	2.04	6.56	30.45

### 3.2.2. Heating

The heating process was carried out using a Carbolite Chamber furnace, capable of temperatures ranging from room temperature to 1000°C, located at the Stevin Lab of TU Delft. The recycled concrete fines (RCF) were heated from room temperature to 900°C and held at that temperature for 30 minutes before being cooled back to room temperature. During the cooling process the RCF stayed in the furnace. The choice of 900°C for heating was based on the study by Verweij (2020), which discusses the effects of heating temperature on hardened cement. Table 3.5 shows the expected conversions as function of temperature. The exact time the samples stayed at 900 °C in the furnace was determined through trial and error.

To find the optimal heating time, the samples were heated for different durations: 30, 60 and 90 minutes. After each heating period, the weight loss was measured to determine when the samples reached full dehydration. The results showed that all heating times caused a weight loss between 20.1% and 20.5%, leading to the conclusion that 30 minutes was sufficient for full dehydration. The mass losses for the different heating times are listed in Table 3.5.

**Table 3.5: Reactions at different temperature ranges (Verweij, 2020)**

Temperature range [°C]	Reaction
0-100	Hydration of unhydrated cement
0-120	Evaporation of free/pore water
200-400	Dehydration of CSH-gel to calcium silicate
400-500	Dehydration of portlandite to calcium oxide (quicklime)
500-600	Carbonation of portlandite to calcite, fast reaction
700-800	Decarbonation of calcite to lime
500-800	Formation of belite
800-900	Formation of alite

**Table 3.6: Mass losses**

Heating duration	Mass loss [%]
30 min	20.49
60 min	20.32
90 min	20.12

In order to not overload the furnace, two target setpoints were used during the heating process of the samples. The first target setpoint was 800 °C which was reached with a heating rate of 10 °C/min. The furnace was then kept at 800 °C for five minutes before heating it up again to 900 °C with a heating rate of 5 °C/min. The samples were placed in a porcelain bowl which was loaded with 517.3 grams of RCF at a time and the furnace had only enough space for one bowl at a time. The samples were cooled down in the oven to room temperature and were stored in plastic zip bags until they were needed for other tests.

### 3.2.3. Carbonation

The carbonation treatment of the RCF was carried out by Rutte Groep. The RCF were exposed to a high concentration of CO<sub>2</sub> for 12 hours at a pressure of about 2 bars. The internal temperature of the carbonation chamber was not measured. Since the chamber was located in a large hall outside and the test took place in winter, the surrounding temperature is assumed to be around 10 °C based on the mean temperatures during that period. However, this is uncertain as the exact temperature was not reported.

It is assumed that carbonation leads to the formation of a reactive silica-gel in the RCF. An additional environmental benefit is that CO<sub>2</sub> is captured by the fines during the process. To measure the amount of CO<sub>2</sub> captured, a thermogravimetric analysis (TGA) was performed on both the untreated and carbonated RCF.

### 3.2.4. Flash calcination

The flash calcination of the RCF was performed using the Flash Calciner from Rutte Groep. This machine rapidly heats and cools small amounts of material. The process starts by heating the machine to the desired temperature. For this research, the temperature was set to the maximum allowed temperature of 800 °C, which corresponds to a maximum core temperature of 700 to 750 °C.

Once the machine is sufficiently heated, the material is pushed in using a rotating screw, which pushes small amounts of material into the heated section of the machine. The material is then exposed to a very high temperature before being quickly cooled back to room temperature as it exits the machine. Inside the Flash Calciner, the material moves within an airflow. The airflow is generated by two blowers, which remain on throughout the entire heating and cooling process.

Flash calcination differs from heating in a regular furnace, where the material is slowly heated and cooled without any movement.

### 3.2.5. Thermogravimetric Analysis and Differential Scanning Calorimetry

Thermogravimetric analyses are conducted on the different samples in order to gain insight into the mass losses that occur during the heating process. This is useful for obtaining information about certain chemical reactions that occur and the outcomes can be compared to existing literature. Also, by analysing the mass losses at different temperatures the presence of certain compounds can be determined. Differential Scanning Calorimetry (DSC) measurements are done at the same time as the TGA by means of a NETZSCH STA 449 F3 Jupiter. The measurements are done under an argon atmosphere and the temperature interval was set to 40 – 1000 °C at a heating rate of 10 K/min. Alumina crucibles are used to put the samples in and to take into account the influence of an empty crucible on the measurements, the first measurement was done with an empty crucible and the results were used as a correction for the results of the other measurements.

In existing literature several characteristic temperature intervals are mentioned at which certain reactions take place in cement paste. An overview of the temperature ranges and the corresponding reactions that take place in the cement paste is given in Table 3.7. In general, the mass losses up to 600 °C are related to the loss of water and above 600 °C to CO<sub>2</sub> release (Scrivener et al., 2016).

**Table 3.7: Characteristic temperature intervals with corresponding reactions (Alarcon-Ruiz et al., 2005)**

Temperature interval [°C]	Reaction
30 – 105	Evaporable water and part of bound water escape. In general, it is considered that all evaporable water has escaped at 120 °C (Noumowe, 1995).
110 – 170	Loss of water from part of carboaluminate hydrates and decomposition of gypsum and ettringite
180 – 300	Loss of bound water from the decomposition of C-S-H and carboaluminate hydrates
450 – 550	Dehydroxylation of portlandite
700 – 900	Decarbonation of calcium carbonate

### 3.3. Flexural and compressive strength tests

The European standard NEN-EN 196-1 describes the testing method for determining the compressive and, optionally, the flexural strength of cement mortar. For those tests, a set of three prismatic test specimens of 40 mm × 40 mm × 160 mm in size are prepared. The strength tests were carried out when the specimens reached an age of 28 days ( $\pm$  8 hours).

The mortar specimens are prepared according to NEN-EN 196-1, which specifies the composition and mixing procedure of the mortar. The mortar consists of the three ingredients cement, sand and water. The ingredients are mixed in the following proportions:

- 1 part cement
- 3 parts CEN Standard sand
- ½ part water (water/cement ratio 0.50)

The mortar is prepared in batches for three test specimens. Table 3.8 specifies the amounts of the ingredients of each batch for the reference samples and the samples that contain untreated RCF. The mix design is similar for the samples that contain treated RCF. However, in the mix design of the samples that contain thermally treated RCF an amount of 3.83 grams of the superplasticizer CUGLA HR con. 35% SPL is added. This amount corresponds to the maximum allowed dose of 0.85 wt. % compared to the weight of the cement.

The mortar is mixed using the HOBART N50 mixer from the Stevin Lab at the TU Delft. The mixing and moulding of the mortar is done by the procedure as described in NEN-EN 196-1. After demoulding the prisms they were stored in the curing room of the Stevin Lab at a relative humidity of at least 95% until they reached the age of 28 days at which the strength tests were performed.

**Table 3.8: Mortar mix designs for reference cements and replacement ratio's 100%, 75% and 50% to prepare three test samples**

Specimen	Cement (g)	Fly ash (g)	BFS (g)	SC fines (g)	Sand (g)	Water (g)
REF1	450	0	0	0	1350	225
REF2	315	135	0	0	1350	225
REF3	135	0	315	0	1350	225
SC1-100	0	0	0	450	1350	225
SC2-100	0	135	0	315	1350	225
SC3-100	0	0	315	135	1350	225
SC1-75	112.5	0	0	337.5	1350	225
SC2-75	78.75	135	0	236.25	1350	225
SC3-75	33.75	0	315	101.25	1350	225
SC1-50	225	0	0	225	1350	225
SC2-50	157.5	135	0	157.5	1350	225
SC3-50	67.5	0	315	67.5	1350	225

flexural strength of the specimens is determined by the three-point loading test with one of the types of apparatus mentioned in section 4.7 of NEN-EN 196-1. During this test, the mortar prism is placed in the apparatus with one side face on the supporting rollers with its longitudinal axis normal to the supports. The load is applied vertically by means of the loading roller to the opposite side face of the prism and increased smoothly at the rate of  $50 \pm 10$  N/s until fracture. The flexural strength of the individual specimens is then calculated with the following formula:

$$R_f = \frac{1.5 \times F_f \times l}{b^3}$$

where

$R_f$	=	<i>the flexural strength [MPa]</i>
$b$	=	<i>the side of the square section of the prism [mm]</i>
$F_f$	=	<i>the load applied to the middle of the prism at fracture [N]</i>
$l$	=	<i>the distance between the supports [mm]</i>

The following values of  $b$  and  $l$  apply to all calculations in this study:

$b$	=	<i>40 mm</i>
$l$	=	<i>100 mm</i>

The flexural strength is calculated as the arithmetic mean of the three individual test results, each rounded at least to the nearest 0.1 MPa. The arithmetic mean should also be rounded to the nearest 0.1 MPa. After the three point loading test, the remaining prism halves be covered with a damp cloth until they are tested in compression.

The compressive strength test is carried out on the halves of the prism broken during the three-point loading test. Each prism half is tested by loading its side faces using the equipment described in sections 4.8 and 4.9 of NEN-EN 196-1. The prism halves are centered laterally to the platens of the machine within  $\pm 0.5$  mm and longitudinally such that the end face of the prism overhangs the platens or auxiliary plates by about 10 mm. The load on the specimens is increased smoothly at the rate of  $2400 \pm 200$  N/s over the entire load application until fracture. The compressive strength of each individual half is then calculated with the following formula:

$$R_c = \frac{F_c}{1600}$$

where

$R_c$	=	<i>the compressive strength [MPa]</i>
$F_c$	=	<i>the maximum load at fracture [N]</i>
1600	=	<i>the area of the platens or auxiliary plates (40 mm x 40 mm) [mm<sup>2</sup>]</i>

### 3.4. Hypotheses

This section contains the hypotheses for the strength tests that are done with the samples.

#### 3.4.1. Samples with untreated RCF

Since the RCF probably mostly consists of cement paste which has already reacted, no reactivity is expected on beforehand without any treatment. Although it is possible that the RCF contains some unhydrated cement paste, it is not expected to be of such a significant amount that it results in measurable strengths for the prisms with a 100% replacement ratio.

The strengths of the samples with partial replacement ratios 50% and 75% are expected to have a measurable value, due to the presence of ordinary Portland cement. It is expected that the samples with a 50% replacement ratio will have higher strengths than the samples with a 75% replacement ratio due to the fact that more OPC is present at a replacement ratio of 50%.

The results that come out of the tests with these samples will function as reference for the samples that contain treated RCF. The results will be used to get insight into the effects of the treatments on the strengths of the samples. The questions that are of interest for the test results from the untreated samples is:

- *What is the strength development over 28 days in mortar prisms in which the OPC is fully replaced by untreated RCF?*
- *How does the strength development of the samples change when the replacement ratios are changed to 75% and 50%?*

#### 3.4.2. Samples with carbonated RCF

Recycled concrete fines undergo mineralization through carbonation, resulting in the acquisition of pozzolanic properties (Bruin, 2023). Consequently, it is expected that the recycled concrete fines will show a certain degree of reactivity. This reactivity can be attributed to the transformation of the recycled concrete fines during the carbonation process, leading to the development of pozzolanic properties and overall performance in concrete applications. Li et al. (2022) outlined the chemical reactions during carbonation, which show the presence of  $\text{CaCO}_3$  and Si-gel after carbonation of recycled hardened cement paste.

By carbonating the RCF, it can be investigated what the effect is of this treatment on the strength development of the samples by comparing the results with the results obtained from the tests with the untreated samples. The question that is to be answered with this treatment is as follows:

- *How does carbonation of the RCF affect the 28-day strength of the mortar prisms, compared to mortar prisms with untreated RCF?*

#### 3.4.3. Samples with further ground RCF

By further grinding of the RCF, the effect of the grinding process on the reactivity can be obtained by comparing the strength test results with the test results of the untreated fraction. It can be expected that the reactivity improves, since the grinding process results in a bigger surface area, which allows for faster and more efficient reactions. However, the RCF fraction already contain the finest possible particle sizes in the range from 0 to 63  $\mu\text{m}$ . Therefore, it can be questioned whether there is still any potential left for a significant improvement. A possible first try is to grind the RCF to 0-32  $\mu\text{m}$ . By carrying out the treatment, the following question can be answered:

- *How does further grinding the RCF to a 0-32  $\mu\text{m}$  range affect the 28-day strength of the mortar prisms, compared to mortar prisms with untreated RCF?*



#### 3.4.4. Samples with thermally treated RCF at 900 °C

The thermal treatment in a furnace at 900 °C for 30 minutes is assumed to fully dehydrate the calcium hydroxide and other hydrated cement phases. The treatment is applied in order to upcycle the RCF and regain some of the reactivity. The possible formation of alite and elite during the treatment makes this treatment promising. It is expected that the prisms with thermally treated RCF will have higher strength compared to the prisms with untreated RCF. The following question is of interest:

- *How does heating of the RCF up to 900 °C affect the 28-day strength of the mortar prisms, compared to mortar prisms with untreated RCF?*

#### 3.4.5. Samples with flash calcined RCF

By flash calcining the RCF it is of interest to investigate the possibility of obtaining a reactive material. A similar process is used during the production of Blast Furnace Slag, which must be rapidly cooled down to obtain a reactive product. Since the flash calcination is done at a high temperature between 700 and 800 °C, the RCF will also be dehydrated. It is expected that the prisms with flash calcined RCF will have higher strength compared to the samples with untreated RCF. It is of interest to answer the following question:

- *How does flash calcination of the RCF affect the 28-day strength of the mortar prisms, compared to mortar prisms with untreated RCF?*

# 4. Results

## 4.1. TGA and DSC

This part contains the results of the TGA and DSC measurements. In Table 3.7, the characteristic dehydration temperature intervals of cementitious materials are listed. Based on the literature review and the fact that only cementitious materials were tested in this study, it is expected that the mass losses mainly occur in three temperature ranges. Namely, 0 – 300 °C, 450 – 550 °C, and 700 – 900 °C (Alarcon-Ruiz et al., 2015). Furthermore, it is expected that the RCF that are heated in a furnace, as well as the RCF that are treated with the Flash Calciner show less mass loss compared to the other RCF. This is due to the fact that in the mentioned two treatments, the RCF are exposed to very high temperatures which causes that a certain amount of water is already lost during the treatments leading to less mass loss during the TG measurements.

Figures Figure 4.1 and Figure 4.2 respectively show the TG and DTG curves of the untreated and treated RCF used in this study. Abrupt mass drops in the TG curves correspond to peaks in the DTG curves. The individual graphs with a closer look can be found in Appendix D: TGA and DSC. It can be observed that in the graphs the mass losses generally occur in the same ranges and that there is a continuous mass loss over the whole range. The continuous mass loss corresponds to the dehydration of calcium silicate hydrates, calcium aluminate hydrates and other minor hydrates (Marsh & Day, 1988). The heated fines were the only sample in which almost no mass loss was observed. The total mass loss was only 0.25%. This indicates that nearly no reactions, evaporation or decomposition occurred, which means that the RCF became nearly thermally stable for temperatures up to 1000 °C after heating the material up to 900 °C and keeping it at that temperature for 30 minutes. During the thermal treatment the material already lost 20% of its mass. That mass loss together with the nearly horizontal TG curve indicates a possible full dehydration of the material.

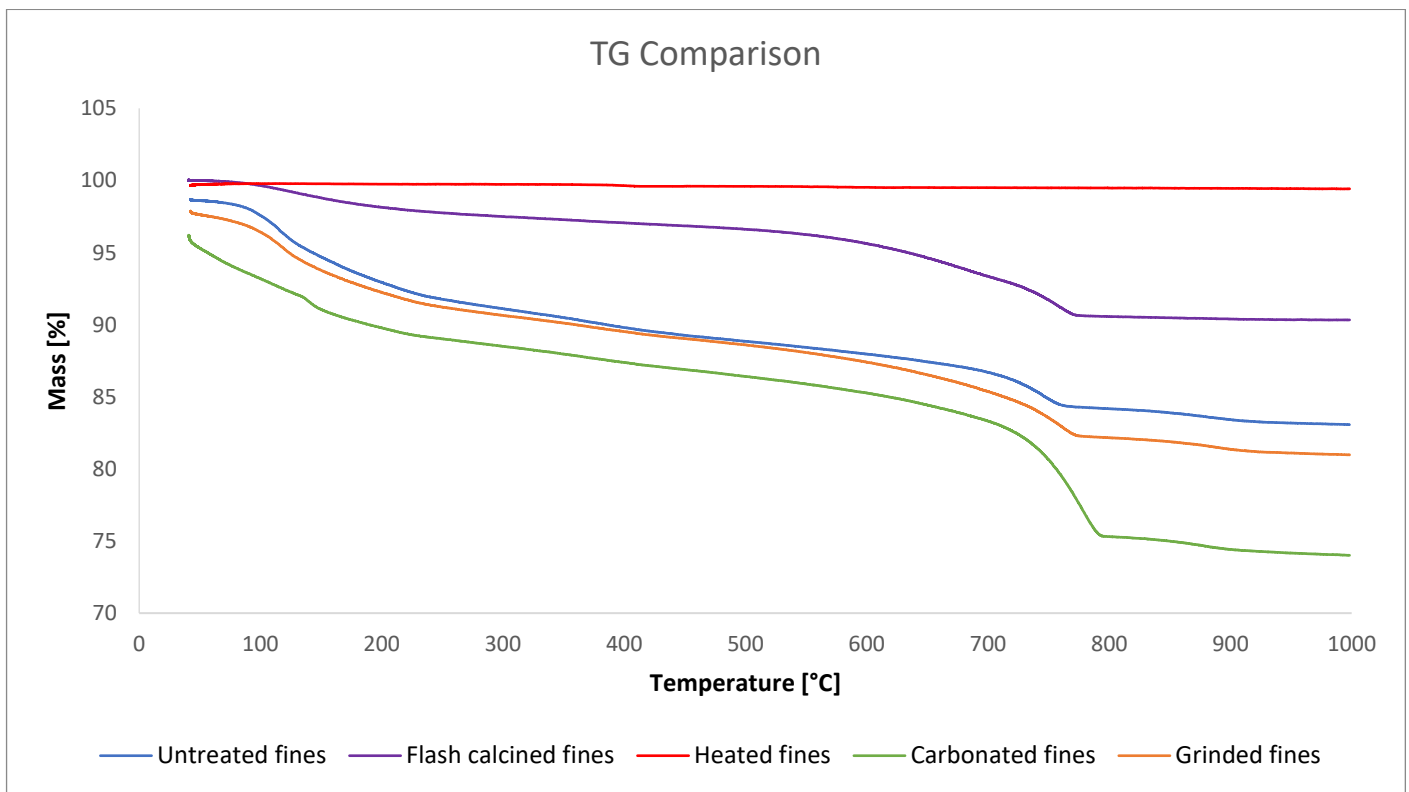
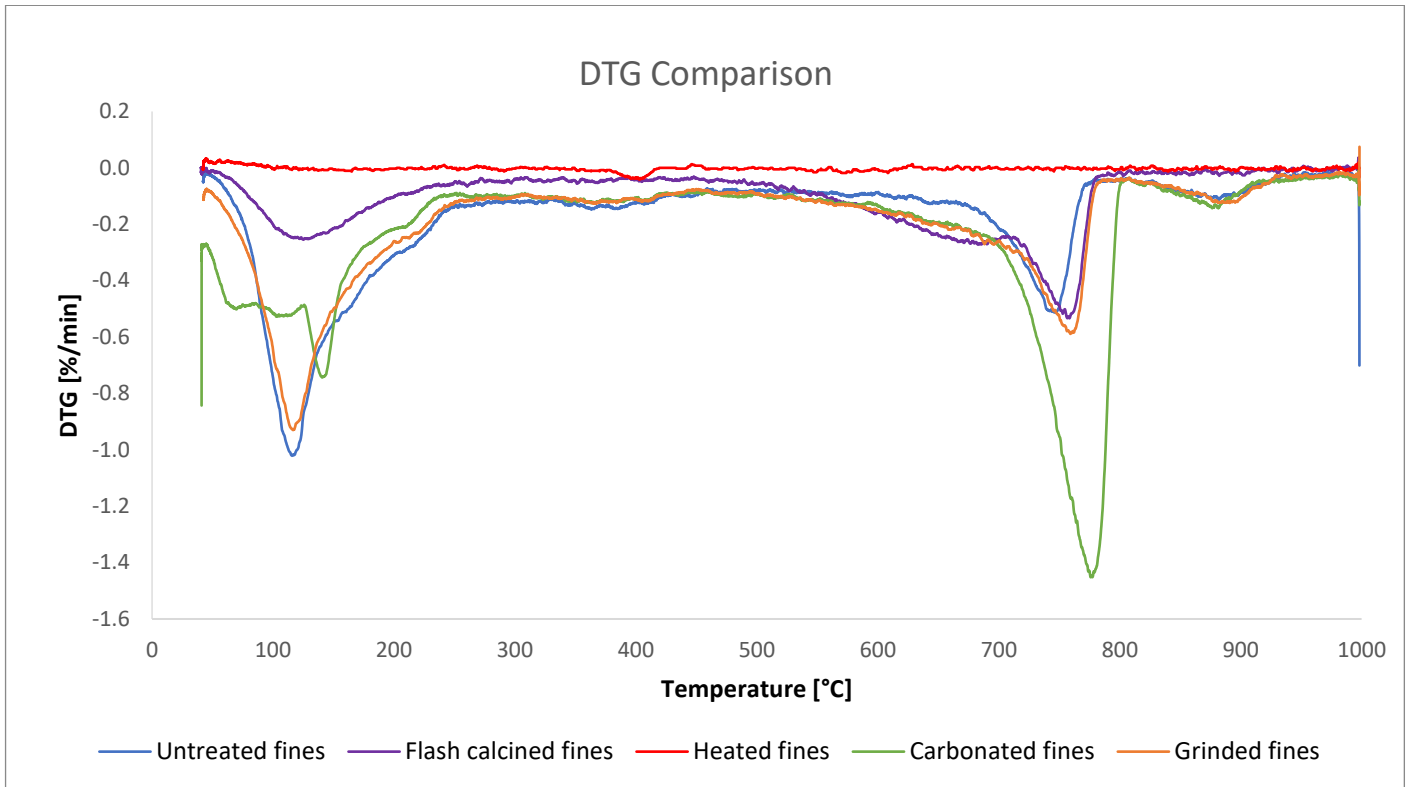


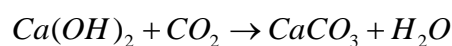
Figure 4.1: Comparison of the TG graphs of all treatments



**Figure 4.2: Comparison of the DTG graphs of all treatments**

The first abrupt drop in mass is observed between 40 – 250 °C with its peak at 115.7 °C. This mass loss corresponds to the evaporation of free water and bound water and the decomposition of gypsum and other hydration products such as ettringite, carboaluminate hydrates and C-S-H. This mass drop occurred for all samples, except for the heated fines. As for the other samples, there are differences in the amount of mass loss in the first range. The untreated, ground and carbonated RCF all had a similar mass loss of approximately 7%, while the flash calcined RCF lost about 2.5% of its mass. This can be explained by the fact that the RCF were exposed to temperatures exceeding 700 °C during the flash calcination process, which led to evaporation of part of the free and bound water, and partial or full dehydration of some previously mentioned hydration products. Also, when looking at the graph of the carbonated RCF, it is noticeable that the mass loss in this first phase is not uniform. A sudden drop occurs at around 140 °C, which can be caused by the decomposition of gypsum. Gypsum dehydrates in two steps, namely at around 100 to 140 °C to hemihydrate and at 140 – 150 °C to anhydrite (Scrivener et al., 2016). However, since this phenomenon is only observed in the carbonated sample and not in the other samples, it is most likely that it is caused by the carbonation of the RCF. Carbonation results in the formation of calcium carbonate, which affects the porosity and can form a sort of passivation layer around C-S-H (Šavija & Luković, 2016). This layer of calcium carbonate may trap water and release it at different rates, which can be the reason why the observed mass loss is not uniform. Another cause could be the decomposition of certain components that were formed during the carbonation process, such as carboaluminates (Wang, et al., 2022). Dehydration of carboaluminates generally occurs between 60 – 200 °C, with peaks at around 140 – 170 °C ((Guan, et al., 2021), (Hay & Celik, 2023)

The second drop occurs around 400 °C and corresponds to the decomposition of Portlandite, which generally happens between 400 and 500 °C (Scrivener et al., 2016). This sudden drop is absent at the carbonated RCF, which can be explained by the carbonation of Portlandite, resulting in the formation of calcium carbonate (Kudlacz et al., 2011):



The mass drop at around 400 °C is also observed at the heated fines. This could mean that there was still a minor component which was not fully decomposed during the treatment. However, it is also possible that a certain reaction took place during the storage of the heated fines.

The third mass drop starts from around 600 °C with its peak between 700 and 800 °C, which corresponds to the decomposition of calcium carbonate. A difference in mass drop between the carbonated RCF and the other samples is observed in this temperature range. While the untreated RCF lost approximately 4% of their mass, the carbonated RCF had a mass loss of around 11%. According to Pan et al. (2016) the amount of CO<sub>2</sub> within the sample corresponds to the mass loss due to the decomposition of calcium carbonate. This indicates an effective CO<sub>2</sub> uptake of around 7% during the carbonation treatment.

The flash calcined and ground RCF had a CO<sub>2</sub> content of approximately 5% and 6%, which are both higher than the untreated RCF. A possible explanation for those differences are that the RCF reacted with CO<sub>2</sub> during storage and/or during the treatment. Especially in the case of the ground fines, this is a logical explanation since the contact surface area of the fines increased during the grinding process, which also increases the reaction rate.

The TG results of the untreated, carbonated, and further ground RCF show another sudden mass drop at around 880 °C, which also corresponds to the decomposition of calcium carbonate. This indicates that the decomposition possibly happened in two steps, which might be related to different polymorphs. However, the TG graphs do not provide enough information to confirm this. Vaterite is an example of a less stable form of calcium carbonate which dissociate earlier than the more stable forms (Villain et al., 2007). It is noticeable that the flash calcined RCF only show one peak that correspond to the decomposition of calcium carbonate.

Figure 4.3 shows the results of the DSC measurements. DSC is a technique that measures the enthalpy changes related to glass transitions. Interpretation of the DSC graphs of hydrated cement is generally very difficult because different reactions occur within the same temperature range, leading to overlapping signals. For this reason, DSC measurements of hydrated cements are generally not used for quantification but rather for identification of the presence of glassy phases or certain hydrates with a characteristic heat development (Scrivener et al., 2016).

The DSC measurements correspond with the TG and DTG curves as the peaks in the DSC curves occur in the same temperature ranges as the mass drops. It can be seen that each sudden mass drop corresponds to an endothermic peak on the DSC curve.

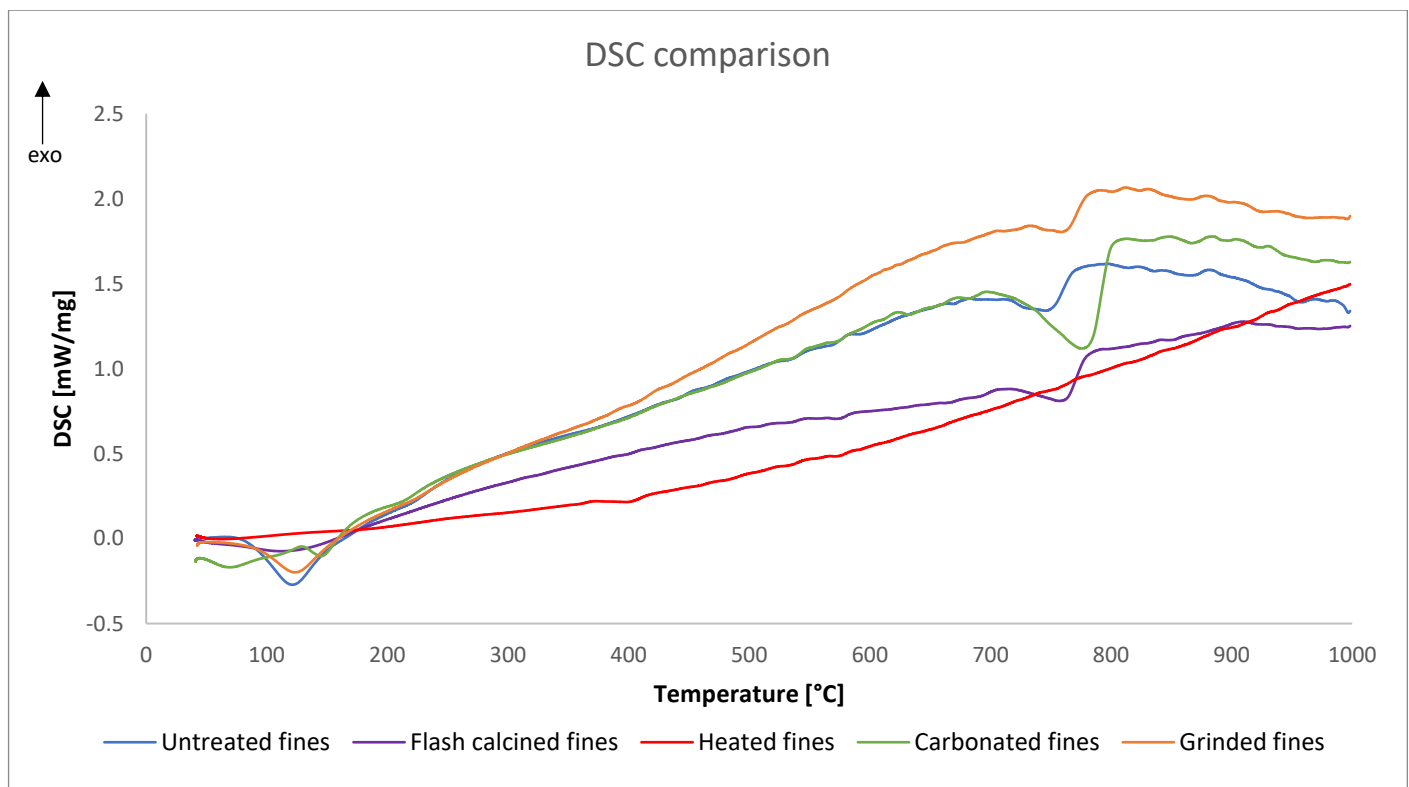


**Figure 4.3: Comparison of the DSC graphs of all treatments**

The second type of RC, which consisted of 50% RCF from CEM I origin and 50% RCF from CEM III origin, were also analyzed in order to assess any differences between the materials. Figures Figure 4.4, Figure 4.5, Figure 4.6 and Figure 4.7 show the comparisons of the TG and DTG curves of both types of RCF in the untreated and flash calcined state.

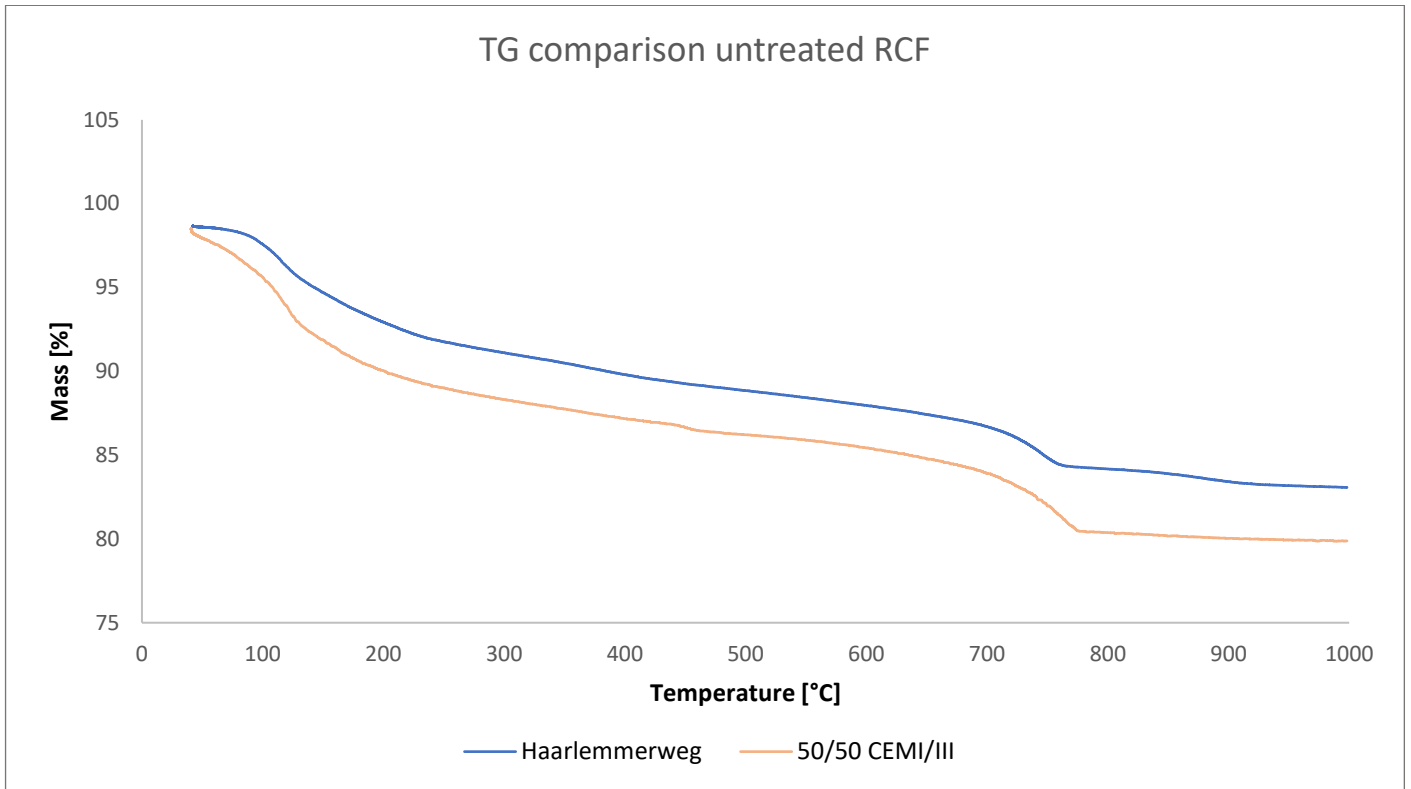


**Figure 4.4: TG comparison between the different untreated RCF types**

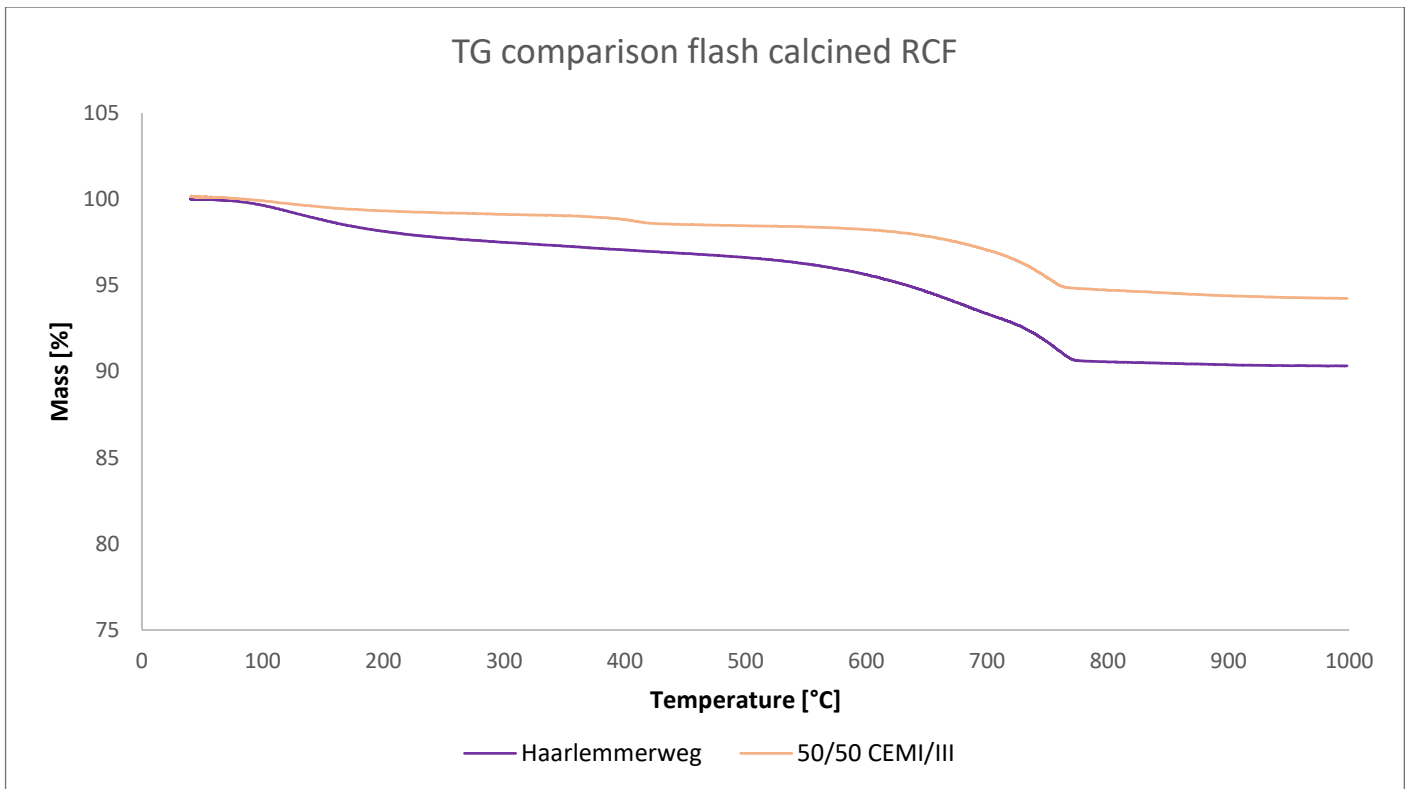


**Figure 4.5: TG comparison between the different flash calcined RCF types**

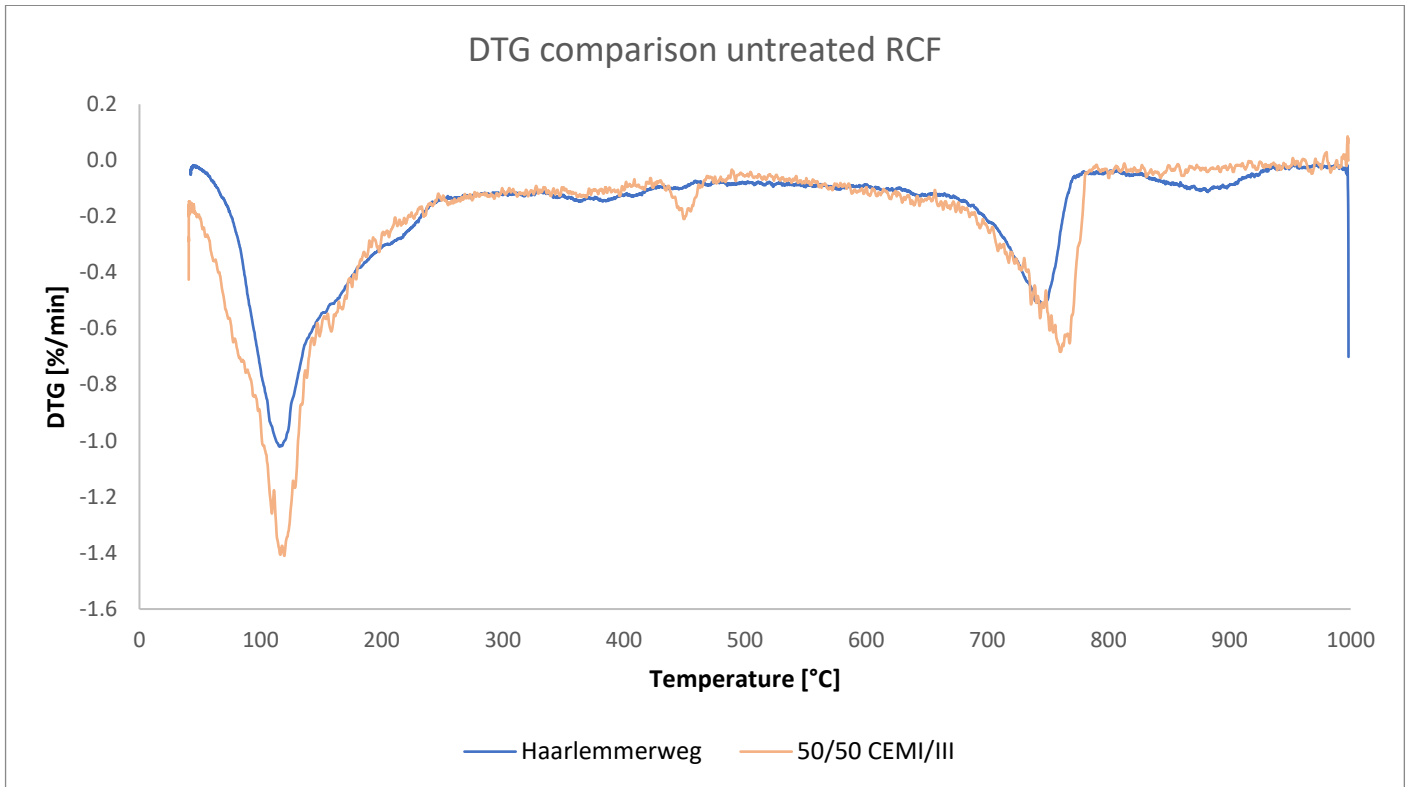


Figure 4.6: DTG comparison between the different untreated RCF types

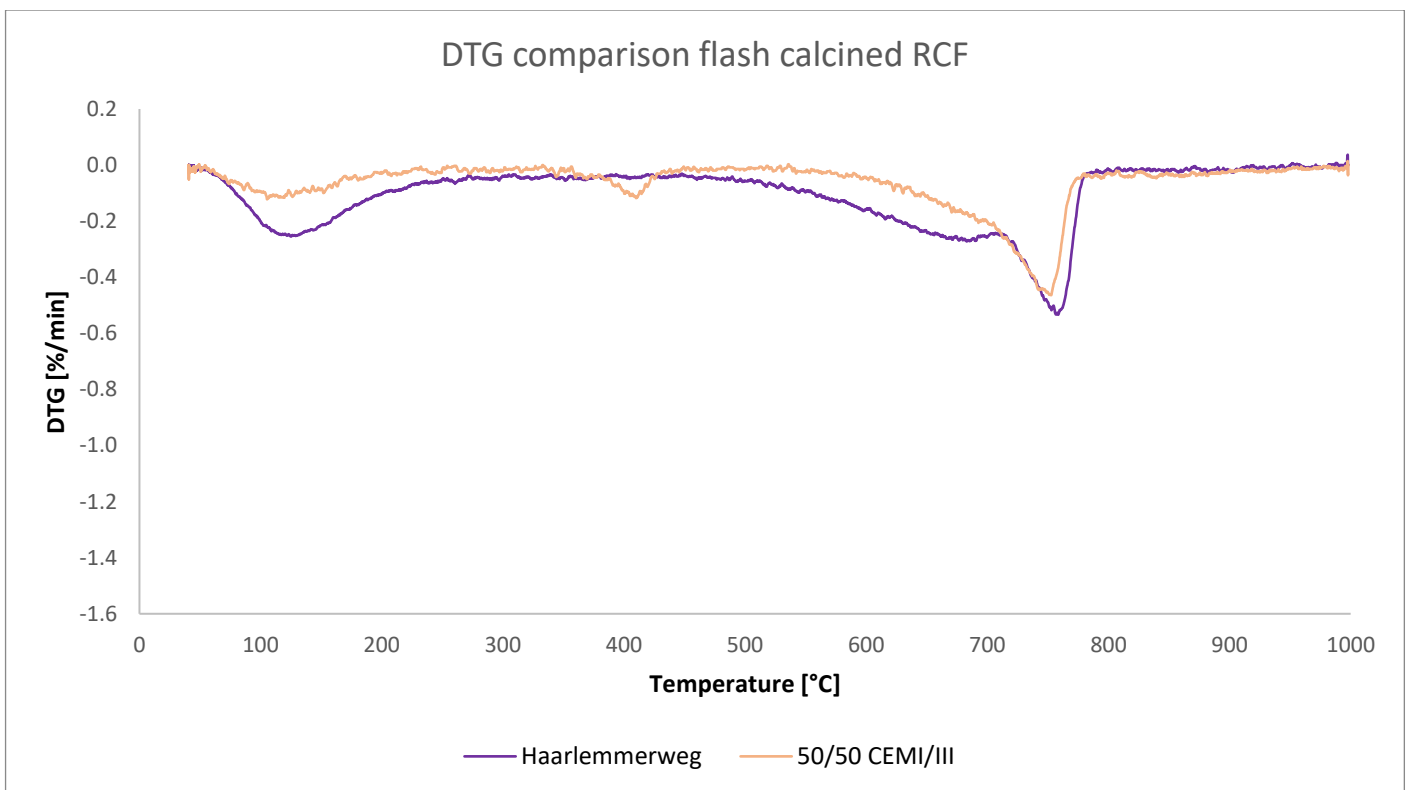


Figure 4.7: DTG comparison between the different flash calcined RCF types

The TG graphs show that the mass losses occur within the same temperature ranges for both samples, which is in line with the expected ranges reported in the literature for cementitious materials. However, notable differences are observed between the two types of RCF.

In the untreated state, the total mass loss of the 50/50 RCF is approximately 4% higher than that of the Haarlemmerweg RCF. The larger peaks in the DTG graph of the 50/50 RCF indicate a possible higher amount of free and bound water, hydration products such as CSH and portlandite and calcium carbonate. This suggests that the 50/50 RCF retained more moisture and carbonation products compared to the Haarlemmerweg RCF.

After flash calcination, the observed trend reverses as the 50/50 RCF exhibit an approximately 4% lower total mass loss than that of the Haarlemmerweg fines. The DTG peaks are generally smaller, except for the peak at around 400 °C, which corresponds to the decomposition of portlandite.

A possible explanation for the lower total mass loss of the flash calcined 50/50 RCF is the difference in storage conditions. The TG analysis of the 50/50 RCF was conducted shortly after flash calcination, while the Haarlemmerweg RCF had been stored for a longer period before testing. This additional storage time likely allowed the Haarlemmerweg RCF to absorb moisture from the air and undergo rehydration reactions, increasing their moisture content. Also, there was more time for carbonation of the RCF, which is in line with the observations in the TG graph temperature range corresponding to the decomposition of calcium carbonate. However, since the observations suggest that the 50/50 RCF originally had a higher content of hydration products and calcium carbonate, flash calcination may have resulted in a greater decomposition of these phases. This could also be a potential explanation for the lower mass loss compared to the Haarlemmerweg RCF.

## 4.2. Flexural and compressive strength tests

This section shows the results that are obtained from the flexural and compressive strength tests on the mortar prisms with the different samples used during this research. The strength tests are done according to NEN-EN 196-1. The strengths are calculated with the fracture loads  $F_f$  and  $F_c$ , which can be found in Appendix C: Strength results. The specimens in which the cement is replaced by RCF are tested in the same manner as the reference specimens to make fair comparisons possible. The replacement ratios are 50%, 75% and 100%.

### 4.2.1. Reference specimens

The reference specimens were tested to measure their flexural and compressive strengths. The strength tests were conducted according to the NEN-EN 196-1 standard and the results are listed in Table 4.1.

**Table 4.1: Flexural ( $R_f$ ) and compressive ( $R_c$ ) strengths of reference prisms [MPa]**

Sample	Mean $R_f$ [MPa]	Mean $R_c$ [MPa]
REF1	8,7	44,3
REF2	7,8	37,2
REF3	8,8	40,4

The mean compressive strengths of the reference prisms reached a maximum value of 44.3 MPa, which is lower than expected. The cement used in these prisms belongs to strength class 52.5, which means that the minimum strength should be 52.5 MPa. None of the specimens met this requirement, making the results insufficient according to NEN-EN 196-1. However, due to time constraints and the consistent preparation process, these results will still be used as a reference for the specimens containing RCF. Since the same cement was used for all specimens, the comparisons remain valid.



#### 4.2.2. Comparison of 'CEM I' variants

This section compares the strength test results of all CEM I variants. Figure 4.8 provides an overview of the average flexural strengths, while Figure 4.9 shows the average compressive strengths of the CEM I variants. The dark blue bars in the charts represent the reference sample. Additionally, Table 4.2 presents both the flexural and compressive strengths of the samples as ratios relative to the reference strengths.

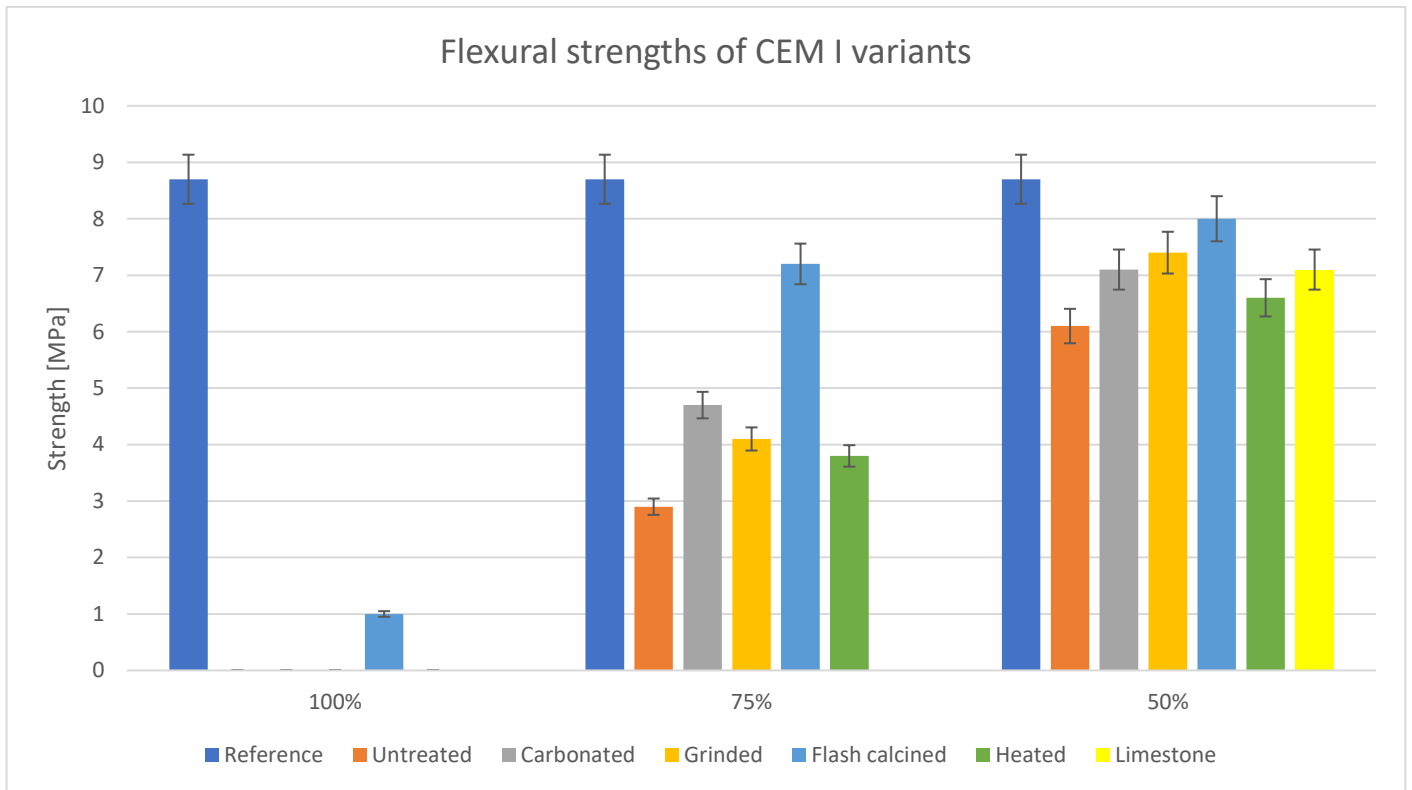


Figure 4.8: Flexural strengths of CEM I variants

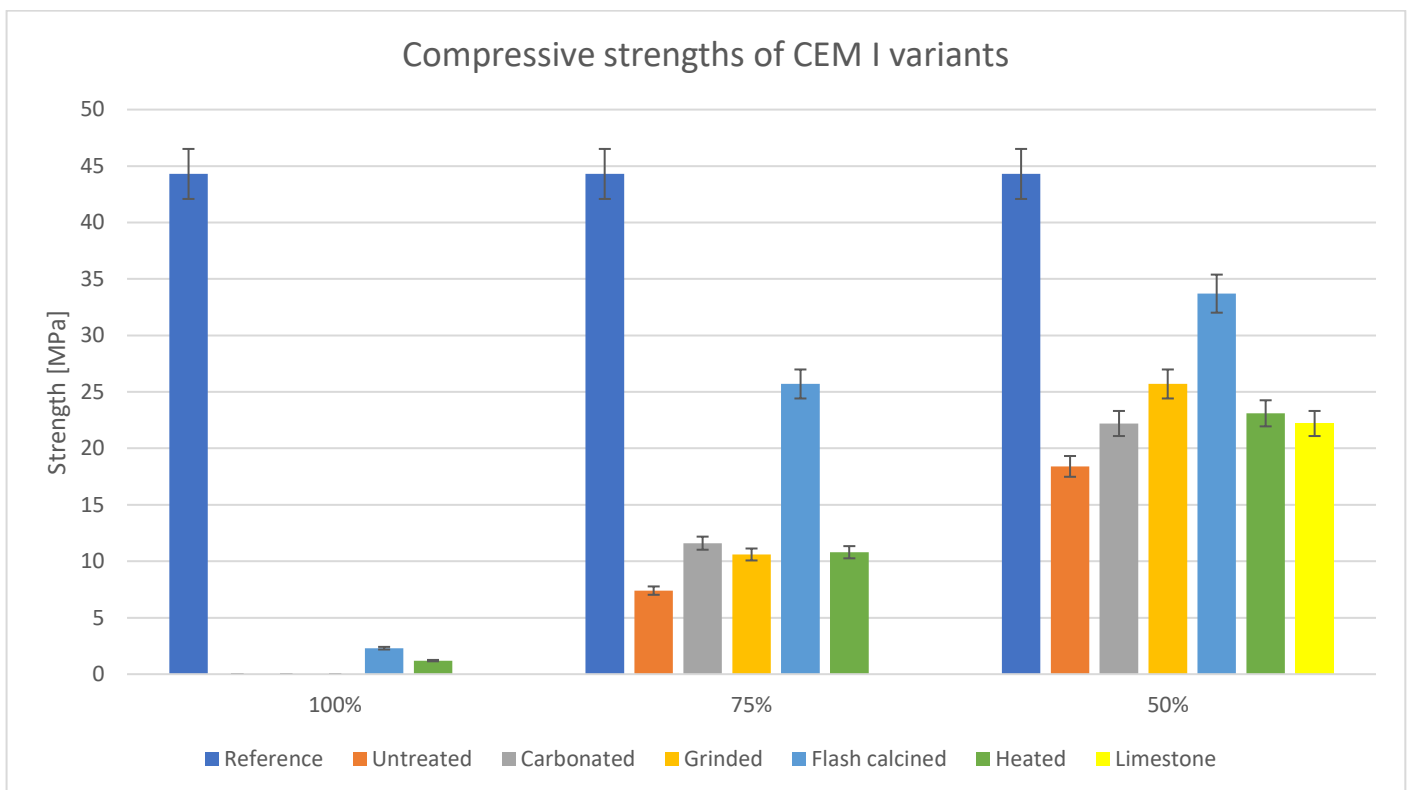


Figure 4.9: Compressive strengths of CEM I variants

**Table 4.2: Flexural ( $R_f$ ) and compressive ( $R_c$ ) strengths of CEM I variants as ratio to reference values**

Sample	Mean $R_f$ [MPa]	Ratio $R_f$ [%]	Mean $R_c$ [MPa]	Ratio $R_c$ [%]
SC1-100	0	0	0	0
SC1-CAR-100	0	0	0	0
SC1-GR-100	0	0	0	0
SC1-FC-100*	1	11.5	2.3	5.2
SC1-HT-100	0	0	1.2	2.7
SC1-75	2.9	33.3	7.4	16.7
SC1-CAR-75	4.7	54.0	11.6	26.2
SC1-GR-75	4.1	47.1	10.6	23.9
SC1-FC-75*	7.2	82.8	25.7	58.0
SC1-HT-75	3.8	43.7	10.8	24.4
SC1-50	6.1	70.1	18.4	41.5
SC1-CAR-50	7.1	81.6	22.2	50.1
SC1-GR-50	7.4	85.1	25.7	58.0
SC1-FC-50	8	92.0	33.7	76.1
SC1-HT-50	6.6	75.9	23.1	52.1
CEM1-LS-50	7.1	81.6	22.2	50.1

Initial observations show that most of the SC1-100 samples had no measurable flexural or compressive strength after 28 days of curing. This was true for all samples except those containing heated RCF or flash-calcined RCF. In the samples with heated RCF, the flexural strength could not be measured, while the compressive strength reached only 2.7% of the reference value. The flash-calcined RCF samples performed slightly better, achieving mean flexural and compressive strengths of 11.5% and 2.3% of the reference values, respectively. It should be noted that the samples marked with an asterisk contain another type of RCF compared to the samples without a mark.

Another notable observation is that the flexural strengths are relatively closer to the reference values compared to the compressive strengths. However, cement is generally weak in flexural and tensile strength, which is evident from the low flexural strength values. In practice, cement is primarily characterized by its compressive strength. This aligns with the European standard EN 197-1, which defines the standard strength of cement based on its compressive strength, not its flexural or tensile strength.

Figure 4.9 shows that the compressive strengths of samples containing both untreated and treated RCF are lower than the reference compressive strength. This is true for all samples. Furthermore, clear trend is observed in these samples: as the replacement ratio decreases, the compressive strength increases. This trend is expected since a lower replacement ratio means that more primary Portland cement is present, resulting in greater reactivity.

When comparing the compressive strengths of individual samples, it is clear that all treatments improved the compressive strength for the 75% and 50% replacement ratios. However, the extent of improvement varies by treatment. Flash calcination stands out, showing a strength increase of 41.3% for SC1-FC-75\* and 34.6% for SC1-FC-50. The other treatments resulted in smaller improvements, with increases of up to 9.5% for SC1-75 and 16.5% for SC1-50. These results suggest that all treatments positively influenced strength development when RCF was combined with primary cement, but flash calcination had the most significant effect.

Lastly, the strength test results for the samples with limestone instead of RCF are interesting. When comparing the flexural strengths, the CEM1-LS-50 samples show a higher value than the samples with untreated or heated RCF and an identical value to the samples with carbonated RCF. Regarding the compressive strengths, the limestone samples also match the strength of the carbonated RCF samples and exceed the strength of the untreated RCF samples. It is important to note that the tests with limestone were conducted only for the 50% replacement ratio.

### 4.2.3. Comparison of 'CEM II' variants

This section compares the strength test results of all CEM II variants. Figure 4.10 provides an overview of the mean flexural strengths for these samples, while Figure 4.11 displays the mean compressive strengths, including the reference values for comparison. Additionally, Table 4.3 presents both the flexural and compressive strengths of the samples expressed as a ratio of the reference strengths.

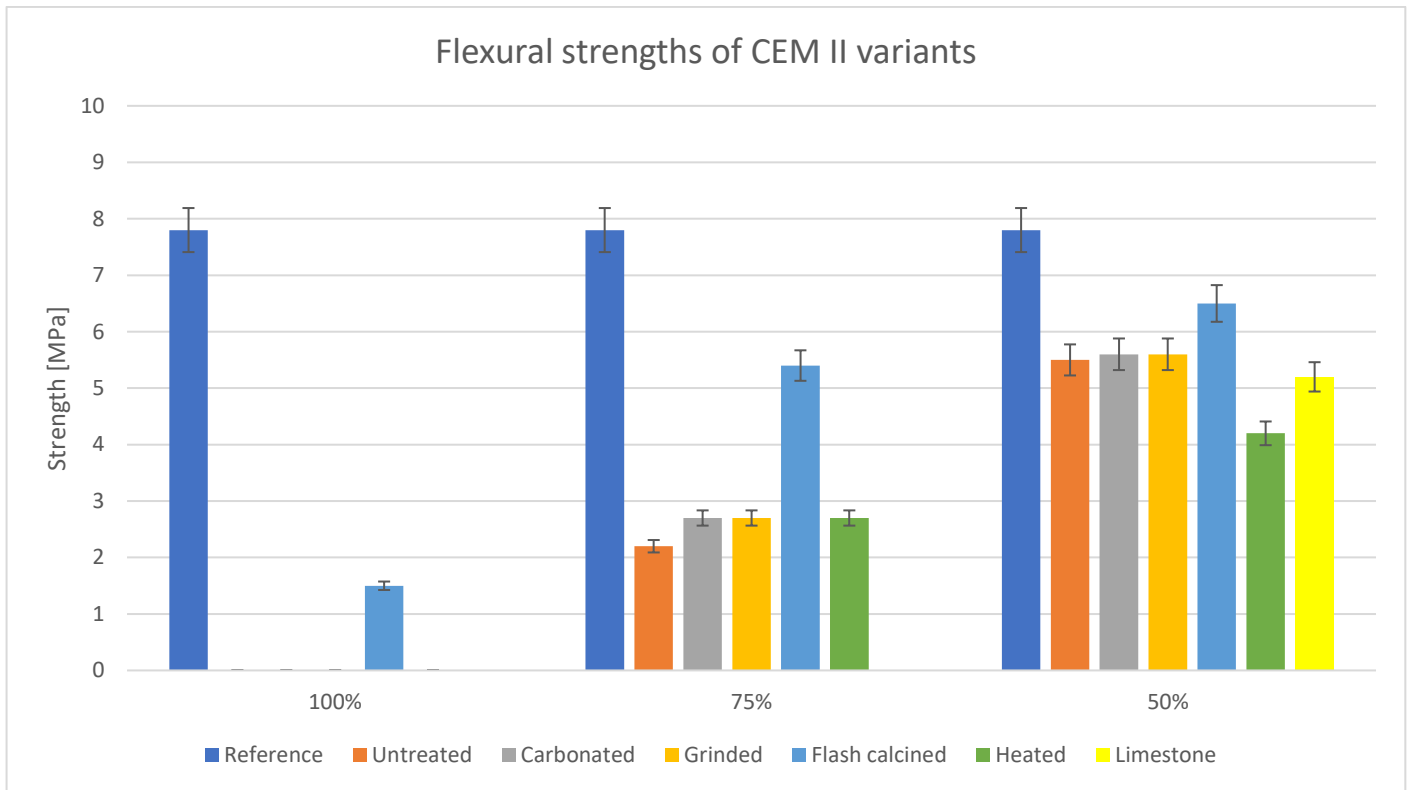


Figure 4.10: Flexural strengths of CEM II variants

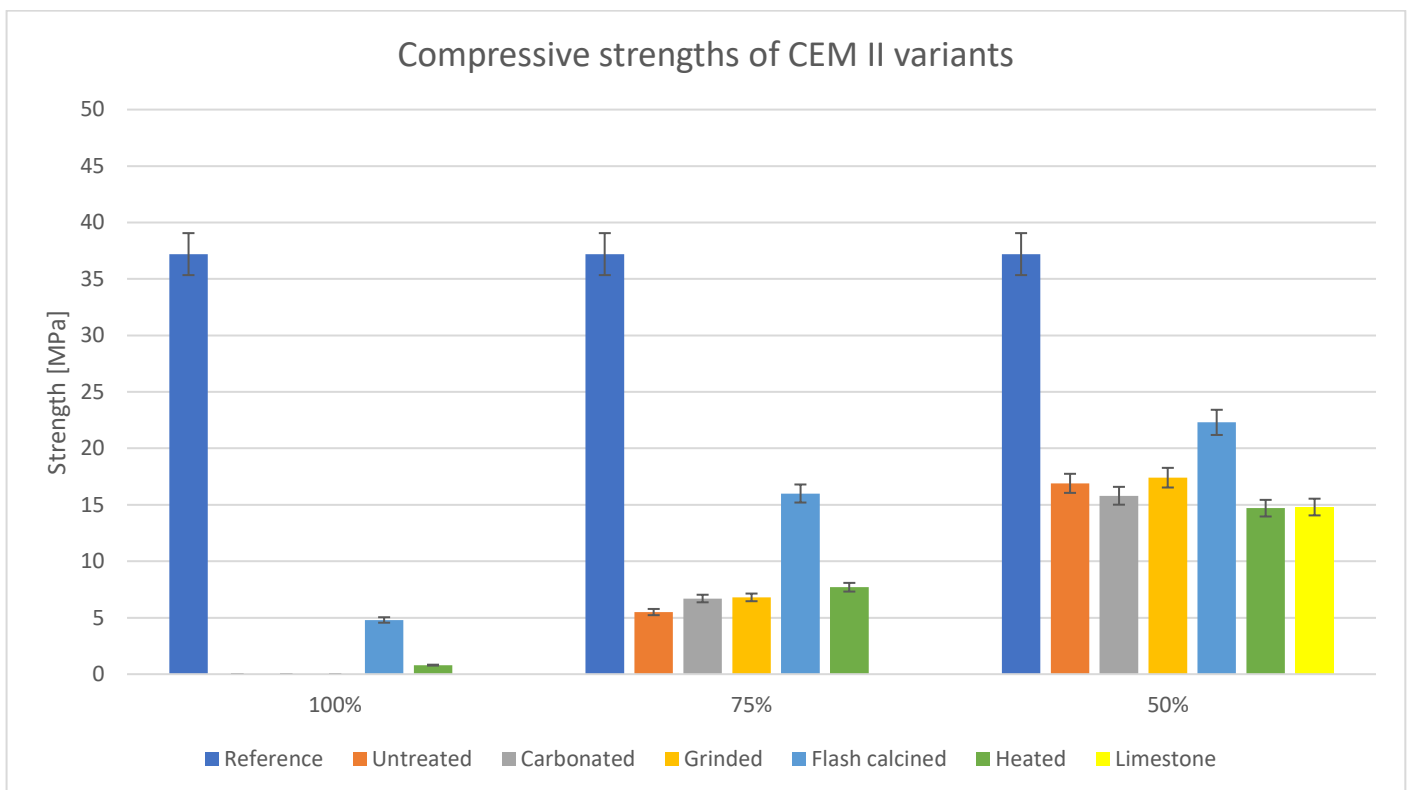


Figure 4.11: Compressive strengths of CEM II variants

**Table 4.3: Flexural and compressive strengths of CEM II variants as ratio to reference values**

Sample	Mean R <sub>f</sub> [MPa]	Ratio R <sub>f</sub> [%]	Mean R <sub>c</sub> [MPa]	Ratio R <sub>c</sub> [%]
SC2-100	0	0	0	0
SC2-CAR-100	0	0	0	0
SC2-GR-100	0	0	0	0
SC2-FC-100*	1.5	19.2	4.8	12.9
SC2-HT-100	0	0.0	0.8	2.2
SC2-75	2.2	28.2	5.5	14.8
SC2-CAR-75	2.7	34.6	6.7	18.0
SC2-GR-75	2.7	34.6	6.8	18.3
SC2-FC-75*	5.4	69.2	16	43.0
SC2-HT-75	2.7	34.6	7.7	20.7
SC2-50	5.5	70.5	16.9	45.4
SC2-CAR-50	5.6	71.8	15.8	42.5
SC2-GR-50	5.6	71.8	17.4	46.8
SC2-FC-50*	6.5	83.3	22.3	59.9
SC2-HT-50	4.2	53.8	14.7	39.5
CEM2-LS-50	5.2	66.7	14.8	39.8

Similar to the CEM I variants, the CEM II samples with a 100% replacement ratio showed no measurable flexural or compressive strength, except for the ones containing heated RCF or flash calcined RCF. Among the SC2-HT-100 samples, the flexural strength remained unmeasurable, while the compressive strength reached a mean value of 2.2% of the reference value. The SC2-FC-100\* samples performed better, with a mean flexural strength of 19.2% of the reference value and a mean compressive strength of 12.9% of the reference value.

Furthermore, the results show that all treatments have led to comparable outcomes for the carbonated, ground and heated samples with a 75% replacement ratio. The flash calcined RCF again stand out with a significantly higher strengths compared to the other samples. The SC2-FC-75\* samples had a mean flexural and compressive strength of respectively 69.2% and 43% of the reference values, while the other treatments led to mean flexural strengths of 34.6% for all samples and mean compressive strengths varying from 18% to 20.7% of the reference value. It should again be noted that the SC2-FC-75\* contained a different type of RCF compared to the other samples. However, for all treatments an improvement in both the flexural and compressive strength was measured compared to the untreated RCF.

When comparing the results for the differently treated samples, the effects varied depending on the replacement ratios. For the heated RCF, compressive strength improved for the 100% and 75% replacement ratios but decreased for the 50% ratio. A similar trend was observed in the flexural strength values, except for the SC2-HT-100 samples, which showed no measurable strength.

Carbonated RCF samples also showed higher compressive and flexural strengths at the 75% replacement ratio but had lower compressive strength at the 50% ratio. However, this decrease in compressive strength did not align with the flexural strength, which slightly improved at the 50% replacement ratio.

For the ground RCF, slight improvements were seen for both the 75% and 50% replacement ratios.

Generally, both average flexural and compressive strengths increased as the replacement ratios decreased, which aligns with expectations due to the higher presence of OPC.

Lastly, the limestone samples had a higher flexural and compressive strength compared to the samples with heated RCF. The other samples showed slightly higher values than the limestone samples, except for the samples with flash calcined RCF, which showed a more significant difference.

#### 4.2.4. Comparison of 'CEM III' variants

This section compares the strength test results of all CEM III variants. Figure 4.12 shows the mean flexural strengths of the CEM III variants, while Figure 4.13 displays the mean compressive strengths. The dark blue bars represent the reference sample. Additionally, Table 4.4 presents both the flexural and compressive strengths of the samples expressed as a ratio of the reference strengths.

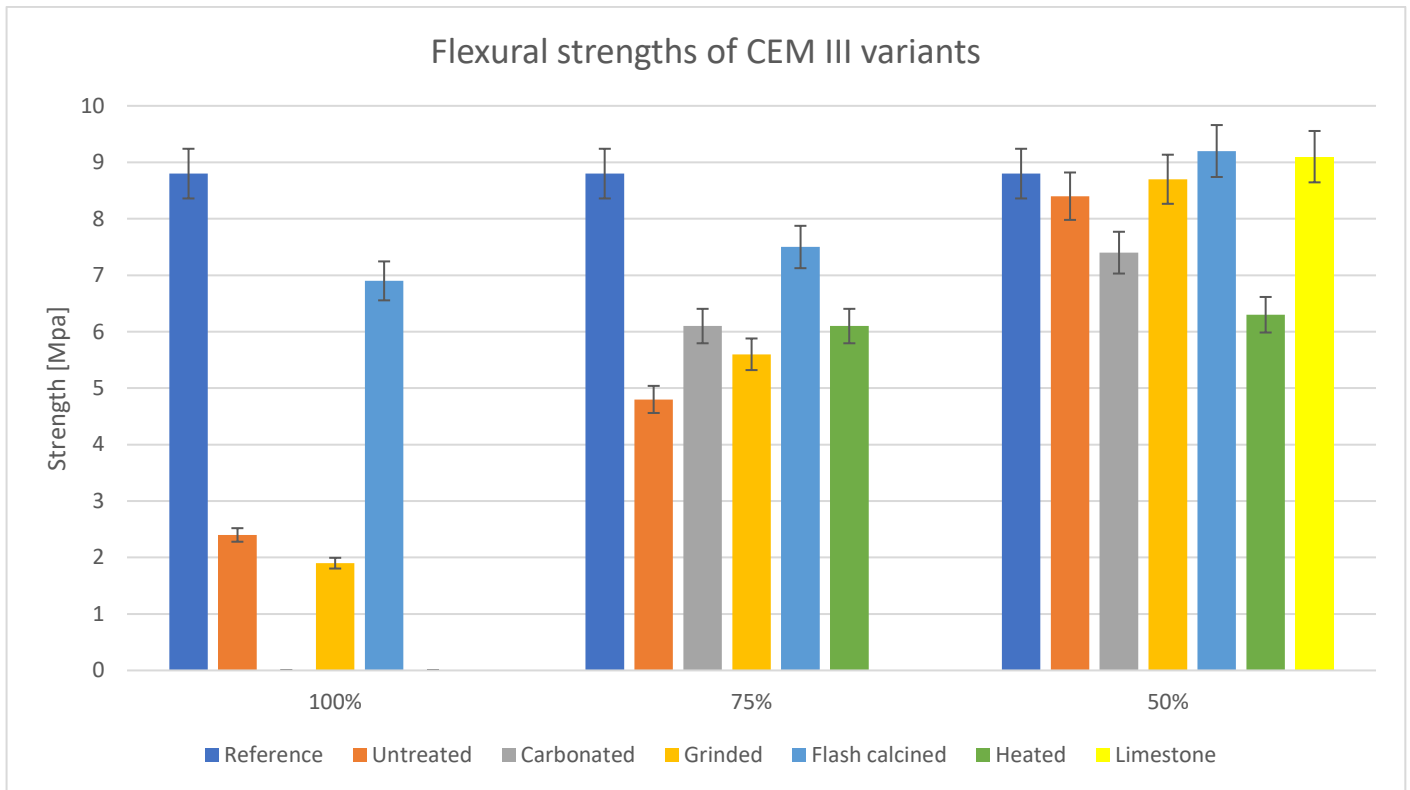


Figure 4.12: Flexural strengths of CEM III variants

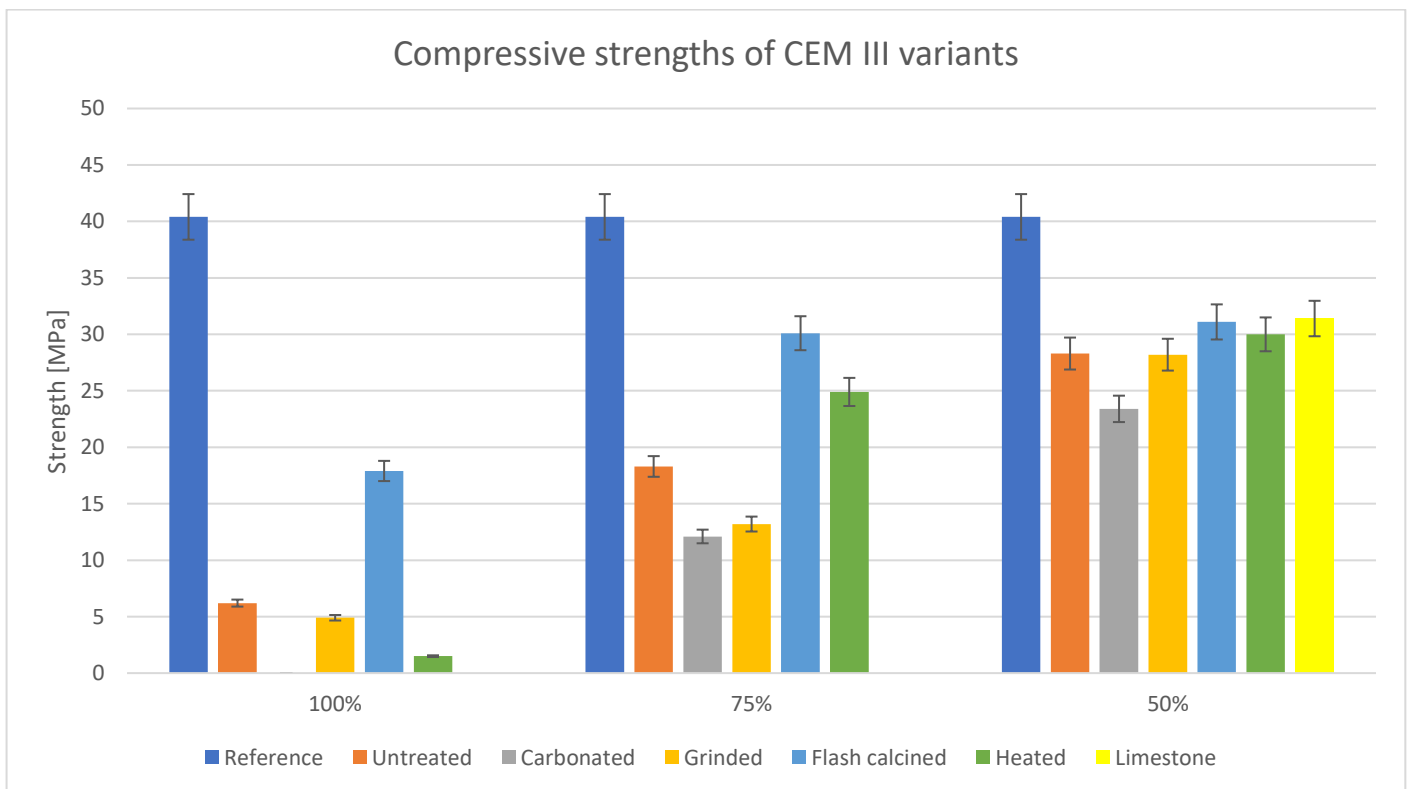


Figure 4.13: Compressive strengths of CEM III variants

**Table 4.4: Flexural and compressive strengths of CEM III variants as ratio to reference values**

Sample	Mean R <sub>f</sub> [MPa]	Ratio R <sub>f</sub> [%]	Mean R <sub>c</sub> [MPa]	Ratio R <sub>c</sub> [%]
SC3-100	2.4	27.3	6.2	15.3
SC3-CAR-100	0	0.0	0	0.0
SC3-GR-100	1.9	21.6	4.9	12.1
SC3-FC-100*	6.9	78.4	17.9	44.3
SC3-HT-100	0	0.0	1.5	3.7
SC3-75	4.8	54.5	18.3	45.3
SC3-CAR-75	6.1	69.3	12.1	30.0
SC3-GR-75	5.6	63.6	13.2	32.7
SC3-FC-75*	7.5	85.2	30.1	74.5
SC3-HT-75	6.1	69.3	24.9	61.6
SC3-50	8.4	95.5	28.3	70.0
SC3-CAR-50	7.4	84.1	23.4	57.9
SC3-GR-50	8.7	98.9	28.2	69.8
SC3-FC-50	9.2	104.5	31.1	77.0
SC3-FC-50*	6.4	72.7	31.5	78.0
SC3-HT-50	6.3	71.6	30	74.3
CEM3-LS-50	9.1	103.4	31.4	77.7

In contrast to the SC1-100 and SC2-100 samples, the SC3-100 sample did have measurable flexural and compressive strengths. The mean flexural strength was 27.3%, and the compressive strength was 15.3% of the reference value. The mean flexural and compressive strengths reach values of up to respectively 95.5% and 70% of the reference value for the SC3-50 samples. This indicates an activating effect of the untreated RCF on the BFS, which will be discussed further in Discussion.

When analyzing the effects of the different treatments, several trends can be observed. Grinding the RCF resulted in lower compressive strengths across all replacement ratios compared to the reference values. For the flexural strength, grinding had a negative effect at the 100% replacement ratio but showed improvement at the 75% and 50% replacement ratios.

Thermal treatment of the RCF heating led to lower compressive strength at the 100% replacement ratio, with unmeasurable flexural strength. However, for the 75% replacement ratio, both the compressive and flexural strengths improved. At the 50% replacement ratio, the compressive strength slightly increased, while the flexural strength decreased.

Carbonation showed mixed results. For the 75% and 50% replacement ratios, the compressive strength was lower compared to the untreated samples. At the 100% replacement ratio, both flexural and compressive strengths remained unmeasurable. The only exception was the flexural strength at the 75% replacement ratio, which increased slightly after carbonation.

Flash calcination continued to produce the highest strengths among all treatments. However, the differences between flash calcination and the other treatments became smaller as the replacement ratio increased, suggesting that flash calcination is less effective at lower replacement ratios when combined with BFS. To explore potential differences between types of RCF, the SC3-FC-50 sample was produced twice using the two varying RCF types. A significant difference was observed in flexural strength: the SC3-FC-50 sample achieved 104.5% of the reference flexural strength, while the SC3-FC-50\* sample reached 72.7%. The compressive strengths of the two samples were closer to each other with 77% and 78% of the reference value, respectively.

Lastly, the samples containing limestone instead of RCF showed surprisingly high strengths. Replacing 50% of the OPC with limestone resulted in flexural and compressive strengths of 103.4% and 77.7% of the reference values, respectively. The compressive strength notably surpasses the average compressive strength observed in the SC3-FC-50 samples.

### 4.3. LCA review

This section contains a literature review on existing life cycle assessments of ordinary Portland cement (OPC) and recycled concrete fines.

#### 4.3.1. Goal definition

The objective of this Life Cycle Assessment (LCA) review is to compare the environmental impacts of recycled concrete fines with those of ordinary Portland cement production. This comparison aims to provide insights into the potential environmental benefits and drawbacks of using recycled cement as opposed to producing new cement based on data retrieved from existing LCAs. The results will inform stakeholders in the construction industry, policy makers, and researchers about the sustainability of recycled concrete fines and help in making informed decisions regarding material use in construction projects.

The primary audience for this LCA review includes construction industry professionals, environmental policy makers, researchers, and sustainability consultants. The findings will also be valuable to organizations aiming to reduce their environmental footprint and promote sustainable building practices.

The findings will be used to inform research and development in recycling technologies. Other possible applications include the guiding of decision-making in construction material selection, support of policy development for sustainable practices and enhancement of public awareness and industry standards regarding sustainable materials.

#### 4.3.2. Scope definition

The functional unit of this LCA review is defined as 1 kg of cement or recycled concrete fines used in concrete production. The chosen system boundaries are cradle-to-gate. This includes the extraction of raw materials, processing, production and transportation up to the point where the cement and recycled concrete fines are ready to be used in concrete.

The processes that are included in the LCA for ordinary Portland cement production are raw material extraction, raw material transportation, clinker production including energy use and emissions, cement grinding and packaging, and transportation to construction sites.

The processes for the production of recycled concrete fines start from the demolition of existing concrete structures, followed by transportation of the concrete rubble to the recycling facility, processing the concrete rubble by crushing and grinding with the Smart Liberator method, additional processing, packaging, and transportation to construction sites.

The impact categories that are considered in this LCA are limited to the eleven basic impact categories that must be included in each LCA according to the Dutch building regulations 'Bouwbesluit-2012 bepalingsmethode'. Construction industries from other continents or countries might follow other regulations and include other impact categories in their LCAs. The required data for this LCA review are obtained from existing LCA studies and datasets. Another important note is that there is limited data available on the environmental impacts of RCF. Lastly, it is assumed that the RCF are a suitable cement substitute, despite the limited knowledge about their functionality. This implies that although it might follow from the LCA review that the RCF are more environmental friendly than OPC, it does not necessarily mean that it can also replace OPC in terms of functionality.

### 4.3.3. Life Cycle Impact analysis

In order to get insight into the environmental impacts of ordinary Portland cement, data has been collected from several studies and listed in Table 4.5. As can be observed from the table, the environmental impacts of some categories are left empty. This is due to the fact that this research considers only the eleven impact categories that are mentioned in the table, while some of the studies did not consider all of them or used other unit equivalents to express them. Also, the studies of Rahla et al.(2019) and De Belie et al. (2012) showed only one value for the ADP impact category and did not make any distinction between fuel or non-fuel. The most relevant impact category for this research is the Global Warming Potential, since one of the main goals of this research is to make a contribution to the developments in science and the building industry regarding a CO<sub>2</sub>-neutral economy. The obtained data shows that the GWP of OPC differs from 0.82 to 0.95 kg CO<sub>2</sub>/kg cement, with a mean of 0.866 kg CO<sub>2</sub>/kg cement. It can be stated that this range is a valid representation of the general GWP of OPC, based on the study of Anderson et al. (2020), who evaluated 102 Environmental Product Declarations for 118 cementitious materials in which a range of approximately 700 to 1000 kg CO<sub>2</sub>/kg cement was found.

**Table 4.5: Environmental impacts per kg of OPC according to different studies**

Source / Unit equivalent	Impact category										
	ADP- non fuel	ADP-fuel	GWP	ODP	POCP	AP	EP	HTP	FAETP	MAETP	TETP
	kg Sb	kg Sb	kg CO <sub>2</sub>	kg CFC-11	kg C <sub>2</sub> H <sub>4</sub>	kg SO <sub>2</sub>	kg PO <sub>4</sub> <sup>3-</sup>	kg 1,4-DB	kg 1,4-DB	kg 1,4-DB	kg 1,4-DB
Rahla et al. (2019)	1,59E <sup>-03</sup>		8.44E <sup>-01</sup>	2.28E <sup>-08</sup>	4.26E <sup>-05</sup>	1.15E <sup>-03</sup>	1.73E <sup>-04</sup>	4.02E <sup>-02</sup>	4.14E <sup>-03</sup>	1.94E <sup>+01</sup>	1.17E <sup>-03</sup>
Zentar et al. (2024)	1.34E <sup>-06</sup>	1.20E <sup>-03</sup>	8.60E <sup>-01</sup>	2.08E <sup>-08</sup>	5.56E <sup>-05</sup>	1.53E <sup>-03</sup>	5.10E <sup>-04</sup>	1.01E <sup>-01</sup>	8.59E <sup>-02</sup>	1.85E <sup>+02</sup>	1.09E <sup>-03</sup>
Jonkers (2021)	6.70E <sup>-07</sup>	5.70E <sup>-04</sup>	8.20E <sup>-01</sup>	5.20E <sup>-09</sup>	2.10E <sup>-04</sup>	2.70E <sup>-03</sup>	3.60E <sup>-04</sup>	5.00E <sup>-02</sup>	6.90E <sup>-04</sup>	5.10E <sup>+00</sup>	6.80E <sup>-04</sup>
De Belie et al. (2012)	1.37E <sup>-03</sup>		8.40E <sup>-01</sup>	-	1.02E <sup>-04</sup>	3.08E <sup>-03</sup>	4.75E <sup>-04</sup>	6.83E <sup>-02</sup>	-	-	-
Josa et al. (2004)	-	-	8.53E <sup>-01</sup>	-	-	9.00E <sup>-05</sup>	-	-	-	-	-
Olagunju et al. (2021)	-	-	9.11E <sup>-01</sup>	7.84E <sup>-08</sup>	-	1.40E <sup>-03</sup>	-	1.21E <sup>-03</sup>	9.92E <sup>-05</sup>	3.83E <sup>-04</sup>	4.38E <sup>-01</sup>
Koullapis (2022)	4.15E <sup>-08</sup>	1.84E <sup>-03</sup>	8.50E <sup>-01</sup>	5.05E <sup>-09</sup>	5.99E <sup>-05</sup>	9.91E <sup>-04</sup>	1.43E <sup>-04</sup>	3.70E <sup>-02</sup>	4.31E <sup>-04</sup>	1.87E <sup>+00</sup>	4.58E <sup>-04</sup>
Bushi et al. (2014)	2.62E <sup>-03</sup>	2.77 E <sup>-03</sup>	9.50E <sup>-01</sup>	1.10E <sup>-11</sup>	-	4.10E <sup>-03</sup>	-	-	-	-	-

The environmental impacts of RCF are difficult to estimate, due to the scarcity of data. Nevertheless, Koullapis (2022) succeeded in making a comprehensive environmental and economic assessment of two innovative concrete recycling technologies and compared them with the traditional crushing recycling method. The two considered innovative recycling technologies were Concrete to Cement and Aggregates (C2CA) and Smart Crushing (SC). The latter method was used for retrieving the RCF that were investigated in this research. Koullapis (2022) used the production of 1 m<sup>3</sup> of concrete as the functional unit of his analysis. He analyzed a mix design in which 20% of the primary cement (CEM III/A) was replaced by RCF with a particle size range of 0 – 125 µm, which corresponds to 68 kg/m<sup>3</sup>. The replacement percentages of sand and gravel were both 100%. Table 4.6 shows the environmental impact of the Smart Crushing process per ton of end-of-life (EoL) concrete. 0.091 ton of the RCF 0 – 125 µm can be retrieved from each ton of EoL concrete. That information is used to calculate the environmental impacts per kg of RCF, which are listed in Table 4.7.



Table 4.6: Environmental impacts of the processing of 1 ton EoL concrete with the Smart Liberator method (Koullapis, 2022)

SC2	Excavator	Impact crusher	Sieve tower	Air separator	SmartLiberator	Horizontal screen	Smartrefiner	Coveyor belts
ADP-minerals	4.02E-09	4.65E-06	5.58E-07	3.91E-07	1.30E-07	1.95E-07	3.58E-07	3.72E-07
ADP-fossil	4.06E-03	3.69E-02	4.42E-03	3.10E-03	1.03E-03	1.55E-03	2.84E-03	2.95E-03
AP	4.59E-03	1.25E-02	1.51E-03	1.05E-03	3.51E-04	5.27E-04	9.66E-04	1.00E-03
EP	1.06E-03	2.87E-03	3.44E-04	2.41E-04	8.04E-05	1.21E-04	2.21E-04	2.30E-04
FAETP	6.13E-02	1.41E-02	1.69E-03	1.19E-03	3.95E-04	5.93E-04	1.09E-03	1.13E-03
GWP100a	6.13E-01	5.03E+00	6.03E-01	4.22E-01	1.41E-01	2.11E-01	3.87E-01	4.02E-01
HTP	7.51E-02	5.22E-01	6.27E-02	4.39E-02	1.46E-02	2.19E-02	4.02E-02	4.18E-02
MAETP	1.04E+02	6.11E+01	7.34E+00	5.14E+00	1.71E+00	2.57E+00	4.71E+00	4.89E+00
ODP	1.05E-07	2.71E-07	3.25E-08	2.27E-08	7.58E-09	1.14E-08	2.08E-08	2.16E-08
POCP	9.98E-05	7.62E-04	9.15E-05	6.40E-05	2.13E-05	3.20E-05	5.87E-05	6.10E-05
TETP	2.09E-04	2.59E-02	3.11E-03	2.17E-03	7.25E-04	1.09E-03	1.99E-03	2.07E-03

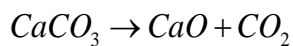
Table 4.7: Environmental impacts per kg of RCF obtained with the Smart Liberator method

Impact category	Unit equivalent	Value per ton of EoL concrete	Value per kg of RCF
ADP non-fuel	kg Sb	6.66E <sup>-06</sup>	7.32E <sup>-08</sup>
ADP fuel	kg Sb	5.69E <sup>-02</sup>	6.25E <sup>-04</sup>
AP	kg SO <sub>2</sub>	2.25E <sup>-02</sup>	2.75E <sup>-04</sup>
EP	kg PO <sub>4</sub> <sup>3-</sup>	5.17E <sup>-03</sup>	5.68E <sup>-05</sup>
FAETP	kg 1.4-DB	8.15E <sup>-02</sup>	8.96E <sup>-04</sup>
GWP	kg CO <sub>2</sub>	7.81E <sup>+00</sup>	8.58E <sup>-02</sup>
HTP	kg 1.4-DB	8.22E <sup>-01</sup>	9.03E <sup>-03</sup>
MAETP	kg 1.4-DB	2.80E <sup>+03</sup>	3.08E <sup>+00</sup>
ODP	kg CFC-11	4.93E <sup>-07</sup>	5.42E <sup>-09</sup>
POCP	kg C <sub>2</sub> H <sub>4</sub>	1.19E <sup>-03</sup>	1.19E <sup>-03</sup>
TETP	kg 1.4-DB	3.73E <sup>-02</sup>	3.73E <sup>-02</sup>

Table 4.7 shows that the GWP of each kg of RCF obtained with the Smart Liberator method is 0.0858 kg CO<sub>2</sub>, which corresponds to approximately 10% of the GWP of producing new OPC. In theory this would mean that by using the Smart Liberator method for cement recycling, the carbon dioxide emissions due to the cement production can be brought down by 90%. However, this implies that the RCF can fully replace the OPC, but that is not yet possible based on the results from this research.

During this research several treatments were applied to the RCF in order to improve the reactivity of the material. Even though the results of all treatments did not show that the RCF can fully replace OPC, it is of interest to have an idea of what the environmental impacts are of the treatments. Especially the CO<sub>2</sub>-emissions are of great interest.

When looking at the treatments that are applied during this research, there are two treatments that involve high temperatures. These are the flash calcination and heating of the RCF. During these treatments CO<sub>2</sub> is released due to the decomposition of calcium carbonate and due to the energy consumption of the flash calciner and oven. Emissions from calcium carbonate decomposition depend on the amount of calcium carbonate present. However, it is debatable whether the carbon dioxide emissions due to decomposition of calcium carbonate, because it is a carbonation product of the carbonation of portlandite. The TGA results during this research indicate that the untreated RCF that is used contain approximately 3% calcium carbonate by mass. The decomposition reaction of calcium carbonate is as follows:



This means that for each mol of decomposed CaCO<sub>3</sub>, one mol of CO<sub>2</sub> comes free. By using the 3% calcium carbonate content and the molecular masses of CaCO<sub>3</sub> and CO<sub>2</sub>, which are respectively 100 g/mol and 44 g/mol, a simple calculation can be made to estimate the released CO<sub>2</sub>. This results in an emission of 0.013 kg CO<sub>2</sub> per kg of RCF, which should be added to the CO<sub>2</sub> emission due to the Smart Liberator recycling process. This leads to a total CO<sub>2</sub> emission of 0.099 kg CO<sub>2</sub>/kg RCF.

The CO<sub>2</sub> emissions due to the energy consumption is difficult to estimate due to the fact that the specific heat capacity of the RCF is unknown. However, for this study the specific heat is estimated at 800 J/(kg °C) based on findings in literature ((Bentz et al., 2011), (Xu & Chung, 2000), (Shafigh et al., 2020), (Mendez, 2019), (Damdelen, 2016)). This means that heating the material from 20 °C to 800 °C requires 624 kJ per kg. Under the assumption of an efficiency of 81%, which corresponds to the thermal efficiency of a FCB Flash Calciner at nominal production rate (Giroud & Pinoncely, 1996), the total energy consumption will be 770 kJ per kg. Assuming that the energy source is supplied by solar panels, which have a GWP of 0.09 kg CO<sub>2</sub>/kWh (Khan et al., 2024), the GWP of thermal treatment of the RCF is 0.019 kg CO<sub>2</sub>/kg RCF.

Adding this value to the previously calculated GWP of 0.099 kg CO<sub>2</sub>/kg RCF results in a total GWP after flash calcination of 0.118 kg CO<sub>2</sub>/kg RCF. This corresponds to a reduction of 86.4% compared to the GWP of OPC.

The carbonation treatment applied during this research resulted in approximately 7% uptake of CO<sub>2</sub> by mass of the RCF. This corresponds to 0.070 kg uptake of CO<sub>2</sub> per kg of RCF. Subtraction of this from the emission during the Smart Crusher process, leads to a total emission of 0.0158 kg CO<sub>2</sub>/kg RCF.

# 5. Discussion

## *Reference mortars*

The results of the strength tests that have been performed during this research show that the mortar prisms that are made with the reference cements do not meet the requirements set by the European standard EN 197-1. Since OPC with strength class 52.5 has been used for the reference prisms, the minimum compressive strength should be 52.5 MPa. However, this was not the case for any of the reference prisms which either indicates that the OPC did not perform as it should have or that something has been consequently going wrong during the preparations of the mortar prisms. For the mixing procedure, the European standard has been followed and making new prisms with the same OPC led to similar results. It is unknown what the exact reason is for the low strengths of the prisms, but in the literature several factors which influence the strength of cement and concrete are mentioned. The primary factors that affect the strength are the water-cement ratio and the porosity, which are correlated with each other ((Mehta & Monteiro, 2006), (Neville & Brooks, 1987)). An increment of one percent of air content leads to 5% decrease of compressive strength (Wong et al., 2011). Other mentioned factors are the cement type, curing conditions, properties of the mixing water and testing parameters (Mehta & Monteiro, 2006). Besides factors that are related to the mixing and testing of cement also the storage conditions of dry cement plays an important role in the strength development. To prevent hydration during storage it is important to store the cement in a dry and well-ventilated environment. The storage time also affects the strength development. Ibrahim (2018) investigated the effect of storage time on the strength development of OPC. He found that OPC loses more than 30% of its 28-day strength after six month of storage and more than 40% after one year of storage.

Although the 28-day strengths of the reference prisms are lower than expected, the results are still used as references for the RCF in this study, because the same OPC has been used and the same procedure has been followed for all samples. Therefore, the results can be compared to each other.

## *Relationship with replacement ratios*

A trend is observed in the 28 day flexural and compressive strengths for all samples in relation to the different replacement ratios. It is obvious that a lower replacement ratio results in higher strength values, regardless of the applied treatments to the RCF. This corresponds to the hypothesis that the presence of more OPC at lower replacement ratios result in higher strengths. A logical explanation for this is that a lower clinker content indicates less hydration products, which results in higher porosity and lower strength (Lu et al., 2018).

## *Performance of untreated RCF at different replacement ratios*

The strength test results of the prisms with untreated RCF indicate that RCF obtained with the Smart Liberator method did not develop any measurable strength over 28 days when fully replacing OPC in the CEM I and CEM II variants, while it did in the CEM III variant with 70% BFS. This indicates that the RCF might function as an activator for BFS. A possible explanation for this activation is the presence of the hydration product Portlandite in the RCF, which was confirmed by the TG analysis. Portlandite is known for its high pH value, making it a suitable activator for BFS (Tonelli et al., 2024) (Aitcin, 2016). This assumption is reinforced by the fact that the strength test results of the CEM III/B variant are generally higher in comparison with the CEM I and CEM II variants for all replacement ratios and all treatments.

The SC1-75, SC2-75 and SC3-75 had flexural strengths that corresponded to 33.3%, 28.2% and 54.5% of their reference values, respectively. The values of the compressive strengths were 16.7%, 14.8% and 45.3%, respectively. This clearly shows that the RCF in combination with BFS has great potential when it comes to replacing OPC. Approximately half of the reference strength can be achieved, while replacing 75% of OPC in the mixture.

The SC1-50, SC2-50 and SC3-50 had flexural strengths that corresponded to 70.1%, 70.5% and 95.5% of the reference value, respectively. For the compressive strengths those values were 41.5%, 45.4% and 70%. While the SC1 and SC2 samples have similar strength ratios for corresponding replacement ratios, the SC3 samples clearly have significantly higher strengths. This further emphasizes the previously mentioned activating effect of the RCF on BFS, indicating a great potential of using RCF as an activator for BFS without any additional treatments.

## *Performance of treated RCF at 100% replacement*

When comparing the strength test results of the prisms containing the treated RCF, only the regular thermal treatment and flash calcination showed a measurable improvement for the compressive strengths of the SC1-

100 and SC2-100 variants. As for the flexural strengths, only the flash calcination resulted in measurable strengths for the SC1-100 and SC2-100 variants. Although the measured strengths were very low, the improvements due to the treatments were measurable, which indicates a possible regain of reactivity of the RCF after exposure to high temperatures. This was also concluded from the studies of Ma et al. (2009) and Shui et al. (2009).

Considering the CEM III variants with 100% replacement ratio, the grinding of the RCF resulted in slightly lower, but comparable flexural and compressive strengths as the samples with untreated RCF. Heating of the RCF resulted in a compressive strength of 3.7% of the reference value, while no flexural strength was measured for the SC3-HT-100. The flexural and compressive strengths of the SC3-FC-100\* were significantly higher than those of the SC3-100. Although the SC3-FC-100\* mix was made of RCF which were different from the RCF used in the SC3-100 mix, it can still be concluded that the flash calcination significantly increased the strength based on the repeated SC3-FC-50 mix. The TG results of the 50/50 RCF (used in SC3-FC-100\*) showed a higher amount of Portlandite than in the other RCF, which indicates probable better reactivity with BFS for the 100% replacement ratio. This also aligns with the slightly higher measured compressive strength of the SC3-FC-50\* prisms. It is expected that portlandite rehydrates after addition of water to the mix, but it might have been that the amount of portlandite after rehydration will be lower than the initial amount due to the reaction of CaO with ambient CO<sub>2</sub> during storage (Menéndez et al., 2012).

The carbonation and regular heating of the RCF clearly reduced the strength of the SC3-100 samples. This can be attributed to the carbonation and decomposition of Portlandite, due to which the activating effect was gone after carbonation and strongly reduced due to the heating. The TG results showed a small mass drop that corresponds to the decomposition of portlandite in the heated fines, which means that some portlandite was still present and/or reformed during storage. It is also expected that some of the initial portlandite is rehydrated after adding water. These are possible explanations for why there was still some strength measured for the SC3-HT-100. However, it was observed that the water demand of the heated RCF was high, although this was mitigated by adding superplasticizer to the mix. It is of interest to perform experiments with varying w/c-ratios in order to find the optimum ratio for better strength development.

#### *Performance of treated RCF at 75% replacement*

For the SC1-75 and SC2-75 samples, all samples with treated RCF showed improvement of both the flexural and compressive strengths of the samples in comparison with the samples with untreated RCF. This indicates that all applied treatments show potential in improving the reactivity of the RCF. In case of the carbonation treatment, the higher strength values are probably caused by the reaction of Portlandite with the Si-gel that is formed during carbonation ((Lu et al., 2018), (Li et al., 2022), (Mao et al., 2024), (Zajac et al., 2024)).

The improvement of the strength after grinding the RCF is possibly related to the higher specific surface area. This is in line with the findings of Liu et al. (2018). Their study showed a clear relation between the final strength and the fineness of supplementary cementitious materials: by refining the particle sizes of the SCMs, the strength of the blended cements was increased.

Carbonation and grinding of the RCF resulted in lower strengths for the SC3-75 samples, while the flash calcination and regular heating resulted in higher strengths. The negative effects of the carbonation and grinding are most likely due to the carbonation of portlandite. The TG results of the ground fines indicated that carbonation took place during and/or after the treatment.

#### *Performance of RCF at 50% replacement*

All treatments resulted in higher strengths for the SC1-50 samples, but not for the SC2-50 samples. For the SC2-50 samples, grinding of the RCF resulted slightly higher compressive strength and flash calcination led to a more significant increase in compressive strength. The carbonation and regular heating resulted in lower compressive strengths. Further research is necessary to determine why those treatments resulted in lower strengths at the 50% replacement ratio, while they improved the strength at 75% replacement. The results indicate a different behavior of the carbonated and heated RCF when used in combination with fly ash.

In the SC1-FC-50 and SC1-HT-50 the same type of RCF were used. The results showed that the flash calcination leads to significantly higher strengths compared to the regular heating, which indicates that the flash calcination shows higher potential as an upcycling method. This corresponds to the findings of Bullard (2015), who investigated the effect of cooling rates on mineralization in Portland cement clinker. He found that a faster cooling regime resulted in the best crystal forming and highest glass content, which is favorable for the reactivity of Portland cement. The same principle might be applicable for RCF, but microstructural analysis is needed to confirm this. However, the cooling regime in the flash calciner is not the only factor that influences the final strengths compared to a regular furnace. Since the RCF move within an airflow and have

a much shorter residence time compared to regular stationary heating, much less agglomeration is caused during flash calcining (Martirena-Hernández, et al., 2024). Agglomeration reduces the specific surface area, leading to less reactivity. However, since no particle size analysis was performed after the thermal treatments, the exact effect remains unknown.

For the SC3-50 variants, the effects of the treatments showed similar trends as those on the SC3-75 variants. The flash calcination again showed that this treatment has a great potential by reaching flexural and compressive strength values of 104.5% and 77% compared to the reference value, respectively. The flash calcined 50/50 RCF resulted in a compressive strength of 78%, which is comparable to the 77% of the other RCF. However, the improvements were less significant compared to those of the SC3-100 and SC3-75 variants, which also applies to the other treatments as the strength values are relatively close to each other. This might be due to the presence of more OPC at the 50% replacement ratio, which could outweigh the effects of the RCF. Reconfirmation of these results is necessary to draw a valid conclusion. Nevertheless, the RCF show a great potential in being used as an activator for BFS.

During the preparations of the samples it was observed that the RCF resulted in a higher water demand, which is why a superplasticizer was used in some of the samples. The high water demand negatively influences the workability and significantly increases porosity which leads to lower strengths (Duan et al., 2020). The water demand was even higher for the flash calcined and heated RCF, corresponding to the outcomes of several studies which investigated the effect of dehydrating cement with thermal treatments ((Cariço et al., 2020), (Wang et al., 2018), (Balducco et al., 2019), (Alberda van Ekenstein, 2020)).

#### *Limestone variants*

The CEM3-LS-50 showed relatively high strength results, reaching up to 77.7% of the compressive strength of the reference sample, while the flash calcined RCF resulted in a strength ratio of 78%. Limestone has the advantages that it functions as a filler, it significantly reduces the water demand and improves the consistency (Singh, 2023). These are possible explanations for the relatively high strengths of the limestone variants, especially since the RCF have a high water demand. Better compaction due to the addition of limestone may also have resulted in higher strengths. As for the RCF, it might be possible that the RCF create more air voids in the mixture, leading to a lower strength. This is especially the case for thermally treated RCF. Menéndez et al. (2012) observed an increase in porosity after rehydration of thermally treated cement paste. Nevertheless, more research is needed to draw a valid conclusion.

#### *Limitations*

A limitation of this presented study is the limited knowledge about the RCF that were used. Although the RCF from the Haarlemmerweg were expected to be a BFS containing cement, the TG analysis did not provide any detailed information about the microstructure of the material. This made it difficult to clearly understand the possible hydration mechanisms of the RCF. Also the effects of the treatments on the microstructure are unknown, making it difficult to explain any observed differences in strength values.

Furthermore, this research only focused on the flexural and compressive strengths of the samples, ignoring the other requirements that the material should meet according to the European standards.

Also, the flash calcined samples of most variants were made from other RCF than the other samples due to limited amount of available material. Although the RCF showed similar performance of the SC3-FC-50 for both types, it is uncertain how the RCF respond to other treatments and replacement ratios.

It is also important to note that for the carbonation of the RCF the efficiency highly depends on the circumstances under which the carbonation takes place ((Li & Wu, 2022), (Teune et al., 2023), (Xu, et al., 2022)). The carbonated RCF that were used in this research were dry carbonated for twelve hours at a pressure of 2 bars and a surrounding temperature which was estimated at 10 °C due to the time of the year in which the treatment was applied. The relative humidity was not measured. In the study of Li and Wu (2022), in which several studies were investigated, it was found that the CO<sub>2</sub> sequestration capacity of the materials tend to increase with temperatures between 20 °C and 80 °C. Based on these findings, there might be possibilities to improve the carbonation treatment that was applied to the RCF in this study.

#### *Comparison with existing literature*

Overall, the strength values that were found during this study correspond very well to the findings in literature. Tang et al. (2020) critically reviewed dozens of studies in which cement was replaced by RCF. Statistical data showed that the median relative compressive strength at a replacement ratio of more than 30% was 56.5% of the reference value. This is similar to the mean value of the samples in this study with a replacement ratio of 50%, which is 58.7%.

# 6. Conclusions and recommendations

## 6.1. Conclusions

The main goal of this research was to investigate the functionality of recycled concrete fines that are obtained with the Smart Liberator method. Reference cements were used to assess the functionality of the RCF. The main research question of this study is as follows:

*'To what extent can recycled concrete fines replace traditional cement?'*

The research question will be answered by first answering the following sub-questions:

1. *What is the impact of different replacement percentages of recycled concrete fines on the compressive and flexural strength of the mortar prisms?*

Based on the results that were obtained during this research, it can be concluded that the compressive and flexural strength of the mortar prisms increase with a decreasing replacement ratio. The main reason for this is the presence of more OPC in the mixture, which means more reactivity and thus more strength development. However, the outcomes highly depend on the type of cement in which the RCF are applied. During this study it was observed that the water demand of the mixture increased with an increasing replacement ratio. This corresponds to the findings in literature which state that RCF generally have a high water absorption. As this led to worse workability and higher porosity, which was observed during this study, it probably had a negative effect on the strength development of the samples from this study. The higher water demand was mitigated by using superplasticizer in the heated and flash calcined RCF mortar mixtures.

2. *What is the effect of the treatment method on the strength of the recycled concrete fines?*

The effects of carbonation, grinding, conventional heating and flash calcination on the strengths of the samples were different for each type of cement in which the treated RCF were applied. There was also a difference observed in the effects of the treatments at varying replacement ratios.

To begin with, the carbonation of the RCF seemed to have a positive effect on the strengths of the SC1-75 and SC2-75. Both the SC1-CAR-75 and SC2-CAR-75 had higher strengths than the corresponding untreated samples. The SC3-CAR-75 had lower strengths than the SC3-75, which was probably caused by the carbonation of portlandite, but also the absence of an activator for the formed Si-gel could be an additional explanation. This same effect was also observed at the SC3-CAR-50 samples. Furthermore, the SC1-CAR-50 had a higher compressive strength than the SC1-50. An explanation for this is the activation of the formed Si-gel by portlandite. The SC2-CAR-50 had a lower compressive strength compared to the SC2-50. It is likely that the fly ash in the mix reacted with portlandite, due to which the Si-gel in the carbonated fines could not be activated. This might have been the reason for the lower strength of the SC2-CAR-50. The carbonation did not have any measurable effects on any of the 100% replacement samples. Improvement of the carbonation treatment and addition of a suitable activator may lead to better results. However, more research is required to draw valid conclusions about the effect of carbonation.

Next, the grinding of the RCF resulted in improvement of the strengths of the SC1 and SC2 samples with 75% and 50% replacement ratios, while it reduced the compressive strengths of all SC3 samples. No improvements were measured for the SC1-100 and SC2-100 samples. The measured higher strengths are probably caused by the increase of the specific surface area of the RCF, which enhanced the reactivity. The observed strength reduction in the SC3 samples is probably caused by carbonation of the ground RCF and absence of an activator for the possibly formed Si-gel. Nevertheless, grinding showed potential in enhancing the reactivity of RCF at 50% replacement in the CEM I variant.

Heating of the RCF increased the compressive strengths of the SC1-100 and SC2-100 samples from 0% to 2.7% and from 0% to 2.2%, respectively. This indicates that the dehydrated RCF are reactive, which corresponds to findings in literature. However, the measured values are rather low. This is probably due to

the high water demand as was also mentioned in previous studies, although this was mitigated by addition of a superplasticizer. The SC3-HT-100 had lower strength than the SC3-100 samples, which is probably caused absence or reduced presence of portlandite after rehydration reactions. Similar observations are made with the 75% and 50% replacement ratios. It was found in literature that portlandite may only partially rehydrate due to formation of stable products during storage. Nevertheless, heating shows potential in regaining reactivity. 50% replacement seems feasible in combination with BFS based on the results from this study, but more research is needed to find the optimal heating conditions and w/c ratio.

Lastly, the flash calcination significantly improved the strengths of all samples. A disadvantage of the flash calcination results was that only the SC1-FC-50 and SC3-FC-50 were made from the same flash calcined RCF, while the other samples were made from RCF of another origin. However, since the SC3-FC-50 showed similar results for both types of RCF, it is expected that the other samples would also give similar results, but this remains uncertain. Nevertheless, the flash calcination showed the greatest potential in improving the reactivity of the RCF. This study demonstrated that it is the most effective treatment across all cement types and replacement ratios. Up to 75% replacement of OPC is feasible in combination with BFS, while CEM I shows potential at 50% replacement ratio. Both combinations resulted in strength ratios close to 80% of the reference samples. Although the flash calcination significantly improved the strength at 50% replacement in the CEM II variant, the final compressive strength ratio was 59.9%.

3. *How do the strength characteristics of mortar prisms with varying recycled concrete fines percentages relate to those of standard mortar mixtures with traditional cement?*

Replacement of OPC by RCF leads to lower strengths for all replacement ratios compared to the reference mortars. The lower the replacement ratio, the higher the strength due to more OPC being present. As for the 100% replacement ratio with untreated RCF, only the SC3-100 had measurable strengths. Nevertheless, there are differences observed in the strength ratios of the SC samples compared to the reference mortars which are related to the type of cement in which the OPC is replaced by RCF. The RCF perform best in the CEM III/B samples. After that follow the CEM I samples in which the OPC is replaced by RCF and the lowest strengths were measured in the CEM II samples. This indicates that the RCF show high potential when used as an activator for BFS.

The reference mortars in this study had lower strength than expected and although there are several possible explanations related to the storage, mixing and testing of the cements, it remains uncertain what the reason was for the lower strengths. The results were still used as a reference since a consistent procedure was applied for all samples.

4. *How does the environmental impact of the recycled concrete fines relate to that of ordinary Portland cement?*

The LCA review showed that the recycled concrete fines obtained from the Smart Liberator method are a good alternative of OPC in terms of environmental impact. Since this research mainly aims to contribute to the development of a carbon neutral, circular economy, the main considered environmental impact is the GWP. The GWP of producing RCF from EoL concrete with the Smart Liberator method is 10% of the GWP of producing OPC. This value increases up to 13.6% after flash calcination. This means that the GWP of cement production can be reduced by 86% if 100% of the cement is replaced by RCF. However, based on the findings in this report, a replacement ratio of 50% is feasible in combination with CEM I, while 75% seems feasible in combination with CEM III. The combined GWP will be 0.492 kg CO<sub>2</sub>/kg cement at 50% replacement and 0.305 kg CO<sub>2</sub>/kg cement at 75% replacement. These are reduction of respectively 43.2% and 64.8%.

***Main question: To what extent can recycled concrete fines replace traditional cement?***

This study showed that their performance is not exactly the same as OPC, but rather depends on factors as the type of cement and the applied treatment. However, the RCF show great potential when used as an activator for BFS with and without any treatment.

When using the RCF as an activator for BFS cements, such as CEM III/B, relative flexural and compressive strength values of 95.5% and 70% can be reached when replacing 50% of the OPC with untreated RCF.

These values increase up to 104.5% and 77% after flash calcination of the RCF, which indicates effective activation of the BFS by RCF. From the treatments the flash calcination consistently lead to the best results for all cement types and replacement ratios. This indicates that flash calcination has the highest potential in capacity to improve the reactivity of RCF and their potential cementitious behaviour. Up to 75% replacement of OPC is feasible when combining flash calcined RCF with BFS cement. In combination with CEM I 50% replacement is feasible after flash calcination.

Carbonation of the RCF showed some potential in combination with CEM I. However, the overall strength values were rather low, possibly due to the absence of an activator for the formed Si-gel. This is also the case for the other variants. It is therefore of interest to incorporate a suitable activator for Si-gel in further research in order to draw a valid conclusion about the treatment.

Heating of the RCF resulted in a very high water demand, although this was mitigated by incorporating a superplasticizer. Nevertheless, it improved the performance of the RCF and therefore shows that reactivity can be regained.

Grinding showed some improvement at the CEM I variant, but it also led to carbonation of the fines. Therefore, addition of an activator might be needed. It may also be used in combination with a carbonation treatment to improve its reactivity.

Nevertheless, the main focus of future research should lie in using flash calcination as an upcycling treatment, since it shows the greatest potential in improving the performance of RCF.

From an environmental perspective, the recycling of concrete fines with the Smart Liberator method show great potential to significantly reduce the GWP of cement production. Based on findings in this study, replacement ratios of 50% in CEM I and 75% in CEM III seem feasible considering strength properties. These ratios lead to combined GWP of respectively 0.492 kg CO<sub>2</sub>/kg cement and 0.305 kg CO<sub>2</sub>/kg cement, corresponding to reductions of 43.2% and 64.8% relative to the GWP of OPC found in literature. At 100% replacement the GWP of cement production could be reduced by 86%. However, there are still improvements to be made in order to fully replace OPC in the future.



## 6.2. Recommendations

This part contains recommendations for further research based on the results in this report.

### *Microstructural characterization and analysis of the RCF*

Further research should focus on obtaining detailed knowledge about the properties and origin of the RCF that are used for the experiments. It is of interest to characterize the RCF with more advanced techniques, such as X-ray fluorescence and X-ray diffraction, to study the microstructural changes in the RCF after treatment and to get to know what the chemical composition is of the untreated and treated RCF. Based on that, it can be exactly known what the effect is of the treatments on the fines. In this study only a TGA was performed, but this did not provide detailed information about the microstructure of the material. Microstructural analysis can provide detailed insight into the reactions that take place in the material during the treatments, which might help in the optimization of the treatments. Furthermore, understanding the properties of the RCF can clarify their reactivity and potential hydration mechanisms. It also makes it easier to explain the observed differences in performance between the treatments.

### *Evaluation of additional performance requirements*

It is of interest to also assess other crucial material properties of concrete incorporating the RCF, such as durability, shrinkage, permeability and freeze-thaw resistance in accordance with European standards. This study only focused on the flexural and compressive strengths, at mortar level, but those properties are not sufficient to assess the potential of replacing OPC by RCF.

### *Reconfirmation of results of flash calcination results for CEM III-variants*

The effect of the flash calcination on the strength of the CEM III variant at 50% replacement was not in line with the other replacement ratios. It seems like the flash calcination did not improve the strength at 50% replacement, while it significantly improved the strengths at 75% and 100% replacement. This makes it of interest to reconfirm the results of the CEM III variants by repeating the tests.

### *Focusing on flash calcination as upcycling treatment*

This study demonstrated that flash calcination showed the greatest potential in improving the performance of RCF, showing significantly better results than other treatments. Future research should therefore mainly focus flash calcination as an upcycling treatment.

### *Optimization of treatments*

Although this study showed that flash calcination leads to significantly better results than other treatments, future research should not neglect those treatments as they also showed some potential in improving the performance of RCF. For example, literature review showed that carbonation conditions like dry or wet carbonation, temperature, pressure and relative humidity influence the carbonation efficiency. It is of interest to investigate the optimal carbonation conditions for the RCF. Also, this study showed that some carbonation occurred after grinding. It is therefore of interest to investigate the combination of grinding and carbonation. Also, conventional heating showed that this regain of reactivity is possible.

### *Combination of fine and coarse fraction*

During this research only the finest fraction of the Smart Liberator RCF was investigated. This fraction has a particle size range of 0 – 63  $\mu\text{m}$ . However, the coarser 63 – 250  $\mu\text{m}$  fraction is assumed to also contain cementitious material. Therefore it is of interest to combine both fractions to possibly enhance the performance of the material, possibly in combination with a treatment.

### *Assessment of strength development over time*

It is of interest to assess the strength development of the RCF samples over time. This can be done by performing strength tests at different ages, such as 1 day, 7 days, 28 days and 90 days. In this way the development of the strength will be clear, which might help with optimizing the performance of the material.

# Bibliography

- Abbas, A., Fathifazl, G., Burkan Isgor, O., Razaqpur, A. G., Fournier, B., & Foo, S. (2007, December 27). Proposed method for determining the residual mortar content of recycled concrete aggregates. *Journal of ASTM International*. doi:10.1520/JAI101087
- Ahmari, S., Ren, X., Toufigh, V., & Zhang, L. (2012, October). Production of geopolymetric binder from blended waste concrete powder and fly ash. *Construction and Building Materials*, pp. 718-729. doi:<https://doi.org/10.1016/j.conbuildmat.2012.04.044>
- Aïtcin, P. -C. (2016). *Science and Technology of Concrete Admixtures*. Canada: Woodhead Publishing.
- Alarcon-Ruiz, L., Platret, G., Massieu, E., & Ehrlicher, A. (2005, March). The use of thermal analysis in assessing the effect of temperature on a cement paste. *Cement and Concrete Research*, pp. 609-613.
- American Coal Ash Association. (2003). *Fly Ash Facts for Highway Engineers*. Aurora.
- Baert, G., Van Driessche, I., Hoste, S., De Schutter, G., & De Belie, N. (2007). Interaction between the Pozzolanic Reaction of Fly Ash and the Hydration of Cement. *12th International Congress on the Chemistry of Cement*. Montréal (Canada). Retrieved from <https://iccc-online.org/fileadmin/gruppen/iccc/proceedings/12/pdf/fin00486.pdf>
- Balasubramanian, A. (2017). *Size reduction by crushing methods*. Mysore: University of Mysore. doi:10.13140/RG.2.2.28195.45606
- Baldusco, R., Nobre, T., Angulo, S., Quarcioni, V., & Cincotto, M. (2019, May 17). Dehydration and Rehydration of Blast Furnace Slag Cement. *Journal of Materials in Civil Engineering*, pp. 1-13.
- Bentz, D., Peltz, M., Durán-Herrera, A., Valdez, P., & Juárez, C. (2011, January). Thermal properties of high-volume fly ash mortars and concretes. *Journal of Building Physics*, pp. 263-275.
- Betonakkoord. (2021, March 3). *Resultaten*. Retrieved from Betonakkoord: <https://www.betonakkoord.nl/wp-content/uploads/sites/43/166796/roadmap-hergebruik-betonreststromen-03.pdf>
- Betonhuis. (2020, April 20). *Cementmarkt in Nederland*. Retrieved from Betonhuis: <https://betonhuis.nl/cement/cementmarkt-nederland#:~:text=30%25%20%C3%A0%2035%25%20betreft%20portlandcementen,hoogovencement%20het%20meest%20wordt%20toegepast>.
- Bordy, A., Younsi, A., Aggoun, S., & Fiorio, B. (2017, February 1). Cement substitution by a recycled cement paste fine: Role of the residual anhydrous clinker. *Construction and Building Materials*, pp. 1-8. doi:<https://doi.org/10.1016/j.conbuildmat.2016.11.080>
- Bouwbestel. (n.d.). *Samenstelling beton 1 m3*. Retrieved from Bouwbestel: <https://www.bouwbestel.nl/blog/samenstelling-beton-1m3.html>
- Braymand, S., Roux, S., Fares, H., Déodonne, K., & Feugeas, F. (2007). Separation and Quantification of Attached Mortar in Recycled Concrete Aggregates. *Waste Biomass Valorization*, pp. 1393-1407. doi:10.1007/s12649-016-9771-2
- Bruin, M. (2023, Oktober 23). Binding CO2 bij hergebruik cementsteen. *Betoniek*, pp. 12-17. Retrieved from <https://www.betoniek-nl.tudelft.idm.oclc.org/binding-co2-bij-hergebruik-cementsteen>
- Bullard, R. (2015). *Effect of cooling rates on mineralization in Portland cement clinker*. Kansas City: University of Missouri.
- Bushi, L., & Meil, J. (2014, January). An Environmental Life Cycle Assessment of Portland-Limestone and Ordinary Portland Cements in Concrete. Canada: Athena Sustainable Materials Institute.
- Carriço, A., Bogas, J., & Guedes, M. (2020, July 30). Thermoactivated cementitious materials - a review. *Construction and Building Materials*.
- CBS. (n.d.). *Hoe groot is onze broeikasgasuitstoot?* Retrieved from CBS: <https://www.cbs.nl/nl-nl/dossier/dossier-broeikasgassen/hoe-groot-is-onze-broeikasgasuitstoot-wat-is-het-doel-#:~:text=In%202021%20bedroeg%20de%20uitstoot,1%20miljard%20kilogram%20CO2>.
- Cement Association of Canada. (n.d.). *How cement and concrete are made*. Retrieved from Website of Cement Association of Canada: <https://cement.ca/the-cement-and-concrete-industry/how-cement-and-concrete-are-made/>
- Chen, P., Wang, J., Wang, L., Xu, Y., Qian, X., & Ma, H. (2017, April 15). Producing vaterite by CO2 sequestration in the waste solution of chemical treatment of recycled concrete aggregates. *Journal of Cleaner Production*, pp. 735-742.

- Chen, W., & Brouwers, H. J. (2006). The reaction of slag in cement: theory and computer modelling. *16th Ibausil, International Conference on Building Materials (Internationale Baustofftagung)*, (pp. 0445-0454). Weimar.
- Chindaprasirt, P., Chotithanorm, C., Cao, H. T., & Sirivivatnanon, V. (2007, July). Influence of fly ash fineness on the chloride penetration of concrete. *Construction and Building Materials*, pp. 356-361. doi:10.1016/j.conbuildmat.2005.08.010
- Chindaprasirt, P., Homwuttivong, S., & Sirivivatnanon, V. (2004, July). Influence of fly ash fineness on strength, drying shrinkage and sulfate resistance of blended cement mortar. *Cement and Concrete Research*, pp. 1087-1092. doi:10.1016/j.cemconres.2003.11.021
- Chindaprasirt, P., Jaturapitakkul, C., & Sinsiri, T. (2007, July). Effect of fly ash fineness on microstructure of blended cement paste. *Construction and Building Materials*, pp. 1534-1541. doi:10.1016/j.conbuildmat.2005.12.024
- ConstructionHow. (2020, April 7). *Manufacturing Process of Cement*. (F. Khan, Editor) Retrieved from ConstructionHow: <https://constructionhow.com/manufacturing-process-of-cement/>
- Damdelen, O. (2016, March). Investigation of Different Types of Cement Material on Thermal Properties of Sustainable Concrete Mixes. *Int. Journal of Engineering Research and Application*, pp. 87-92.
- De Belie, N., & Van den Heede, P. (2012, April). Environmental impact and life cycle assessment (LCA) of traditional and 'green' concretes: Literature review and theoretical calculations. *Cement & Concrete composites*, pp. 431-442.
- Di Maio, F., Lotfi, S., Bakker, M., Hu, M., & Vahidi, A. (2017). HISER International Conference. *Advances in Recycling and Management of Construction and Demolition Waste* (pp. 209-219). Delft: TU Delft Library.
- Duan, Z., Singh, A., Xiao, J., & Hou, S. (2020, September 10). Combined use of recycled powder and recycled coarse aggregate derived from construction and demolition waste in self-compacting concrete. *Construction and Building Materials*.
- Escalante, J., Gómez, L., Johal, K., Mendoza, G., Mancha, H., & Méndez, J. (2001, June 20). Reactivity of blast-furnace slag in Portland cement blends hydrated under different conditions. *Cement and Concrete Research*, pp. 1403-1409. Retrieved from [https://doi.org/10.1016/S0008-8846\(01\)00587-7](https://doi.org/10.1016/S0008-8846(01)00587-7)
- Fink, J. (2015). Cement additives. In *Petroleum Engineer's Guide to Oil Field Chemicals and Fluid* (2nd ed., pp. 317-376). Oxford: Gulf Professional Publishing. Retrieved from <https://doi.org/10.1016/B978-0-12-803734-8.00010-2>
- Florea, M. V., Ning, Z., & Brouwers, H. J. (2013, October). *Publicaties*. Retrieved from Slimbreker: <https://www.slimbreker.nl/publicaties.html>
- Florea, M. V., Ning, Z., & Brouwers, H. J. (2014, January 15). Activation of liberated concrete fines and their application in mortars. *Construction and Building Materials*, pp. 1-12. doi:<https://doi.org/10.1016/j.conbuildmat.2013.09.012>
- Florea, M. V., Ning, Z., & Brouwers, H. J. (2014). *Smart crushing of concrete and activation of liberated concrete fines*. Eindhoven: TU/e.
- Gebremariam, A. T., Di Maio, F., Vahidi, A., & Rem, P. (2020, December). Innovative technologies for recycling End-of-Life concrete waste in the built environment. *Resources, Conservation and Recycling*. Retrieved from <https://doi.org/10.1016/j.resconrec.2020.104911>
- Giroud, V., & Pinoncely, A. (1996). Twelve years flash calciner performances of service to fuel saving and high quality in alumina calcining. *Fourth international alumina quality workshop*, (pp. 149-161). Darwin.
- Goto, S., H., F., Tsuda, T., Ooshiro, K., Yamamoto, S., & Ioku, K. (2007). Structure analysis of glass of CaO-Al<sub>2</sub>O<sub>3</sub>-SiO<sub>2</sub> system by means of NMR. *12th International Congress on the Chemistry of Cement*. Montreal: International Congress on the Chemistry of Cement.
- Gruskovnjak, A., Lothenbach, B., Holzer, L., Figi, R., & Winnefeld, F. (2006, July). Hydration of alkali-activated slag: comparison with ordinary Portland cement. *Advances in Cement Research*, pp. 119-128.
- Guan, Q., Xia, J., Wang, J., Leng, F., Zhou, Y., & Cao, C. (2021). Recycling Blast Furnace Ferronickel Slag as a Replacement for Paste in Mortar: Formation of Carboaluminate, Reduction of White Portland Cement, and Increase in Strength. *Materials*.
- Hay, R., & Celik, K. (2023, August 15). Performance enhancement and characterization of limestone calcined clay cement (LC3) produced with low-reactivity kaolinitic clay. *Construction and Building Materials*.

- Hemalatha, T., & Ramaswamy, A. (2017, March 20). A review on fly ash characteristics - Towards promoting high volume utilization in developing sustainable concrete. *Journal of Cleaner Production*, pp. 546-559.
- Hendriks, C. A., Worrel, E., De Jager, D., Blok, K., & Riemer, P. (1999). Emission Reduction of Greenhouse Gases from the Cement Industry. *Greenhouse Gas Control Technologies: Proceedings of the 4th International Conference on Greenhouse Gas Control Technologies, 30 August-2 September 1998, Interlaken, Switzerland* (pp. 939-944). Interlaken: Elsevier Science Ltd.
- Ibrahim, A. J. (2018). The Effect of Storage Period on the Physical and Mechanical Properties of Portland Cement. *Civil and Environmental Research*, pp. 1-5.
- International Energy Agency & World Business Council for Sustainable Development. (2018). *Techology Roadmap*.
- Issa, T. M., Sitarz, M., Mróz, K., & Różycki, M. (2023, March 9). Geopolymers - Base Materials and Properties of Green Structural Materials. *Materials Proceedings*. Retrieved from <https://doi.org/10.3390/materproc2023013043>
- Jawed, I., Skalny, J., Bach, T., Schubert, P., Bijen, J., Grube, H., . . . Ward, M. A. (1991). Hardened mortar and concrete with fly ash. In K. Wesche, *Fly Ash in Concrete: Properties and Performance* (pp. 42-159). Abingdon: Taylor & Francis.
- Jonkers, H. (2021). *CIE4100 - Concrete LCA dataset*. Retrieved from Brightspace TU Delft.
- Jonkers, H. M. (2021). Reader CIE4100 - Materials and Ecological Engineering. Delft: TU Delft.
- Josa, A., Aguado, A., Heino, A., Byars, E., & Cardim, A. (2004, July). Comparative analysis of available life cycle inventories of cement in the EU. *Cement and Concrete Research*, pp. 1313-1320.
- Kalinowska-Wichrowska, K., Kosior-Kazberuk, M., & Pawluczuk, E. (2020, January 1). The Properties of Composites with Recycled Cement Mortar Used as a Supplementary Cementitious Material. *Materials*, p. 64. doi:<https://doi.org/10.3390/ma13010064>
- Koullapis, K. (2022). *Environmental and economic assessment of innovative concrete recycling systems*. Delft: TU Delft.
- Kudlacz, K., Ruiz-Agudo, E., & Rodriguez-Navarro, C. (2011). Carbonation of Portlandite (Ca)(OH)<sub>2</sub> - A pseudomorphic, dissolution/precipitation replacement reaction. *Geophysical Research Abstracts*. Granada.
- Lehne, J., & Preston, F. (2018). *Making Concrete Change*. London: The Royal Institute of International Affairs.
- Li, L., & Wu, M. (2022, June). An overview of utilizing CO<sub>2</sub> for accelerated carbonation treatment in the concrete industry. *Journal of CO<sub>2</sub> Utilization*.
- Li, L., Liu, Q., Huang, T., & Peng, W. (2022, October 1). Mineralization and utilization of CO<sub>2</sub> in construction and demolition wastes recycling for building materials: A systematic review of recycled concrete aggregate and recycled hardened cement powder. *Elsevier*.
- Liu, S., Zhang, T., Guo, Y., Wei, J., & Yu, Q. (2018, May 1). Effects of SCMs particles on the compressive strength of micro-structurally designed cement paste: inherent characteristic effect, particle size refinement effect and hydration effect. *Powder Technology*, pp. 1-11.
- Lotfi, S., Deja, J., Rem, P., Mróz, R., Van Roekel, E., & Van der Stelt, H. (2013). *A Mechanical Process For In Situ Recycling of EOL Concrete*.
- Lu, B., Shi, C., Zhang, J., & Wang, J. (2018, October 20). Effects of carbonated hardened cement paste powder on hydration and microstructure of Portland cement. *Construction and Building Materials*, pp. 699-708.
- Ma, X. W., Han, Z. X., Li, X. Y., & Meng, F. L. (2009, August 1). Thermal treatment of waste concrete and the rehydration properties of the dehydrated cement paste. *Journal of Qingdao Technological University*, pp. 93-97.
- Mao, Y., Drissi, S., He, P., Hu, X., Zhang, J., & Shi, C. (2024, January). Quantifying the effects of wet carbonated recycled cement paste powder on the properties of cement paste. *Cement and Concrete Research*.
- Marchon, D., & Flatt, R. (2016). Mechanisms of cement hydration. In P. Aïtcin, & R. Flatt, *Science and Technology of Concrete Admixtures* (pp. 129-145). Cambridge: Woodhead Publishing. Retrieved from <https://doi.org/10.1016/B978-0-08-100773-0.00005-8>
- Marsh, B. K., & Day, R. L. (1988). Pozzolan and cementitious reactions of fly ash in blended cement pastes. *Cement and Concrete Research*, pp. 301-310.

- Martirena-Hernández, J., Antoni, M., Oquendo-Machado, Y., Borrajo-Perez, R., Alujas-Diaz, A., & Almenares-Reyes, R. (2024, September 18). Impact of calcination technology on properties of calcined clays. *RILEM Technical Letters*, pp. 190-197.
- Matthes, W., Vollpracht, A., Villagrán, Y., Kamali-Bernard, S., Hooton, D., Gruyaert, E., . . . De Belie, N. (2017). Ground Granulated Blast-Furnace Slag. In W. Matthes, A. Vollpracht, Y. Villagrán, S. Kamali-Bernard, D. Hooton, E. Gruyaert, . . . N. De Belie, *Properties of Fresh and Hardened Concrete Containing Supplementary Cementitious Materials* (pp. 1-53). Cham: Springer. doi:[https://doi.org/10.1007/978-3-319-70606-1\\_1](https://doi.org/10.1007/978-3-319-70606-1_1)
- Mehdizadeh, H., Cheng, X., Mo, K., & Ling, T.-C. (2022, July 22). Upcycling of waste hydrated cement paste containing high-volume supplementary cementitious materials via CO<sub>2</sub> pre-treatment. *Journal of Building Engineerin*.
- Mehdizadeh, H., Ling, T., Cheng, X., Pan, S., & Mo, K. (2021, January 28). CO<sub>2</sub> Treatment of Hydrated Cement Powder: Characterization and Application Consideration. *Journal of Materials in Civil Engineering*.
- Mehdizadeh, H., Ling, T.-C., Cheng, X., & Mo, K. (2020, April 22). Effect of particle size and CO<sub>2</sub> treatment of waste cement powder on properties of cement paste. *Canadian Journal of Civil Engineering*, pp. 522-531.
- Mehta, P. K., & Monteiro, P. J. (2006). *Concrete: Microstructure, Properties and Materials* (3rd ed.). New York: McGraw-Hill.
- Mejía, E., Navarro, P., Vargas, C., Tobón, J. I., & Osorio, W. (2016). Characterization of construction and demolition waste in order to obtain Ca and Si using a citric acid treatment. *Dyna*(83), pp. 94-101. doi:<http://dx.doi.org/10.15446/dyna.v83n199.56394>
- Mendez, J. (2019). *Thermal Properties of Cement-based Composites*. Ouro Preto: Universidade Federal de Ouro Preto.
- Menéndez, E., Andrade, C., & Vega, L. (2012, January 14). Study of dehydration and rehydration processes of portlandite in mature and young cement pastes. *Journal of Thermal Analysis and Calorimetry*, pp. 443-450.
- Miller, S. A., Horvath, A., & Monteiro, P. J. (2016, July 25). Readily implementable techniques can cut annual CO<sub>2</sub> emissions from the production of concrete by over 20%. *Environmental Research Letters*. doi:10.1088/1748-9326/11/7/074029
- Neville, A., & Brooks, J. (1987). *Concrete Technology* (2nd ed.). Harlow, England: Pearson Education.
- Noumowe, A. (1995). *Effet de hautes températures (20-600 C) sur le béton: cas particulier de béton a hautes performances*. Lyon: INSA.
- Oksri-Nelfia, L., Mahieux, P.-Y., Amiri, O., Turcry, P., & Lux, J. (2016). Reuse of recycled crushed concrete fines as mineral addition in cementitious materials. *Materials and Structures*, pp. 3239-3251. doi:<https://doi.org/10.1617/s11527-015-0716-1>
- Olagunju, B. D., & Olanrewaju, O. A. (2021). Life Cycle Assessment of Ordinary Portland Cement (OPC) Using both Problem Oriented (Midpoint) Approach and Damage Oriented Approach (Endpoint). In A. Petrillo, & F. De Felice, *Product Life Cycle - Opportunities for Digital and Sustainable Transformation* (p. 114). Naples: IntechOpen.
- Ottelé, M. (2022, May 17). Positief toekomstbeeld dankzij nieuwe recyclingmethoden beton. *Cement*, pp. 26-34.
- Pan, S. Y., Chang, E. E., Kim, H., Chen, Y. H., & Chiang, P. C. (2016, April 15). Validating carbonation parameters of alkaline solid wastes via integrated thermal analyses: Principles and applications. *Journal of Hazardous Materials*, pp. 253-262.
- Payá, J., Borrachero, M. V., Monzó, J., Soriano, L., & Tashima, M. M. (2012, May 1). A new geopolymeric binder from hydrated-carbonated cement. *Materials Letters*, pp. 223-225. doi:<https://doi.org/10.1016/j.matlet.2012.01.132>
- Pepe, M., Filho, R. D., Koenders, E. A., & Martinelli, E. (2014, October 30). Alternative processing procedures for recycled aggregates in structural concrete. *Construction and Building Materials*, pp. 124-132. doi:<http://dx.doi.org/10.1016/j.conbuildmat.2014.06.084>
- Portland Cement Association. (n.d.). *Cement & Concrete*. Retrieved from Cement: <https://www.cement.org/cement-concrete>
- Qin, L., & Gao, X. (2019, April 15). Recycling of waste autoclaved aerated concrete powder in Portland cement by accelerated carbonation. *Waste Management*, pp. 254-264.

- Rahla, K. M., Mareus, R., & Bragança, L. (2019, May 20). Comparative sustainability assessment of binary blended concretes using Supplementary Cementitious Materials (SCMs) and Ordinary Portland Cement (OPC). *Journal of Cleaner Production*, pp. 445-459.
- Richardson, I. G., Wilding, C. R., & Dickson, M. J. (1989, October). The hydration of blast furnace slag cements. *Advances in Cement Research*, pp. 147-157.
- Rijksoverheid. (n.d.). *Nederland circulair in 2050*. Retrieved from Rijksoverheid: <https://www.rijksoverheid.nl/onderwerpen/circulaire-economie/nederland-circulair-in-2050>
- Sakai, E., Miyahara, S., Ohsawa, S., Lee, S. H., & Daimon, M. (2005, June). Hydration of fly ash cement. *Cement and Concrete Research*, pp. 1135-1140. doi:10.1016/j.cemconres.2004.09.008
- Satyendra. (2013, April 10). *Blast Furnace Slag*. Retrieved from Ispatguru: <https://www.ispatguru.com/blast-furnace-slag/>
- Satyendra. (2013, April 21). *Fly Ash*. Retrieved from Ispatguru: <https://www.ispatguru.com/fly-ash/>
- Šavija, B., & Luković, M. (2016, August). Carbonation of cement paste: understanding, challenges and opportunities. *Construction and Building Materials*, pp. 285-301. Retrieved from <https://doi.org/10.1016/j.conbuildmat.2016.04.138>
- Schoon, J., De Buysser, K., Van Driessche, I., & De Belie, N. (2015, April). Fines extracted from recycled concrete as alternative raw material for Portland cement clinker production. *Cement & Concrete Composites*, pp. 70-80. Retrieved from <https://doi.org/10.1016/j.cemconcomp.2015.01.003>
- Scrivener, K., Snellings, R., & Lothenbach, B. (2016). *A Practical Guide to Microstructural Analysis of Cementitious Materials*. Boca Raton: Taylor & Francis Group.
- Shafigh, J., Asadi, I., Akhiani, A., Mahyuddin, N., & Hashemi, M. (2020, September). Thermal properties of cement mortar with different mix proportions. *Materiales de Construcción*.
- Shehata, M. H., & Thomas, M. D. (2000, July). The effect of fly ash composition on the expansion of concrete due to alkali-silica reaction. *Cement and Concrete Research*, pp. 1063-1072. Retrieved from [https://doi.org/10.1016/S0008-8846\(00\)00283-0](https://doi.org/10.1016/S0008-8846(00)00283-0)
- Shui, Z., Xuan, D., Chen, W., Yu, R., & Zhang, R. (2009, January). Cementitious characteristics of hydrated cement paste subjected to various dehydration temperatures. *Construction and Building Materials*, pp. 531-537. doi:<https://doi-org.tudelft.idm.oclc.org/10.1016/j.conbuildmat.2007.10.016>
- Singh, V. (2023). 16 - Advances . In V. Singh, *The Science and Technology of Cement and Other Hydraulic Binders* (pp. 613-624). Woodhead Publishing.
- Snellings, R., Mertens, G., & Elsen, J. (2012, January 1). Supplementary Cementitious Materials. *Reviews in Mineralogy & Geochemistry*, pp. 211-278. doi:10.2138/rmg.2012.74.6
- Song, S., Sohn, D., Jennings, H., & Mason, T. O. (2000, January). Hydration of alkali-activated ground granulated blast furnace slag. *Journal of Materials Science*, pp. 249-257.
- Tam, V. W., Soomro, M., & Evangelista, A. C. (2021, June 21). Quality improvement of recycled concrete aggregate by removal of residual mortar: A comprehensive review of approaches adopted. *Construction and Building Materials*. doi:<https://doi.org/10.1016/j.conbuildmat.2021.123066>
- Teune, I., Schollbach, K., Florea, M., & Brouwers, H. (2023, November 15). Carbonation of hydrated cement: The impact of carbonation conditions on CO<sub>2</sub> sequestration, phase formation, and reactivity. *Journal of Building Engineering*.
- The Guardian. (2019, February 25). *Concrete: the most destructive material on Earth*. Retrieved from The Guardian: <https://www.theguardian.com/cities/2019/feb/25/concrete-the-most-destructive-material-on-earth>
- The Netherlands Standardization Institute. (2011, Oktober). *Documenten*. Retrieved from NEN Connect: <https://connect.nen.nl/Portal>
- Tonelli, M., Camerini, R., Baglioni, P., & Ridi, F. (2024, August 16). Activation of ground granulated blast-furnace slag with calcium hydroxide nanoparticles towards the consolidation of adobe. *Construction and Building Materials*.
- Topic, J., Fládr, J., & Prošek, Z. (2017, March). Flexural and Compressive Strength of the Cement Paste with Recycled Concrete Powder. *Advanced Materials Research*, pp. 65-69. doi:<https://doi.org/10.4028/www.scientific.net/amr.1144.65>
- Topič, J., Prošek, Z., & Plachý, T. (2017). Influence of increasing amount of recycled concrete powder on mechanical properties of cement paste. *IOP Conference Series: Materials Science and Engineering* 236. Prague: IOP Publishing Ltd.
- Uygunoğlu, T. (2011, July). Reuse of hydrated mortar as partial replacement material in cement. *Advances in Cement Research*, pp. 113-122. doi:<https://doi.org/10.1680/adcr.9.00053>

- Van der Wegen, G. (2020, February 11). Een overzicht van innovatieve recyclingmethoden. *Betoniek*, pp. 12-16.
- Van Jaarsveld, J. G., Van Deventer, J. S., & Lorenzen, L. (1997, July). The potential use of geopolymeric materials to immobilise toxic metals: Part 1. Theory and applications. *Minerals Engineering*, pp. 659-669. Retrieved from [https://doi.org/10.1016/S0892-6875\(97\)00046-0](https://doi.org/10.1016/S0892-6875(97)00046-0)
- Verweij, M. (2020, September 23). Terugwinnen van cement uit beton. *Betoniek*, pp. 28-33. Retrieved from <https://www.betoniek.nl/terugwinnen-van-cement-uit-beton>
- Wang, A., Zhang, C., & Sun, W. (2004, November). Fly ash effects: II. The active effect of fly ash. *Cement and Concrete Research*, pp. 2057-2060. doi:<https://doi.org/10.1016/j.cemconres.2003.03.001>
- Wang, J., Mu, M., & Liu, Y. (2018, November 30). Recycled cement. *Construction and Building Materials*, pp. 1124-1132.
- Wang, J., Xu, L., Li, M., He, H., Wang, Y., Xiang, D., . . . Zhao, H. (2022, July 1). Effect of pre-carbonation on the properties of cement paste subjected to high temperatures. *Journal of Building Engineering* .
- Wesche, K. (1991). *Fly Ash in Concrete: Properties and Performance*. New York: Taylor & Francis.
- Wong, H., Pappas, A., Zimmerman, R., & Buenfeld, N. (2011, October). Effect of entrained air voids on the microstructure and mass transport properties of concrete. *Cement and Concrete Research*, pp. 1067-1077.
- Xu, Y., & Chung, D. (2000, June). Improving silica fume cement by using silane. *Cement and Concrete Research*, pp. 1305-1311.
- Xu, Z., Zhang, Z., Huang, J., Yu, K., Zhong, G., Chen, F., . . . Wang, Y. (2022, September 5). Effects of temperature, humidity and CO<sub>2</sub> concentration on carbonation of cement-based materials: A review. *Construction and Building materials*.
- Zajac, M., Song, J., Ullrich, P., Skocek, J., Ben Haha, M., & Skibsted, J. (2024, January). High early pozzolanic reactivity of alumina-silica gel - A study of the hydration of composite cements with carbonated recycled concrete paste. *Cement and Concrete Research*.
- Zentar, R., & Almokdad, M. (2024, January 12). Flash-calcined sediments versus raw sediments: A comparative life cycle assessment of SCMs. *Construction and Building Materials*.
- Zhang, H. (2011). Cement. In H. Zhang, *Building materials in civil engineering* (pp. 46-80). Cambridge: Woodhead Publishing.

# Appendices

## Appendix A: Cement standards

In this section the applicable rules for OPC and blast furnace cement will be discussed. The rules that are applicable to the cement types may vary per continent or per country. Therefore, multiple cement standards exist around the world. The cement standard that is of interest in this research is the European standard EN 197-1, since the cementitious material which is investigated comes from the Dutch concrete industry. In the Netherlands, the European standard EN 197-1 is also referred to as the Dutch standard NEN-EN 197-1 (The Netherlands Standardization Institute, 2011). The EN 197-1 standard defines and gives the specifications and conformity criteria for common cements. In this standard reference is made to EN 196 norms, which specify the methods of testing cement.

### Composition

In the five main cement types as mentioned in section 2.2, the European standard EN 197-1 distinguishes 27 products in which the composition differs for each product. Ordinary Portland cement or CEM I has only one product, also named CEM I. Portland-composite cement or CEM II is available in 19 different types. Of interest for this thesis is CEM II/B-V. Blast furnace cement or CEM III is available in three types: CEM III/A, CEM III/B and CEM III/C. CEM III/B is of interest for this thesis. The main constituents of CEM I, CEM II/B-V and CEM III/B are Clinker (K), Blast furnace slag (S) and Siliceous fly ash (V). Table A1 shows the values for the composition of the mentioned cement types in percentages by mass.

**Table A1: Composition of CEM I, CEM II/B-V and CEM III/B cements according to EN 197-1**

Main type	Notation	Main constituents			Minor additional constituents
		Clinker (K)	Blast furnace slag (S)	Siliceous fly ash (V)	
<b>CEM I</b>	CEM I	95-100	-	-	0-5
<b>CEM II</b>	CEM II/B-V	65-79	-	21-35	0-5
<b>CEM III</b>	CEM III/B	20-34	66-80	-	0-5

EN 197-1 describes the minor additional constituents as specially selected materials. These can consist of inorganic mineral materials from nature or derived from the clinker production process. Other possible minor additional constituents for cements are, unless specified as main constituent, the following materials:

- Portland cement clinker (K)
- Granulated blast furnace slag (S)
- Pozzolanic materials (P, Q)
- Fly ashes (V, W)
- Burnt shale (T)
- Limestone (L, LL)
- Silica fume (D)

### *Minor additional constituents*

The minor additional constituents enhance the physical properties of cement after being properly prepared and because of their particle size distribution. In respect of hydraulic or pozzolan properties, the minor additional constituents are not subject to any requirements. They can be inert or have pozzolanic, slightly hydraulic or latent hydraulic properties. However, there are other applicable requirements. Depending on their manufacturing or delivery condition, the minor additional constituents must be correctly processed. This includes selection, homogenization, drying, and comminution. They may not significantly raise the cement's water need, lower the reinforcement's corrosion protection, or in any other manner weaken the material's resistance to deterioration.



### Additives

Next to the minor additional constituents, there are the so called additives. These are added to the cement for improvement of its properties or manufacture. Their maximum quantity is, except for pigments, limited to 1.0% by mass of the cement. Organic additives on a dry basis may not exceed 0.2% by mass of the cement. Higher quantities are possible, but they must be explicitly mentioned by the manufacturer. The additives may not worsen the qualities of cement, concrete, or mortar manufactured from cement, or stimulate corrosion of the reinforcement. The type of additive that is incorporated in cement is dependent on the application of the cement. Examples of additives are accelerators, gels, extenders, retarders, foamers, dispersants, fluid-loss additives and weighting agents (Fink, 2015).

### Other requirements

The European standard EN 197-1 distinguishes mechanical, physical, chemical and durability requirements for the cements.

### Mechanical and physical requirements

Figure A1 gives shows the mechanical and physical requirements for the following three standard cement strength classes: class 32.5, class 42.5 and class 52.5. The letters L, N and R are classes of standard cement classes and refer to respectively low early strength, ordinary early strength and high early strength, of which class L is only applicable for CEM III cements.

Strength class	Compressive strength MPa				Initial setting time	Soundness (expansion)
	Early strength		Standard strength			
	2 days	7 days	28 days		min	mm
32,5 L <sup>a</sup>	-	≥ 12,0	≥ 32,5	≤ 52,5	≥ 75	≤ 10
32,5 N	-	≥ 16,0				
32,5 R	≥ 10,0	-				
42,5 L <sup>a</sup>	-	≥ 16,0	≥ 42,5	≤ 62,5	≥ 60	
42,5 N	≥ 10,0	-				
42,5 R	≥ 20,0	-				
52,5 L <sup>a</sup>	≥ 10,0	-	≥ 52,5	-	≥ 45	
52,5 N	≥ 20,0	-				
52,5 R	≥ 30,0	-				

<sup>a</sup> Strength class only defined for CEM III cements.

Figure A1: Mechanical and physical requirements of standard cement strength classes according to EN 197-1

Another physical requirement which is not included in the figure is the heat of hydration. The heat of hydration of low heat common cements, identified by the notation 'LH', may not exceed the characteristic value of 270 J/g. This should be determined in accordance with either one of the following European standards: EN 196-8 at 7 days or EN 196-9 at 41 hours.

### Chemical requirements

EN 197-1 gives requirements for the following chemical properties of cement: loss on ignition, insoluble residue, sulfate content, chloride content and pozzolanicity. These requirements are listed as characteristic values in Figure A2. The second column lists the European standards that are applicable to the tests of the considered properties.

1	2	3	4	5
Property	Test reference	Cement type	Strength class	Requirements <sup>a</sup>
Loss on ignition	EN 196-2	CEM I CEM III	All	≤ 5,0 %
Insoluble residue	EN 196-2 <sup>b</sup>	CEM I CEM III	All	≤ 5,0 %
Sulfate content (as SO <sub>3</sub> )	EN 196-2	CEM I CEM II <sup>c</sup> CEM IV CEM V	32,5 N 32,5 R 42,5 N	≤ 3,5 %
			42,5 R 52,5 N 52,5 R	≤ 4,0 %
		CEM III <sup>d</sup>	All	
Chloride content	EN 196-2	all <sup>e</sup>	All	≤ 0,10 % <sup>f</sup>
Pozzolanicity	EN 196-5	CEM IV	All	Satisfies the test

<sup>a</sup> Requirements are given as percentage by mass of the final cement.

<sup>b</sup> Determination of residue insoluble in hydrochloric acid and sodium carbonate.

<sup>c</sup> Cement types CEM II/B-T and CEM II/B-M with a T content > 20 % may contain up to 4,5 % sulfate (as SO<sub>3</sub>) for all strength classes.

<sup>d</sup> Cement type CEM III/C may contain up to 4,5 % sulfate.

<sup>e</sup> Cement type CEM III may contain more than 0,10 % chloride but in that case the maximum chloride content shall be stated on the packaging and/or the delivery note.

<sup>f</sup> For pre-stressing applications cements may be produced according to a lower requirement. If so, the value of 0,10 % shall be replaced by this lower value which shall be stated in the delivery note.

Figure A2: Chemical requirements for common cements according to EN 197-1

#### Durability requirements

The choice of cement has an influence on the durability of concrete, mortar and grouts. This is particularly the case in extreme environmental conditions. Examples of the properties that determine the durability of the materials are chemical resistance, frost resistance and protection of reinforcement. However, there are no specific requirements for cements, but the choice of cement should follow the appropriate standards for concrete or mortar which are valid in the environment where the concrete or mortar is used.

However, EN 197-1 gives additional requirements for sulfate resisting (SR) cements, which are listed in Figure A3.

1	2	3	4	5
Property	Test reference	Cement type	Strength class	Requirements <sup>a</sup>
Sulfate content (as SO <sub>3</sub> )	EN 196-2	CEM I-SR 0 CEM I-SR 3 CEM I-SR 5 <sup>b</sup>	32,5 N 32,5 R 42,5 N	≤ 3,0 %
		CEM IV/A-SR CEM IV/B-SR	42,5 R 52,5 N 52,5 R	≤ 3,5 %
C <sub>3</sub> A in clinker <sup>c</sup>	EN 196-2 <sup>d</sup>	CEM I-SR 0	All	= 0%
		CEM I-SR 3		≤ 3 %
		CEM I-SR 5		≤ 5 %
	- <sup>e</sup>	CEM IV/A-SR CEM IV/B-SR		≤ 9 %
Pozzolanicity		EN 196-5	CEM IV/A-SR CEM IV/B-SR	All

<sup>a</sup> Requirements are given as percentage by mass of the final cement or clinker as defined in the table.

<sup>b</sup> For specific applications cements CEM I-SR 5 may be produced according to a higher sulfate content. If so the numerical value of this requirement for higher sulfate content shall be declared on the delivery note.

<sup>c</sup> The test method for the determination of C<sub>3</sub>A content of clinker from an analysis of the final cement is under development in CEN/TC51.

<sup>d</sup> In the specific case of CEM I, it is permissible to calculate the C<sub>3</sub>A content of clinker from the chemical analysis of the cement. The C<sub>3</sub>A content shall be calculated by the formula: C<sub>3</sub>A = 2,65 A – 1,69 F (see 5.2.1).

<sup>e</sup> Until the test method is finalised the C<sub>3</sub>A content of clinker (see 5.2.1) shall be determined on the basis of the analysis of clinker as part of the manufacturer's Factory Production Control (EN 197-2:2000, 4.2.1.2).

Figure A3: Requirements for sulfate resisting cements according to EN 197-1

## Requirements for different applications

This section discusses the existing rules and requirements according to European standards for the applications mentioned in the previous paragraph.

### Partial cement substitution/inert filler (type I addition)

According to NEN-EN 206, the general suitability as type I addition is established for:

- Filler aggregate conforming to EN 12620 or [A1>EN 13055<A1]
- Pigments that comply with EN 12878

The European standard NEN-EN 12620 lists the essential characteristics and their requirements for fillers which are intended to be used for preparation of concrete for use in civil engineering works, such as roads and buildings. The following six characteristics are essential for fillers in concrete:

#### 1. Fineness/particle size and density:

Figure A4 shows the grading requirements for fillers according to NEN-EN 12620. These requirements are assessed with the air jet sieving test method described in NEN-EN 933-10. There are no specific requirements given for the particle density. However, NEN-EN 12620 states that, when required, the particle density shall be determined in compliance with EN 1097-6 and the obtained results should be disclosed upon request, stating the method of determination and the calculations used.

Sieve size mm	Percentage passing by mass	
	Overall range for individual results	Producer's maximum declared range <sup>a</sup>
2	100	–
0,125	85 to 100	10
0,063	70 to 100	10

<sup>a</sup> Declared grading range on the basis of the last 20 values (see Table H.1, line 1). 90 % of the results shall be within this range, but all the results shall be within the overall grading range (see column 2 above).

Figure A4: Grading requirements for filler aggregate

#### 2. Composition/content:

For the sake of durability and safety it is important to control and limit the chloride content in concrete. The water-soluble chloride ion content of natural aggregates for concrete shall, when required, be determined in compliance with NEN-EN 1744-1, clause 7. However, for recycled aggregates chlorides may be combined in the calcium aluminate and other phases, which are unlikely to be extracted using water in the procedure described in NEN-EN 1744-1, clause 7. Chloride ion contents are likely to be low for most recycled aggregates. For recycled aggregates, determination of the acid-soluble chloride ion content should be done in compliance with NEN-EN 1744-5.

If necessary, the acid-soluble sulfate content of aggregates and filler aggregates used in concrete should be determined in compliance with NEN-EN 1744-1, clause 12, and declared based on the appropriate category mentioned in Figure A5.

Aggregate	Acid soluble sulfate content Percentage by mass	Category AS
Aggregates other than air-cooled blastfurnace slag	≤ 0,2	AS <sub>0,2</sub>
	≤ 0,8	AS <sub>0,8</sub>
	> 0,8	AS <sub>Declared</sub>
	No requirement	AS <sub>NR</sub>
Air-cooled blastfurnace slag	≤ 1,0	AS <sub>1,0</sub>
	> 1,0	AS <sub>Declared</sub>
	No requirement	AS <sub>NR</sub>

Figure A5: Categories for maximum values of acid-soluble sulfate content

Furthermore, the total sulfur content of the aggregates and filler aggregates, determined in compliance with NEN-EN 1744-1, clause 11, may not exceed the following values:

- 2 % S by mass for air-cooled blast furnace slag.
- 1 % S by mass for aggregates other than air-cooled blast furnace slag

If the aggregates contain pyrrhotite, which is an unstable form of iron sulfide (FeS), special precautions are necessary. In such cases, a maximum total sulfur content of 0,1 % as S shall be applicable. Aggregates and filler aggregates that contain organic or other substances in proportions that alter the rate of setting and hardening of concrete shall be assessed for the effect on stiffening time and compressive strength in compliance with NEN-EN 1744-1, 15.3. These proportions must not:

- Increase the stiffening time of mortar test specimens by more than 120 min;
- Decrease the compressive strength of mortar test specimens by more than 20 % at 28 days

The presence of organic material should be determined in accordance with NEN-EN 1744-1. Also, the presence of lightweight contaminators that alter the rate of setting and hardening of concrete shall be tested in accordance with this standard.

If deemed necessary, an analysis of the impact of water-soluble components in the recycled aggregates on the cement paste's initial setting time shall be conducted, following EN 1744-6 guidelines. The alterations in initial setting time, denoted by  $t_e$ , must satisfy the criteria specified in Figure A6.

Change in initial setting time, $t_e$ (min)	Category (A)
$\leq 10$	A10
$\leq 40$	A40
$> 40$	A <sub>Declared</sub>
No requirement	A <sub>NR</sub>

**Figure A6: Categories for influence of water-soluble materials from recycled aggregates on the initial setting time of cement paste**

### 3. Cleanliness

The declaration of fines content in filler aggregate shall conform to the respective category specified in Figure A7 as determined by the method outlined in EN 933-1. The requirements for fines content of filler aggregate shall comply with the provisions outlined in Figure A4.

Aggregate	0,063 mm sieve Percentage passing by mass	Category $f$
Coarse aggregate	$\leq 1,5$	$f_{1,5}$
	$\leq 4$	$f_4$
	$> 4$	$f_{\text{Declared}}$
	No requirement	$f_{\text{NR}}$
Natural graded 0/8 mm aggregate	$\leq 3$	$f_3$
	$\leq 10$	$f_{10}$
	$\leq 16$	$f_{16}$
	$> 16$	$f_{\text{Declared}}$
	No requirement	$f_{\text{NR}}$
All-in aggregate	$\leq 3$	$f_3$
	$\leq 11$	$f_{11}$
	$> 11$	$f_{\text{Declared}}$
	No requirement	$f_{\text{NR}}$
Fine aggregate	$\leq 3$	$f_3$
	$\leq 10$	$f_{10}$
	$\leq 16$	$f_{16}$
	$\leq 22$	$f_{22}$
	$> 22$	$f_{\text{Declared}}$
	No requirement	$f_{\text{NR}}$

Figure A7: Categories for maximum values of fines content

#### 4. Volume stability

If the properties of the aggregate lead to disruptive shrinkage cracking of concrete, the drying shrinkage associated with aggregates used in structural concrete must be evaluated in accordance with EN 1367-4. The drying shrinkage should not exceed 0.075% as required, and the results of the test must be reported. For recycled aggregates, Annex A should also be considered.

For air-cooled blast furnace slag aggregate, the following requirements apply:

- When tested in compliance with NEN-EN 1744-1998, 19.1, air-cooled blast furnace slag aggregate must be free from dicalcium silicate disintegration
- When tested in compliance with NEN-EN 1744-1998, 19.2, air-cooled blast furnace slag aggregate must be free from iron disintegration

#### 5. Release of other dangerous substances

Documentation providing information on the origin and nature of the raw material, including maps illustrating the location and extraction strategy, shall be provided. The producer is accountable for ensuring that the content of hazardous substances identified is in compliance with the limits set by the relevant provisions applicable in the place where the aggregate will be used.

For recycled aggregates an input control of the raw material to be recycled should also be documented. The procedures for input control during recycling must specify the following:

- Nature of the raw material
- Source and place of origin (the processing depot suffices for the source of recycled aggregates)
- Supplier and transporting agent

The following requirements must be met by the factory production control system:

- Procedures must be in place to identify and control materials, which can include measures for maintaining and adjusting processing equipment, inspecting or testing materials during processing, and modifying processes during inclement weather.
- Procedures must be in place to identify and control hazardous materials identified in H.3.3 to ensure that they do not exceed applicable limits.

- Procedures must be in place to ensure that materials are put into stock in a controlled manner and that storage locations and contents are identified.
- Procedures must be in place to ensure that materials taken from stock have not deteriorated to a point where their conformity is compromised.
- The product must be identifiable up to the point of sale in terms of source and type.

## 6. Durability against freeze-thaw

To comply with the requirement for frost resistant concrete in freezing and thawing conditions, the aggregate's resistance to freezing, as determined by EN 1367-1 or EN 1367-2, shall be declared according to the relevant category stated in Figure A8 or Figure A9. However, it should be noted that this clause applies to coarse aggregates, which are not considered in this study.

Freeze-thaw Percentage loss of mass <sup>a</sup>	Category <i>F</i>
≤ 1	<i>F</i> <sub>1</sub>
≤ 2	<i>F</i> <sub>2</sub>
≤ 4	<i>F</i> <sub>4</sub>
> 4	<i>F</i> <sub>Declared</sub>
No requirement	<i>F</i> <sub>NR</sub>
<sup>a</sup> In extreme situations of cold weather and/or salt or de-icing salt saturation, then tests using a salt solution or urea as detailed in <a href="#">A1</a> EN 1367-1:2007 <a href="#">A1</a> , annex B, may be more appropriate. The limits in this table would not apply.	

Figure A8: Categories for maximum values of freeze-thaw resistance

Magnesium sulfate value Percentage loss of mass	Category <i>MS</i>
≤ 18	<i>MS</i> <sub>18</sub>
≤ 25	<i>MS</i> <sub>25</sub>
≤ 35	<i>MS</i> <sub>35</sub>
> 35	<i>MS</i> <sub>Declared</sub>
No requirement	<i>MS</i> <sub>NR</sub>

Figure A9: Categories for maximum magnesium sulfate soundness

### **Cementitious material (type II addition)**

NEN-EN 206 establishes the general suitability as type II addition for:

- Fly ash conforming to EN 450-1
- Silica fume conforming to EN 13263-1
- Ground granulated blast furnace slag conforming to EN 15167-1

### The k-value concept:

The amounts of both type I and type II additions to be used in concrete should be based on initial research as described in appendix A of NEN-EN 206. The k-value concept is used to determine the suitability of type II additions in concrete. This concept is based on comparing the durability behavior of a reference concrete with a certain type of cement and a test concrete in which the cement has been partially replaced by a filler as a function of the water-cement ratio and the filler content. Another possibility is, if applicable, to use strength as a substitute criterion for durability.

Two other concepts that may be used in combination with the k-value concept are the concept for the equivalent performance of concrete (ECPC) and the concept for the equivalent performance of combinations (EPCC). When complying with these concepts, type I and II additions other than the generally suitable fillers may also be taken into account.

The k-value concept allows for the inclusion of type II fillers by replacing the water-cement ratio with 'water-(cement + k \* filler) ratio'. Additionally, the amount of (cement + k \* filler) should be at least equal to the minimum cement content required for the environmental class.

There are different requirements for the previously mentioned type II additions, which also depend on the type of cement that is being used in combination with the type II addition. Tables A2, A3 and A4 list the requirements for the generally suitable type II additions.

**Table A2: K-value of fly ash according to NEN-EN 206 and NEN 8005**

<b>Type II addition</b>	Fly ash in compliance with EN 450-1
<b>Requirements according to NEN-EN 206</b>	<ul style="list-style-type: none"> <li>▪ A k-value of 0.4 is allowed for concrete which contains CEM I and CEM II/A cements according to EN 197-1.</li> <li>▪ In combination with CEM I, the maximum allowed amount of fly ash that may be taken into account should meet the following requirement:               <ul style="list-style-type: none"> <li>- fly ash/cement mass ratio <math>\leq 0.33</math></li> </ul> </li> <li>▪ In combination with CEM II/A, the maximum allowed amount of fly ash that may be taken into account should meet the following requirement:               <ul style="list-style-type: none"> <li>- fly ash/cement mass ratio <math>\leq 0.25</math></li> </ul> </li> <li>▪ If a larger amount of fly ash is used, the extra amount may not be used for the calculation of the water-(cement + k * fly ash) ratio and the minimum cement content.</li> </ul>
<b>Requirements according to NEN 8005</b>	<ul style="list-style-type: none"> <li>▪ In the Netherlands, a k-value of 0.2 is allowed for concrete which contains CEM III/A and/or CEM III/B and fly ash with a binder function for all strength and environmental classes.</li> <li>▪ The maximum allowed amount of fly ash in combination with CEM III/A and/or CEM III/B should meet the following requirement:               <ul style="list-style-type: none"> <li>▪ fly ash/cement mass ratio <math>\leq 0.25</math></li> </ul> </li> <li>▪ When using a combination of different cements, the k-value can be determined with linear interpolation between the k-values based on the mass ratios of the cements.</li> </ul> <p>The above also applies to fly ashes that do not comply with NEN-EN 450-1, but for which the suitability for usage in concrete is proved with the concepts in NEN-EN 206.</p>

**Table A3: k-value of silica fume according to NEN-EN 206**

<b>Type II addition</b>	Class 1 silica fume in compliance with EN 13263-1
<b>Requirements according to NEN-EN 206</b>	<ul style="list-style-type: none"> <li>▪ For concrete which contains CEM I and CEM II/A (except for cement that contains silica fume) in compliance with EN 197-1, the following k-values are allowed:               <ul style="list-style-type: none"> <li>▪ k = 2.0 for a required water-cement ratio <math>\leq 0.45</math></li> <li>▪ k = 2.0 for a required water-cement ratio <math>&gt; 0.4</math>, except for environmental classes XC and XF: in these cases k = 1.0</li> </ul> </li> <li>▪ The maximum allowed amount of class 1 silica fume that may be taken into account should meet the following requirement:               <ul style="list-style-type: none"> <li>▪ silica fume/cement mass ratio <math>\leq 0.11</math></li> </ul> </li> </ul>



	<ul style="list-style-type: none"> <li>▪ If a larger amount of class 1 silica fume is used, the extra amount may not be used for the calculation of the water-(cement + k * fly ash) ratio and the minimum cement content.</li> <li>▪ The amount of cement may not be lowered with more than 30 kg/m<sup>3</sup> below the minimum required cement content according to the applying environmental class.</li> </ul>
--	--

**Table A4: k-value of silica fume according to NEN-EN 206 and NEN 8005**

<b>Type II addition</b>	Ground granulated blast furnace slag in compliance with EN 15167-1
<b>Requirements according to NEN-EN 206</b>	<ul style="list-style-type: none"> <li>▪ The k-value and the maximum allowed amount of ground granulated blast furnace slag (GGBFS) that should be accounted for, should comply with the regulations that apply at the location of use.</li> </ul>
<b>Requirements according to NEN 8005</b>	<ul style="list-style-type: none"> <li>▪ No k-value has been established for GGBFS in the Netherlands.</li> </ul>

Concept for the equivalent performance of concrete (ECPC):

The 'concept for the equivalent performance of concrete' may only be applied to concrete with cement types that comply with EN 197-1 in combination with one or more fillers. It allows for deviation from the minimum cement content and maximum water-cement ratio requirements if specific fillers and types of cement are used, provided that their production location and properties are clearly defined and documented.

Considering the specified requirements in NEN EN 206-1, it should be demonstrated that the concrete performs equally when comparing it to a reference cement that meets the requirements for the applying environmental class. Special attention should be given to the performance of the concrete when exposed to environmental influences.

NEN 8005 notes that the CUR-recommendation 48 may be consulted for the elaboration of the ECPC.

Concept for the equivalent performance of combinations (EPCC):

In accordance with the principles of the "concept for equivalent performance of combinations," a specified set of combinations of cement that meets EN 197-1 and filler(s) with proven suitability (as stated in 5.1.1) is permissible. These combinations can be fully considered concerning the prescribed requirements for the concrete's maximum water-cement ratio and minimum cement content. The methodology consists of the following steps:

1. Identify a type of cement that complies with a European standard for cement and has the same or a comparable composition as the intended combination;
2. Evaluate whether the concrete types produced with the combination are comparable in terms of strength and durability to concrete made for the relevant environmental class with the identified type of cement;
3. Implement a production control that ensures that these requirements for the concrete types produced with the combination are documented and implemented.

**Raw material for geopolymerization**

According to Van Jaarsveld et al. (1997), any material that contains pozzolanic compounds or a source of silica and alumina that can dissolve easily in an alkaline solution can be used as a source of geopolymer precursor species, making it suitable for geopolymerization. A simple conclusion that follows from this statement is that it is the only requirement for a material to be usable as a raw material for geopolymerization. However, the choice of the raw material depends on several factors, such as costs, type of application and availability (Issa et al., 2023). Two types of raw materials can be distinguished: primary raw materials and secondary raw materials. The secondary raw materials are of interest for this study.

Issa et al. (2023) mention four main secondary raw materials for geopolymerization: fly ash, granulated blast furnace slag, red mud and rice husk ash. Especially fly ash is of main interest for geopolymer synthesis due to its unique characteristics, such as high workability, low water demand, widespread availability and aluminosilicate content. Some other raw materials mentioned by Issa et al. (2023) are steel slag, silica fume, high magnesium nickel slag, coal gangue, waste glass and volcanic ash.

The properties of elements based on geopolymers can be superior and more durable than structures formed by interconnecting Portland cement. The microstructure of geopolymer materials is particularly affected by the composition of the amorphous phase, the oxide content and, most importantly, the fineness of the particles

Important to mention is that geopolymers need activation solutions. The presence of strongly alkaline activators is essential, due to the fact that they facilitate the dissolution of the aluminosilicate source, promoting the creation of stable hydrates with minimal solubility and the development of a dense structure with these hydrates (Issa et al., 2023).

Although Alkali activators are the most common, there are also some compositions that rely on usage of acidic activators. Moreover, previous research indicated that acid-based geopolymers have superior mechanical properties and higher temperature resistance compared to alkali-based geopolymers (Issa et al., 2023).

### ***Admixture for improving concrete sustainability***

The general requirements for admixtures for concrete, grout and mortar are covered by NEN-EN 934-1. This European standard covers the requirements that are common to all admixtures. NEN-EN 934 sections 2 to 5 provide a detailed explanation of the specific requirements that define an admixture's performance in a cementitious mix. Figure A10 shows the general requirements from NEN-EN 934-1.

	Property	Test method	Requirements
1	Homogeneity <sup>a</sup>	Visual	Homogeneous when used. Segregation shall not exceed the limit stated by the manufacturer.
2	Colour <sup>a</sup>	Visual	Uniform and similar to the description declared by the manufacturer.
3	Effective component <sup>a</sup>	EN 480-6 <sup>b</sup>	Infra red spectra to show no significant change with respect to the effective component when compared to the reference spectrum provided by the manufacturer.
4	Absolute density <sup>a</sup> (for liquid admixtures only)	ISO 758 <sup>c</sup>	$D \pm 0,03$ if $D > 1,10$ kg/l $D \pm 0,02$ if $D \leq 1,10$ kg/l where D is manufacturer's stated value of density.
5	Conventional dry material content <sup>a</sup>	EN 480-8 <sup>d</sup>	$0,95T \leq X \leq 1,05T$ if $T \geq 20$ % $0,90T \leq X \leq 1,10T$ if $T < 20$ % T is manufacturer's stated value % by mass; X is test result % by mass.
6	pH value <sup>a</sup> (for liquid admixtures only)	ISO 4316	Manufacturer's stated value $\pm 1$ or within manufacturer's stated range.
7	Total chlorine <sup>a†</sup>	EN ISO 1158 <sup>g</sup>	Either $\leq 0,10$ % by mass <sup>e</sup> or not above manufacturer's stated value.
8	Water soluble chloride <sup>a</sup>	EN 480-10	Either $\leq 0,10$ % by mass <sup>e</sup> or not above manufacturer's stated value.
9	Alkali content (Na <sub>2</sub> O equivalent) <sup>a</sup>	EN 480-12	Not above manufacturer's stated maximum value in % by mass.
10	Corrosion behaviour	EN 480-14	See clause 5.
11	Silicon dioxide SiO <sub>2</sub> content <sup>a h i</sup>	EN 196-2 (procedure 13)	Not above manufacturer's stated maximum value in % by mass. 0

<sup>a</sup> Manufacturer's stated values and characteristics shall be provided in writing to the user upon request.

<sup>b</sup> If the method in EN 480-6 is not suitable, the manufacturer shall specify a documented alternative test method.

<sup>c</sup> ISO 758 is the reference method. Another method may be used provided that it can show essentially the same results as the method in ISO 758.

<sup>d</sup> If the method in EN 480-8 is not suitable, the manufacturer shall specify a documented alternative test method.

<sup>e</sup> Where the chloride content is  $\leq 0,10$  % by mass the admixture may be described as "chloride free".

<sup>f</sup> If there is no significant difference between the total chlorine and the water soluble chloride content, only the water soluble chloride content should be determined in subsequent tests on the admixture involved.

<sup>g</sup> The procedure in EN ISO 1158 shall be modified as follows:

- Increase the sample size in method B to 0,1 g of dry admixture;
- Use silver nitrate and ammonium thiocyanate solutions at 0,01 N.

<sup>h</sup> The silicon dioxide content is only required when silica (see A.1) is a constituent intended to exceed 5 % by mass of the admixture.

<sup>i</sup> This requirement does not apply to natural sand.

**Figure A10: General requirements for admixtures**

## Appendix B: Mixing procedure according to NEN-EN 196-1

1. Weigh the cement and water by means of the balance
2. Carefully pour the water and cement into the mixer bowl, ensuring that no water or cement is lost. The addition should be completed within 10 seconds.
3. Immediately after the water and cement come into contact, start the mixer at a low speed and simultaneously initiate the timing of the mixing stages. Additionally, record the time to the nearest minute as the "zero time," which will serve as the reference point for demoulding specimens and determining strength. After 30 seconds of initial mixing, gradually add the sand over the next 30 seconds. Switch the mixer to high speed and continue mixing for an additional 30 seconds.
4. Pause the mixer for 90 seconds. During the first 30 seconds, use a rubber or plastic scraper to remove any mortar adhering to the walls and bottom of the bowl, and place it back in the middle of the bowl.
5. Resume mixing at high speed for 60 seconds.

After mixing, the test specimens are moulded. In this research prisms with a size of 40 mm × 40 mm × 160 mm are used. The procedure for preparing these specimens is as follows:

1. Prepare the mortar mixture according to the specified procedure.
2. Immediately after preparing the mortar, proceed to mould the specimens.
3. Securely clamp the mould and hopper onto the jolting table.
4. Using a suitable scoop, introduce the first layer of mortar into each mould compartment in one or more increments. Each layer should be approximately 300 grams.
5. Spread the mortar layer evenly by utilizing a large spreader. Hold the spreader almost vertically, with its shoulders in contact with the top of the hopper. Draw it forward and backward once along each mould compartment.
6. Compact the first mortar layer by subjecting it to 60 jolts from the jolting apparatus.
7. Introduce the second layer of mortar, ensuring that there is an excess of mortar. Level it with a small spreader.
8. Compact the second layer by applying an additional 60 jolts using the jolting apparatus.
9. Gently lift the mould from the jolting table and remove the hopper.
10. Immediately strike off the excess mortar using a metal straightedge. Hold the straightedge almost vertically, but inclined in the direction of striking. Slowly move the straightedge with a transverse sawing motion once in each direction.
11. Repeat the striking off procedure with the straightedge held at a more acute angle to smooth the surface.
12. Wipe off the mortar left on the perimeter of the mould as a result of the striking-off.
13. Label or mark the moulds for identification purposes.

After preparation of the test specimens and before testing, they are conditioned for a time period of 28 days according to the following procedure:

### *Before demoulding:*

1. Prepare a sheet of plastic with an approximate size of 210 mm × 185 mm × 6 mm.
2. Place the plastic sheet on top of the mould, covering it completely.
3. Without delay, place each covered mould on a horizontal base in the moist air room or cabinet as specified in section 4.1 of NEN-EN 196-1.
4. Ensure that the moist air has access to all sides of the mould. Do not stack the moulds on top of each other.
5. Each mould should be removed from storage at its appropriate time for demoulding.

### *Demoulding of the specimens for 28 day test:*

1. Carry out demoulding between 20 hours and 24 hours after moulding, taking care not to damage the specimens. Demoulding may be delayed by 24 hours if the mortar has not acquired sufficient strength at 24 hours to be handled without risk of damage. Any delay in demoulding should be recorded in the test report.
2. Suitably mark specimens selected for curing in water for identification, e.g. by water-resistant ink or crayon.

*Curing of the specimens in 95% relative humidity curing room:*

1. After demoulding the prisms, they are stored in a moist air curing room with a relative humidity of 95%.
2. The specimens are kept in the curing room for 28 days  $\pm$  8 hours.
3. Carry out strength test at 28 days  $\pm$  8 hours.

## Appendix C: Strength results

### Reference prisms

**Table C1: Fracture loads of reference prisms [N]**

Sample	F <sub>f</sub> prism 1	F <sub>f</sub> prism 2	F <sub>f</sub> prism 3	Mean F <sub>f</sub> [N]
REF1	3523	3726	3911	3720
REF2	3239	3257	3516	3337,3
REF3	3442	3689	4146	3759

**Table C2: Flexural strengths of reference prisms [MPa]**

Sample	R <sub>f</sub> prism 1	R <sub>f</sub> prism 2	R <sub>f</sub> prism 3	Mean R <sub>f</sub> [MPa]
REF1	8,3	8,7	9,2	8,7
REF2	7,6	7,6	8,2	7,8
REF3	8,1	8,6	9,7	8,8

**Table C3: Maximum compressive load at fracture of reference prisms [N]**

Sample	F <sub>c</sub> prism 1	F <sub>c</sub> prism 2	F <sub>c</sub> prism 3	Mean F <sub>c</sub> [N]
REF1	71486	66094	68966	
	76117	73184	69712	70926,5
REF2	59513	60681	57471	
	57286	61900	59819	59445
REF3	64217	64715	65027	
	65193	64427	64287	64644,3

**Table C4: Compressive strengths of reference prisms [MPa]**

Sample	R <sub>c</sub> prism 1	R <sub>c</sub> prism 2	R <sub>c</sub> prism 3	Mean R <sub>c</sub> [Mpa]
REF1	44.7	41.3	43.1	
	47.6	45.7	43.6	44.3
REF2	37.2	37.9	35.9	
	35.8	38.7	37.4	37.2
REF3	40.1	40.4	40.6	
	40.7	40.3	40.2	40.4

## Prisms with untreated RCF

**Table C5: Fracture loads of prisms containing untreated RCF [N]**

Sample	F <sub>f</sub> prism 1	F <sub>f</sub> prism 2	F <sub>f</sub> prism 3	Mean F <sub>f</sub> (N)
SC1-100	0	0	0	0
SC2-100	0	0	0	0
SC3-100	925	975	1135	1011.7
SC1-75	1258	1295	1215	1256
SC2-75	987	876	987	950
SC3-75	2579	1493	- no result -	2036
SC1-50	2640	2603	2548	2597
SC2-50	2289	2560	2190	2346.3
SC3-50	3683	3615	3430	3576

**Table C6: Flexural strength of prisms containing untreated RCF [MPa]**

Sample	R <sub>f</sub> prism 1	R <sub>f</sub> prism 2	R <sub>f</sub> prism 3	Mean R <sub>f</sub> [MPa]
SC1-100	0	0	0	0
SC2-100	0	0	0	0
SC3-100	2.2	2.3	2.7	2.4
SC1-75	2.9	3.0	2.8	2.9
SC2-75	2.3	2.1	2.3	2.2
SC3-75	6.0	3.5	- no result -	4.8
SC1-50	6.2	6.1	6.0	6.1
SC2-50	5.4	6.0	5.1	5.5
SC3-50	8.6	8.5	8.0	8.4

**Table C7: Maximum compressive loads of the prisms containing untreated RCF [N]**

Sample	F <sub>c</sub> prism 1	F <sub>c</sub> prism 2	F <sub>c</sub> prism 3	Mean F <sub>c</sub> [N]
SC1-100	0	0	0	
	0	0	0	0
SC2-100	0	0	0	
	0	0	0	0
SC3-100	9291	10069	9877	
	9864	10000	10031	9855.3
SC1-75	12226	10881	12046	
	13211	11643	11079	11847.7
SC2-75	8421	8587	8797	
	8735	8834	9210	8764
SC3-75	28047	29629	30442	
	29938	28185	29124	29227.5
SC1-50	32164	30411	26566	
	32132	27335	28198	29467.7
SC2-50	26755	27410	29068	
	26269	23228	29736	27077.7
SC3-50	46252	48924	45628	
	41505	49107	40560	45329.3

**Table C8: Compressive strengths of prisms containing untreated RCF [MPa]**

<b>Sample</b>	<b>R<sub>c</sub> prism 1</b>	<b>R<sub>c</sub> prism 2</b>	<b>R<sub>c</sub> prism 3</b>	<b>Mean R<sub>c</sub> [MPa]</b>
SC1-100	0	0	0	
	0	0	0	0
SC2-100	0	0	0	
	0	0	0	0
SC3-100	5,8	6,3	6,2	
	6,2	6,3	6,3	6,2
SC1-75	7,6	6,8	7,5	
	8,3	7,3	6,9	7,4
SC2-75	5,3	5,4	5,5	
	5,5	5,5	5,8	5,5
SC3-75	17,5	18,5	19,0	
	18,7	17,6	18,2	18,3
SC1-50	20,1	19,0	16,6	
	20,1	17,1	17,6	18,4
SC2-50	16,7	17,1	18,2	
	16,4	14,5	18,6	16,9
SC3-50	28,9	30,6	28,5	
	25,9	30,7	25,4	28,3



## Prisms with carbonated RCF

**Table C9: Fracture loads of prisms containing carbonated RCF [N]**

Sample	F <sub>f</sub> prism 1	F <sub>f</sub> prism 2	F <sub>f</sub> prism 3	Mean F <sub>f</sub> [N]
SC1-CAR-100	0	0	0	0
SC2-CAR-100	0	0	0	0
SC3-CAR-100	0	0	0	0
SC1-CAR-75	2159	1906	1906	1990.3
SC2-CAR-75	1203	1141	1154	1166
SC3-CAR-75	2677	2616	2560	2617.7
SC1-CAR-50	2850	3128	3078	3018.7
SC2-CAR-50	2394	2406	2400	2400
SC3-CAR-50	3541	2967	3023	3177

**Table C10: Flexural strength of prisms containing carbonated RCF [MPa]**

Sample	R <sub>f</sub> prism 1	R <sub>f</sub> prism 2	R <sub>f</sub> prism 3	Mean R <sub>f</sub> [MPa]
SC1-CAR-100	0	0	0	0
SC2-CAR-100	0	0	0	0
SC3-CAR-100	0	0	0	0
SC1-CAR-75	5.1	4.5	4.5	4.7
SC2-CAR-75	2.8	2.7	2.7	2.7
SC3-CAR-75	6.3	6.1	6.0	6.1
SC1-CAR-50	6.7	7.3	7.2	7.1
SC2-CAR-50	5.6	5.6	5.6	5.6
SC3-CAR-50	8.3	7.0	7.1	7.4

**Table C11: Maximum compressive loads of the prisms containing carbonated RCF [N]**

Sample	F <sub>c</sub> prism 1	F <sub>c</sub> prism 2	F <sub>c</sub> prism 3	Mean F <sub>c</sub> [N]
SC1-CAR-100	0	0	0	
	0	0	0	0
SC2-CAR-100	0	0	0	
	0	0	0	0
SC3-CAR-100	0	0	0	
	0	0	0	0
SC1-CAR-75	18796	19596	18877	
	18275	18616	17643	18633,8
SC2-CAR-75	10751	11104	9766	
	10602	10484	11618	10720,8
SC3-CAR-75	18684	18808	20432	
	18827	18375	21282	19401,3
SC1-CAR-50	35063	36002	38316	
	31722	34962	37389	35575,7
SC2-CAR-50	22893	23284	28822	
	25715	24647	26471	25305,3
SC3-CAR-50	39854	38397	38303	
	39248	32151	36998	37491,8

**Table C12: Compressive strength of prisms containing carbonated RCF [MPa]**

<b>Sample</b>	<b>R<sub>c</sub> prism 1</b>	<b>R<sub>c</sub> prism 2</b>	<b>R<sub>c</sub> prism 3</b>	<b>Mean R<sub>c</sub> [MPa]</b>
SC1-CAR-100	0,0	0,0	0,0	
	0,0	0,0	0,0	0,0
SC2-CAR-100	0,0	0,0	0,0	
	0,0	0,0	0,0	0,0
SC3-CAR-100	0,0	0,0	0,0	
	0,0	0,0	0,0	0,0
SC1-CAR-75	11,7	12,2	11,8	
	11,4	11,6	11,0	11,6
SC2-CAR-75	6,7	6,9	6,1	
	6,6	6,6	7,3	6,7
SC3-CAR-75	11,7	11,8	12,8	
	11,8	11,5	13,3	12,1
SC1-CAR-50	21,9	22,5	23,9	
	19,8	21,9	23,4	22,2
SC2-CAR-50	14,3	14,6	18,0	
	16,1	15,4	16,5	15,8
SC3-CAR-50	24,9	24,0	23,9	
	24,5	20,1	23,1	23,4

## Prisms with ground RCF

**Table C13: Fracture loads of prisms containing further ground RCF [N]**

Sample	F <sub>f</sub> prism 1	F <sub>f</sub> prism 2	F <sub>f</sub> prism 3	Mean F <sub>f</sub> [N]
SC1-GR-100	0	0	0	0
SC2-GR-100	0	0	0	0
SC3-GR-100	845	709	913	822,3
SC1-GR-75	1727	1684	1820	1743,7
SC2-GR-75	1012	1154	1252	1139,3
SC3-GR-75	2381	2474	2369	2408
SC1-GR-50	3245	3078	3165	3162,7
SC2-GR-50	2270	2406	2468	2381,3
SC3-GR-50	3689	3473	4022	3728

**Table C14: Flexural strength of prisms containing further ground RCF [MPa]**

Sample	R <sub>f</sub> prism 1	R <sub>f</sub> prism 2	R <sub>f</sub> prism 3	Mean R <sub>f</sub> [MPa]
SC1-GR-100	0,0	0,0	0,0	0,0
SC2-GR-100	0,0	0,0	0,0	0,0
SC3-GR-100	2,0	1,7	2,1	1,9
SC1-GR-75	4,0	3,9	4,3	4,1
SC2-GR-75	2,4	2,7	2,9	2,7
SC3-GR-75	5,6	5,8	5,6	5,6
SC1-GR-50	7,6	7,2	7,4	7,4
SC2-GR-50	5,3	5,6	5,8	5,6
SC3-GR-50	8,6	8,1	9,4	8,7

**Table C15: Maximum compressive loads of the prisms containing further ground RCF [N]**

Sample	F <sub>c</sub> prism 1	F <sub>c</sub> prism 2	F <sub>c</sub> prism 3	Mean F <sub>c</sub> [N]
SC1-GR-100	0	0	0	
	0	0	0	0,0
SC2-GR-100	0	0	0	
	0	0	0	0,0
SC3-GR-100	7594	7446	8421	
	7477	5910	9988	7806,0
SC1-GR-75	17513	16676	17395	
	16763	17252	16236	16972,5
SC2-GR-75	8470	10633	11562	
	10961	11166	12046	10806,3
SC3-GR-75	22000	21659	21009	
	21511	19862	20228	21044,8
SC1-GR-50	43705	35762	45318	
	45407	36159	40313	41110,7
SC2-GR-50	25134	27713	34174	
	27687	27252	25109	27844,8
SC3-GR-50	47493	43749	41669	
	51682	39569	46333	45082,5

**Table C16: Compressive strength of prisms containing further ground RCF [MPa]**

<b>Sample</b>	<b>R<sub>c</sub> prism 1</b>	<b>R<sub>c</sub> prism 2</b>	<b>R<sub>c</sub> prism 3</b>	<b>Mean R<sub>c</sub> [MPa]</b>
SC1-GR-100	0,0	0,0	0,0	
	0,0	0,0	0,0	0,0
SC2-GR-100	0,0	0,0	0,0	
	0,0	0,0	0,0	0,0
SC3-GR-100	4,7	4,7	5,3	
	4,7	3,7	6,2	4,9
SC1-GR-75	10,9	10,4	10,9	
	10,5	10,8	10,1	10,6
SC2-GR-75	5,3	6,6	7,2	
	6,9	7,0	7,5	6,8
SC3-GR-75	13,8	13,5	13,1	
	13,4	12,4	12,6	13,2
SC1-GR-50	27,3	22,4	28,3	
	28,4	22,6	25,2	25,7
SC2-GR-50	15,7	17,3	21,4	
	17,3	17,0	15,7	17,4
SC3-GR-50	29,7	27,3	26,0	
	32,3	24,7	29,0	28,2

## Prisms with heated RCF

**Table C17: Fracture loads of prisms containing heated RCF [N]**

Sample	F <sub>f</sub> prism 1	F <sub>f</sub> prism 2	F <sub>f</sub> prism 3	Mean F <sub>f</sub> [N]
SC1-HT-100	0	0	0	0
SC2-HT-100	0	0	0	0
SC3-HT-100	0	0	0	0
SC1-HT-75	1561	1666	1592	1606.3
SC2-HT-75	1098	1166	1147	1137
SC3-HT-75	2461	2758	2634	2617.7
SC1-HT-50	2733	3085	2690	2836
SC2-HT-50	1857	1733	1814	1801.3
SC3-HT-50	2560	2529	3004	2697.7

**Table C18: Flexural strength of prisms containing heated RCF [MPa]**

Sample	R <sub>f</sub> prism 1	R <sub>f</sub> prism 2	R <sub>f</sub> prism 3	Mean R <sub>f</sub> [MPa]
SC1-HT-100	0.0	0.0	0.0	0.0
SC2-HT-100	0.0	0.0	0.0	0.0
SC3-HT-100	0.0	0.0	0.0	0.0
SC1-HT-75	3.7	3.9	3.7	3.8
SC2-HT-75	2.6	2.7	2.7	2.7
SC3-HT-75	5.8	6.5	6.2	6.1
SC1-HT-50	6.4	7.2	6.3	6.6
SC2-HT-50	4.4	4.1	4.3	4.2
SC3-HT-50	6.0	5.9	7.0	6.3

**Table C19: Maximum compressive loads of the prisms containing heated RCF [N]**

Sample	F <sub>c</sub> prism 1	F <sub>c</sub> prism 2	F <sub>c</sub> prism 3	Mean F <sub>c</sub> [N]
SC1-HT-100	1943	1986	1906	
	1956	1801	1882	1912.3
SC2-HT-100	0	1573	1684	
	1499	1363	1598	1286.2
SC3-HT-100	2270	2381	2363	
	2270	2338	2628	2375.0
SC1-HT-75	17965	15641	16205	
	17575	18821	17240	17241.2
SC2-HT-75	11981	12133	11463	
	13007	12777	12814	12362.5
SC3-HT-75	41700	38154	42520	
	40301	39406	36487	39761.3
SC1-HT-50	33638	38719	40036	
	37231	31709	40541	36979.0
SC2-HT-50	25708	21753	23271	
	24238	22924	23482	23562.7
SC3-HT-50	46132	48180	50961	
	44915	47128	50648	47994.0

**Table C20: Compressive strength of prisms containing heated RCF [MPa]**

<b>Sample</b>	<b>R<sub>c</sub> prism 1</b>	<b>R<sub>c</sub> prism 2</b>	<b>R<sub>c</sub> prism 3</b>	<b>Mean R<sub>c</sub> [MPa]</b>
SC1-HT-100	1.2	1.2	1.2	
	1.2	1.1	1.2	1.2
SC2-HT-100	0.0	1.0	1.1	
	0.9	0.9	1.0	0.8
SC3-HT-100	1.4	1.5	1.5	
	1.4	1.5	1.6	1.5
SC1-HT-75	11.2	9.8	10.1	
	11.0	11.8	10.8	10.8
SC2-HT-75	7.5	7.6	7.2	
	8.1	8.0	8.0	7.7
SC3-HT-75	26.1	23.8	26.6	
	25.2	24.6	22.8	24.9
SC1-HT-50	21.0	24.2	25.0	
	23.3	19.8	25.3	23.1
SC2-HT-50	16.1	13.6	14.5	
	15.1	14.3	14.7	14.7
SC3-HT-50	28.8	30.1	31.9	
	28.1	29.5	31.7	30.0

## Prisms with flash calcined RCF

**Table C21: Fracture loads of prisms containing flash calcined RCF [N]**

Sample	F <sub>f</sub> prism 1	F <sub>f</sub> prism 2	F <sub>f</sub> prism 3	Mean F <sub>f</sub> [N]
SC1-FC-100*	432	500	389	440.3
SC2-FC-100*	685	635	598	639.3
SC3-FC-100*	2930	3035	2869	2944.7
SC1-FC-75*	2973	3091	3202	3088.7
SC2-FC-75*	2153	2375	2338	2288.7
SC3-FC-75*	3017	3226	3300	3181
SC1-FC-50	3288	3473	3541	3434
SC2-FC-50*	2751	2862	2677	2763.3
SC3-FC-50	4004	4059	3658	3907
SC3-FC-50*	2832	2733	2659	2741.3

**Table C22: Flexural strength of prisms containing flash calcined RCF [MPa]**

Sample	R <sub>f</sub> prism 1	R <sub>f</sub> prism 2	R <sub>f</sub> prism 3	Mean R <sub>f</sub> [MPa]
SC1-FC-100*	1.0	1.2	0.9	1.0
SC2-FC-100*	1.6	1.5	1.4	1.5
SC3-FC-100*	6.9	7.1	6.7	6.9
SC1-FC-75*	7.0	7.2	7.5	7.2
SC2-FC-75*	5.0	5.6	5.5	5.4
SC3-FC-75*	7.1	7.6	7.7	7.5
SC1-FC-50	7.7	8.1	8.3	8.0
SC2-FC-50*	6.4	6.7	6.3	6.5
SC3-FC-50	9.4	9.5	8.6	9.2
SC3-FC-50*	6.4	6.2	6.4	6.4

**Table C23: Maximum compressive loads of the prisms containing flash calcined RCF [N]**

Sample	F <sub>c</sub> prism 1	F <sub>c</sub> prism 2	F <sub>c</sub> prism 3	Mean F <sub>c</sub> [N]
SC1-FC-100*	3356	4417	2967	
	3504	3640	3837	3620.2
SC2-FC-100*	8088	8427	7076	
	6823	7699	7539	7608.7
SC3-FC-100*	28173	30133	25689	
	30303	30599	26749	28607.7
SC1-FC-75*	42355	41921	48048	
	40181	36645	37684	41139.0
SC2-FC-75*	24808	28488	22459	
	23203	28185	26483	25604.3
SC3-FC-75*	45123	49434	49428	
	46277	49057	49586	48150.8
SC1-FC-50	51037	54694	54292	
	59021	51081	53717	53973.7
SC2-FC-50*	37450	35986	36821	
	34199	33978	35838	35712.0
SC3-FC-50	53551	51273	46686	
	49189	50124	47587	49735
SC3-FC-50*	48533	51765	47531	
	54088	47247	53022	50364.3

**Table C24: Compressive strength of prisms containing flash calcined RCF [MPa]**

<b>Sample</b>	<b>R<sub>c</sub> prism 1</b>	<b>R<sub>c</sub> prism 2</b>	<b>R<sub>c</sub> prism 3</b>	<b>Mean R<sub>c</sub> [MPa]</b>
SC1-FC-100*	2.1	2.8	1.9	
	2.2	2.3	2.4	2.3
SC2-FC-100*	5.1	5.3	4.4	
	4.3	4.8	4.7	4.8
SC3-FC-100*	17.6	18.8	16.1	
	18.9	19.1	16.7	17.9
SC1-FC-75*	26.5	26.2	30.0	
	25.1	22.9	23.6	25.7
SC2-FC-75*	15.5	17.8	14.0	
	14.5	17.6	16.6	16.0
SC3-FC-75*	28.2	30.9	30.9	
	28.9	30.7	31.0	30.1
SC1-FC-50	31.9	34.2	33.9	
	36.9	31.9	33.6	33.7
SC2-FC-50*	23.4	22.5	23.0	
	21.4	21.2	22.4	22.3
SC3-FC-50	33.5	32.0	29.2	
	30.7	31.3	29.7	31.1
SC3-FC-50*	30.3	32.4	29.7	
	33.8	29.5	33.1	31.5



## Appendix D: TGA and DSC

### Untreated RCF

Figure D1 shows the results of the TGA and DSC measurements of the untreated RCF. When looking at the TG and DTG graphs multiple abrupt mass losses and a continuous mass loss over the whole range are observed. The continuous mass loss corresponds to the dehydration of calcium silicate hydrates, calcium aluminate hydrates and other minor hydrates (Marsh & Day, 1988). The first abrupt drop in mass is observed between 40 – 250 °C with its peak at 115.7 °C. This mass loss corresponds to the evaporation of free water and bound water and the decomposition of gypsum and the other hydration products ettringite, carboaluminate hydrates and C-S-H. The second drop occurs around 400 °C and corresponds to the decomposition of Portlandite, which generally happens between 400 and 500 °C (Scrivener, Snellings, & Lothenbach, 2016). The third drop occurs between 700 and 800 °C and corresponds to the decomposition of calcium carbonate. The last sudden drop in mass occurs at around 882 °C, which also corresponds to the decomposition of calcium carbonate. Each sudden drop in mass on the TG curve corresponds to a peak on the DTG curve and an endothermic peak on the DSC curve. The total mass loss from the beginning to the end is 15.65%.

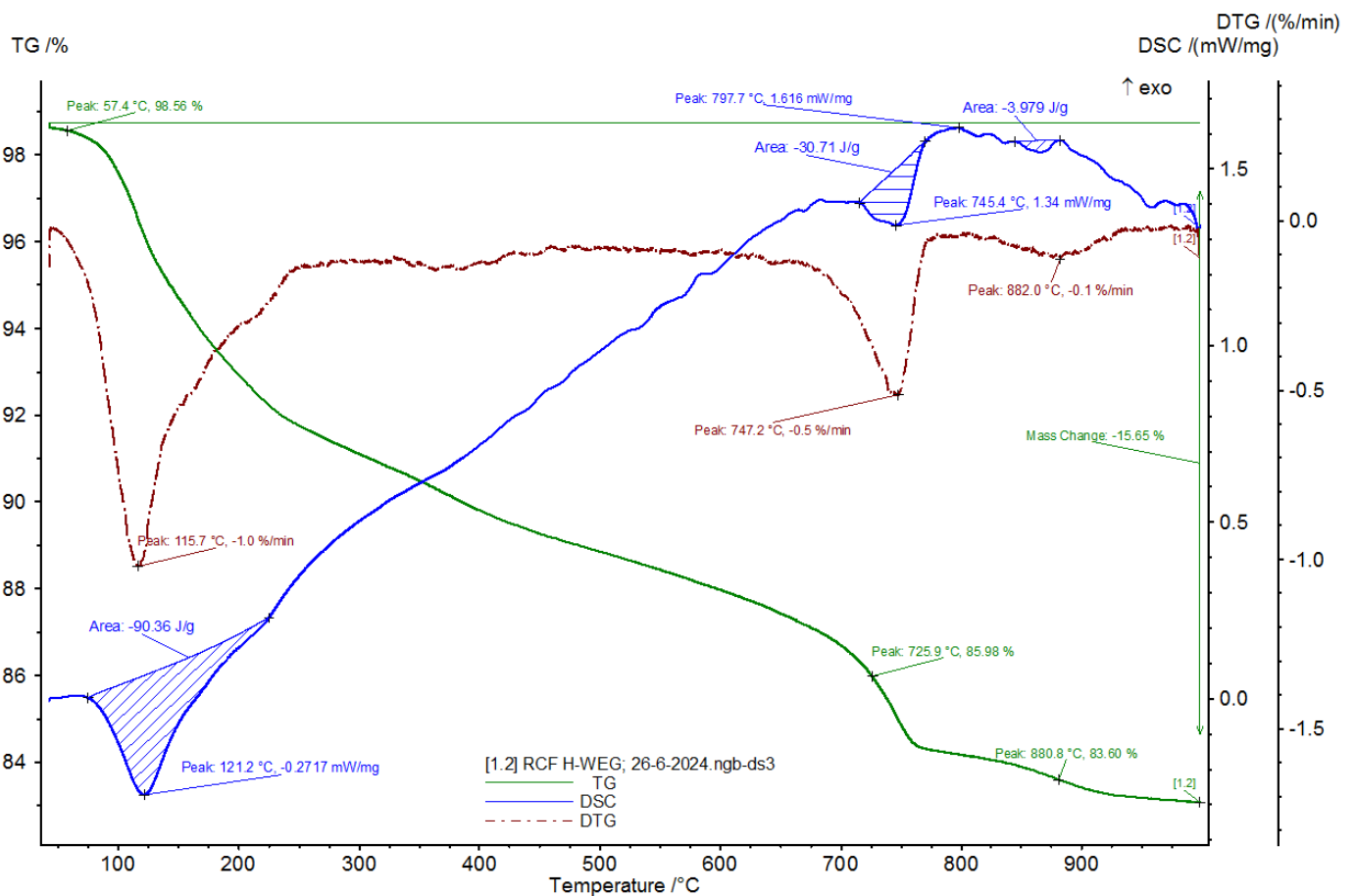
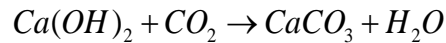


Figure D1: TGA and DSC results of untreated RCF

## Carbonated RCF

Figure D2 shows the results of the TGA and DSC measurements of the carbonated RCF. Similar to the untreated RCF the first significant mass loss occurs between 40 and 250 °C and corresponds to the evaporation of free water and bound water and the decomposition of gypsum and the other hydration products ettringite, carboaluminate hydrates and C-S-H. However, it is noticeable that the mass loss in this first phase is not smooth. A sudden drop occurs at around 140 °C, which can be caused by the decomposition of gypsum. Gypsum dehydrates in two steps, namely at around 100 to 140 °C to hemihydrate and at 140 – 150 °C to anhydrite (Scrivener, Snellings, & Lothenbach, 2016). There is no significant change in slope noticeable between 250 and 700 °C, while generally cementitious materials show a sudden drop at around 400 – 500 °C due to the decomposition of Portlandite. The absence of this sudden mass drop at the carbonated RCF can be explained by the carbonation of Portlandite, resulting in the formation of calcium carbonate (Kudlacz, Ruiz-Agudo, & Rodriguez-Navarro, 2011):



The next sudden mass drops occur between 700 and 800 °C and at around 876.4 °C and correspond to the decomposition of calcium carbonate. It can be observed that this mass drop corresponds to approximately 10% of the sample mass. Pan et al. (2016) states that the amount of CO<sub>2</sub> within the sample corresponds to the mass loss due to the decomposition of calcium carbonate, which indicates that the RCF contain approximately 10 wt.% CO<sub>2</sub> after carbonation and approximately 3% before. The continuous mass loss over the whole range corresponds to the dehydration of calcium silicate hydrates, calcium aluminate hydrates and other minor hydrates (Marsh & Day, 1988). The sudden drops in mass correspond to endothermic peaks on the DSC curve. The total mass loss of the sample is 22.21%.

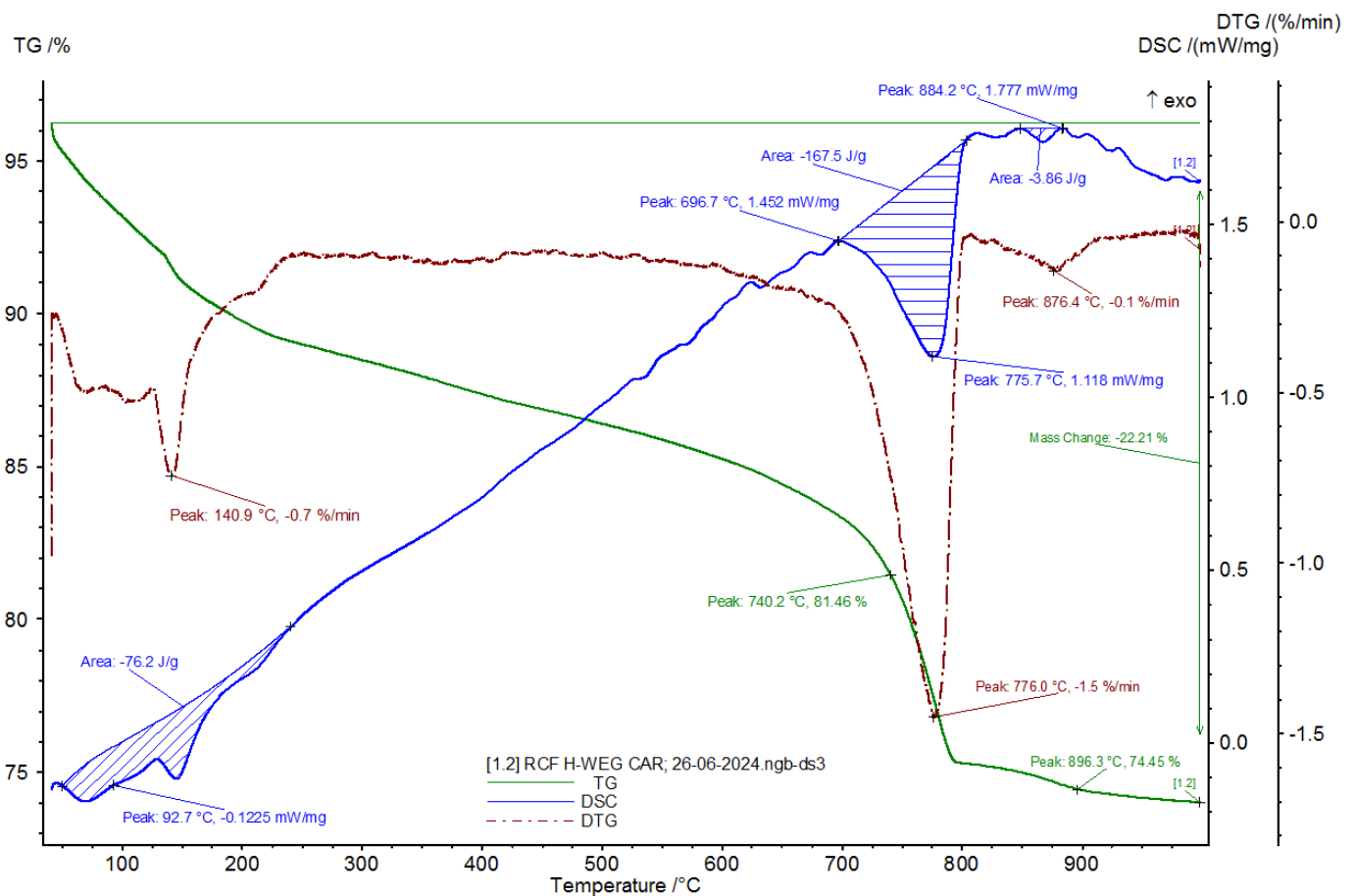


Figure D2: TGA and DSC results of carbonated RCF

## Further ground RCF

The TGA and DSC results of the further ground RCF sample are shown in Figure D3. The first drop in mass occurs between 40 and 250 °C with a smooth peak in the DTG curve. This mass loss is related to the evaporation of free water and bound water and the decomposition of gypsum and the other hydration products ettringite, carboaluminate hydrates and C-S-H. A small drop in mass occurs at around 400 °C and corresponds to the decomposition of Portlandite. The mass losses that correspond to the decomposition of calcium carbonate occur between 700 and 900 °C and seem to happen in two steps. Over the whole range a continuous mass loss is observed, which corresponds to the dehydration of calcium silicate hydrates, calcium aluminate hydrates and other minor hydrates (Marsh & Day, 1988). The total mass loss of the sample is 16.82%.

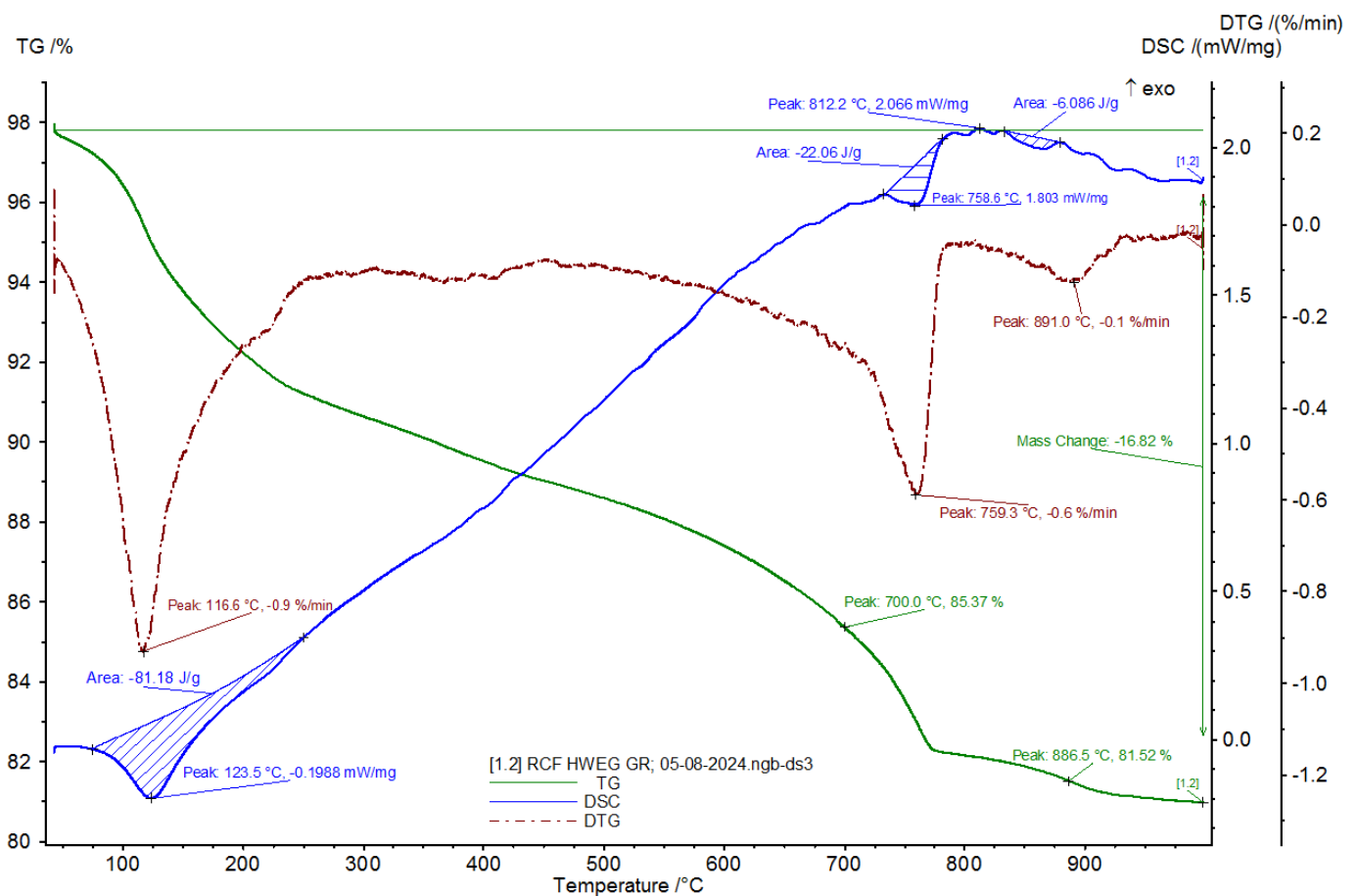


Figure D3: TGA and DSC results of further ground RCF

## Flash calcined RCF

The TGA and DSC results of the flash calcined RCF are shown in Figure D4. The first mass loss occurs between 40 and 250 °C, which generally corresponds to the evaporation of free water and bound water and the decomposition of gypsum and the other hydration products such as ettringite, carboaluminate hydrates and C-S-H. However, since the RCF is flash calcined at a temperature between 700 and 800 °C there should be no free water present in the sample and part of the hydration products should be decomposed. Although, a small amount of moist might be taken up from the air during storage. This is confirmed by the graph since the mass loss at 125.3 °C is only 0.78%. The next mass loss starts from around 500 °C, with its peak between 600 and 800 °C. This corresponds to the decomposition of calcium carbonate, which indicates that the calcium carbonate did not or not fully decompose during the treatment.

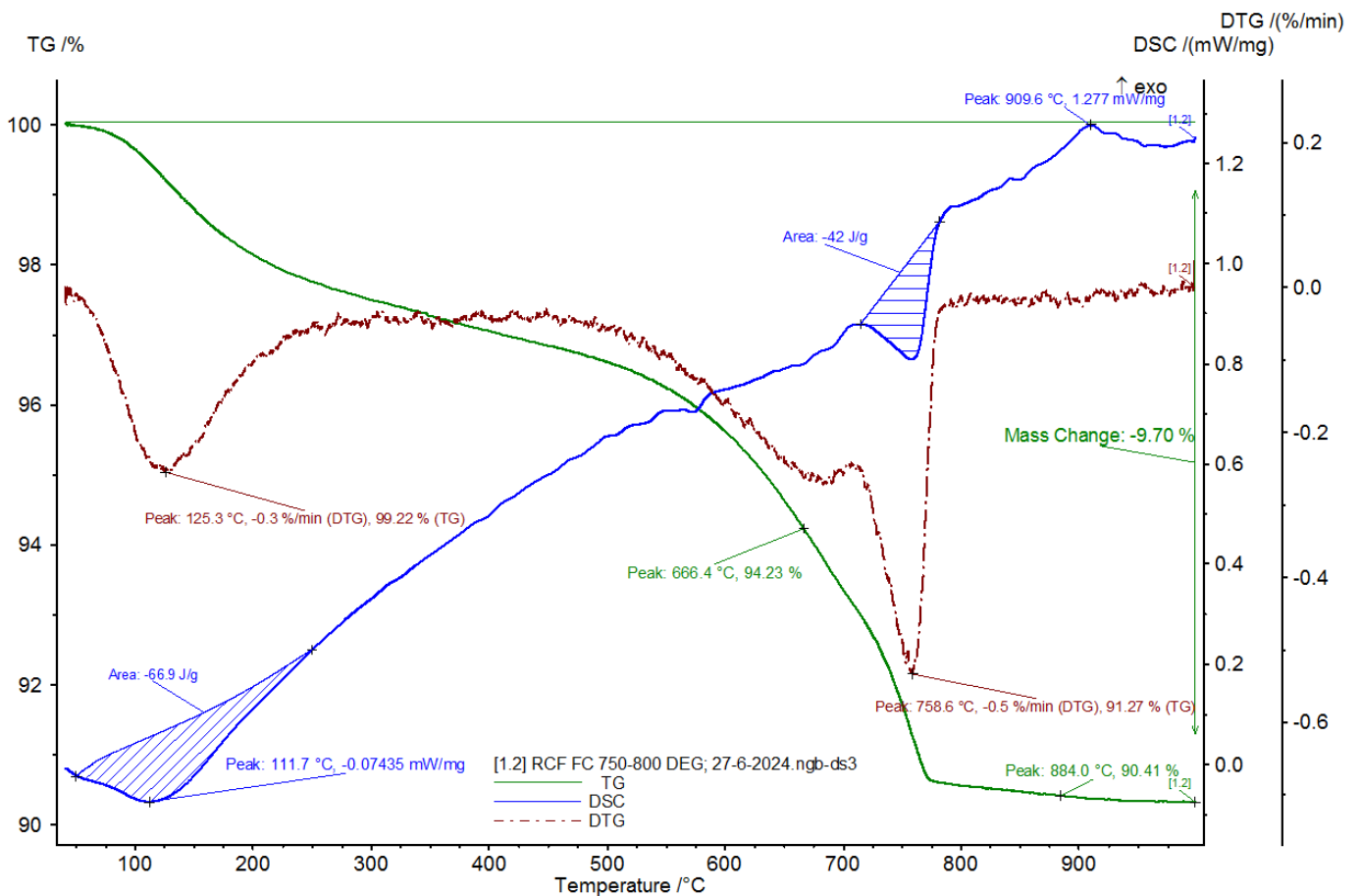


Figure D4: TGA and DSC results of flash calcined RCF

## Heated RCF

Figure D5 shows the TG and DSC curves of the heated RCF. It is observed that the total mass loss during the measurement is only 0.25%, which is negligibly small. This indicates that nearly no reactions, evaporation or decomposition occurred, which means that the RCF became nearly thermally stable for temperatures up to 1000 °C after heating the material up to 900 °C and keeping it at that temperature for one hour. During the thermal treatment the material already lost 20% of its mass. That mass loss together with the nearly horizontal TG curve indicates a possible full dehydration of the material. However, at around 400 °C a small sudden drop in mass occurred. That could mean that there was still a minor component which was not fully decomposed during the treatment.

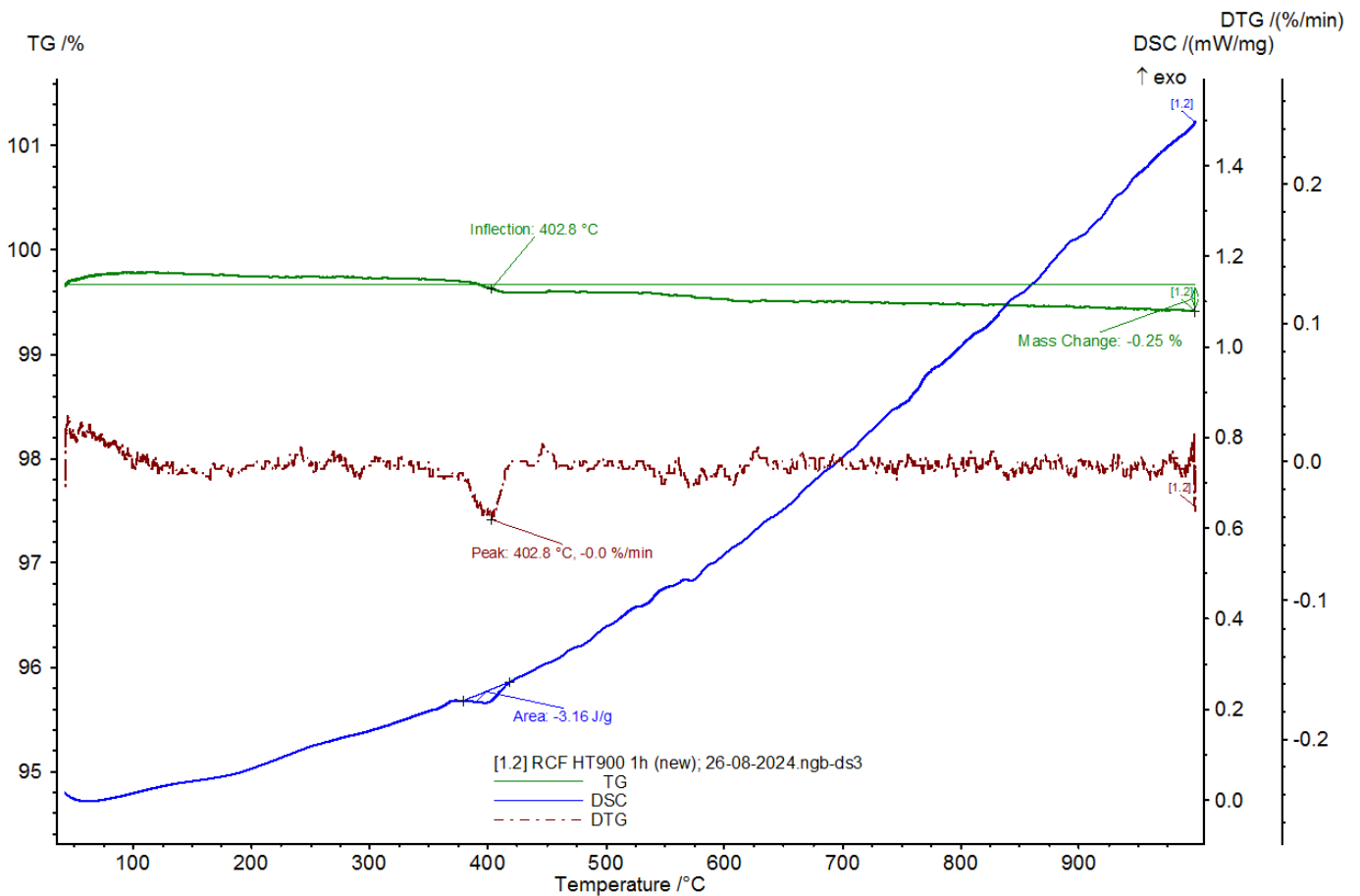


Figure D5: TGA and DSC results of heated RCF